To the Graduate Council:

I am submitting herewith a thesis written by Gregory Thomas Marks entitled "Sedimentology of the Clinch Sandstone (Lower Silurian) at Powell Mountain, Southwestern Virginia." I have examined the final copy of this thesis for form and content and recommend that it be accepted in partial fulfillment of the requirements for the degree of Master of Science, with a major in Geology.

Steven G. Driese, Major Professor

We have read this thesis
and recommend its acceptance:

Accepted for the Council:

Vice Provost
and Dean of The Graduate School

STATEMENT OF PERMISSION TO USE

In presenting this thesis in partial fulfillment of the requirements for a Master's degree at The University of Tennessee, Knoxville, I agree that the Library shall make it available to borrowers under rules of the Library. Brief quotations from this thesis are allowable without special permission, provided that accurate acknowledgment of the source is made.

Permission for extensive quotation from or reproduction of this thesis may be granted by my major professor, or in his absence, by the Head of Interlibrary Services when, in the opinion of either, the proposed use of the material is for scholarly purposes. Any copying or use of the material in this thesis for financial gain shall not be allowed without my written permission.

Signature Gregory L. Marks

Date August, 1987

SEDIMENTOLOGY OF THE CLINCH SANDSTONE (LOWER SILURIAN) AT POWELL MOUNTAIN, SOUTHWESTERN VIRGINIA

A Thesis

Presented for the

Master of Science

Degree

The University of Tennessee, Knoxville

Gregory Thomas Marks

December 1987

DEDICATION

To my mom and dad, whose love and countless sacrifices made everything possible.

ACKNOWLEDGEMENTS

My deepest expression of gratitude is extended to my advisor, Dr. Steven G. Driese, for guidance, advice and being a constant source of encouragement during this project.

Recognition is also extended to Dr. Arnseth and Dr. Broadhead for their suggestions and comments during manuscript preparation. Final thanks go to Mark Fischer for his constructive and stimulating discussions during field work at Powell Mountain.

This research was supported by grants from the Discretionary Fund of the Department of Geological Sciences, the Appalachian Basin Industrial Associates and Sigma Xi. Special funding was provided by a research scholarship from Mobil Exploration and Producing Services, Dallas, Texas.

ABSTRACT

The sedimentology of the Clinch Sandstone (Lower Silurian) was analyzed at Powell Mountain, southwestern Virginia in order to ascertain the paleoenvironmental factors leading to its deposition. At this location, the Clinch is divided into the lower Hagan Shale Member and upper Poor Valley Ridge Sandstone Member, each of which is further subdivided into four facies representing distinctive depositional environments. Facies A/HS , a thick calcareous quartzarenite, directly overlies the subaerially exposed tidal flat deposits of the Upper Ordovician Juniata Formation. Sub-facies B1/HS and B2/HS of the Hagan are differentiated by subtle differences in lithology, sedimentary structures, bedding geometry and mineralogical character. Sub-facies B1/HS is composed of very thinly interbedded, very fine-grained, calcareous quartzarenite and interbedded shale. Sub-facies B2/HS consists of very thinly interbedded, very fine-grained, calcareous quartzarenite, wackestone/packstone units and interbedded shale. Facies C/HS is a medium to dark-gray, fissile to slightly blocky shale. Three individual units comprise Facies D/HS consisting of a bryozoan packstone, a fossiliferous quartzarenite and a ferruginous sandstone conglomerate.

The Poor Valley Ridge Sandstone is also divided into four facies. Facies A/PVR consists of medium-bedded, compound cross-stratified, fine-grained quartzarenite containing intercalations of shale less than 2 cm thick. Ubiquitous trough cross-stratification is enclosed

within large-scale second-order bounding surfaces. Facies B/PVR is composed of a heavily bioturbated, fine to coarse-grained, clay-rich, quartzarenite. Facies C/PVR is composed of fissile to slightly blocky shale. Facies D/PVR is the lowermost facies within the Poor Valley Ridge, and it constitutes the transitional contact with the underlying Hagan Shale. The lithology of D/PVR consists of interbedded subarkose to quartzarenite and intervening shale, with the former exhibiting mineralogical, textural, geometrical and sedimentological changes upward within this facies. Capping the Clinch Sandstone at Powell mountain is the maroon and gray mudstone, siltstone and sandstone of the basal Rose Hill Formation.

Facies of the Hagan Shale represent deposition within laterally contiguous subenvironments on a shallow-marine shelf. Deposition took place within the transition zone and on the middle shelf, both above and below fairweather wave base. Facies A/HS is interpreted to represent the shallowest, most nearshore deposits of the Late Ordovician, Early Silurian marine transgression. Facies B/HS represents deposition in a marine, sublittoral, storm-shelf setting. The thin sandstone and wackestone/packstone units show several features consistent with deposition from episodic, high-energy storm events punctuating the background sedimentation of mud and fine silt. Facies C/HS represents similar but more prolonged periods of quiet-water sedimentation than the interbedded shale of B/HS. Facies D/HS represents deposition by rippled or megarippled sand shoals which occasionally prograded into the offshore area of Hagan deposition.

The four facies of the Poor Valley Ridge Sandstone are interpreted to have been deposited in various subenvironments within a marine-shelf sand wave setting. The large-scale, second-order bounding surfaces of Facies A/PVR represent foreset planes of giant sand waves; internal trough cross-stratification was formed by the migration of sinuous crested dunes capping these large, flow-transverse bedforms. Facies B/PVR represents fairweather deposits during times of reduced sand wave activity. Facies C/PVR represents suspension-fallout deposits which collected in the troughs between sand waves. The upward coarsening/thickening sandstone-and-shale sequence of Facies D/PVR is interpreted as a transitional deposit representing the distal zones of Facies A/PVR. A zone of small sand waves was the first of the Poor Valley Ridge progradational clastic wedge which covered Hagan sediments during the Lower Silurian transgression. As progradation culminated later in the Silurian, tidal flat and offshore sand shoal deposits of the Rose Hill Formation covered the area.

TABLE OF CONTENTS

CHAPTER		PAGE
I.	INTRODUCTION	1
	Background	1
	Purpose	4
	Stratigraphic Position and Age	5
	Previous Work	9
	Study Area	16
	Methods	19
II.	FACIES DESCRIPTION	21
	Introduction	21
	The Hagan Shale Member	21
	General	21
	Facies A/HS Basal Sandstone	23
	Facies B/HS-Interbedded Sandstone and Shale	30
	Sub-facies B1/HS	30
	Sub-facies B2/HS	36
	Facies C/HS-Shale	46
	Facies D/HS-Isolated Quartzarenite and Iron-Rich Packstone	47
	Poor Valley Ridge Member	59
	General	59
	Facies A/PVR-Compound Cross-Stratified Quartzarenite	59
	Facies B/PVR-Bioturbated Sandstone	69
	Facies C/PVR-Shale	74
	Facies D/PVR-Interbedded Sandstone and Shale	77
III.	PALEOENVIRONMENTAL INTERPRETATIONS	85
	Hagan Shale Member	85
	Modern Storm Deposits	85
	Individual Facies Interpretation	91
	Facies A/HS	91
	Facies B/HS	96
	Facies C/HS	106
	Facies D/HS	109
	Poor Valley Ridge Sandstone Member	115
	General	115
	Modern Sand Waves	116
	Definition	116
	Occurrence	119
	Formation	121
	Lateral Variations	122
	Internal Structures	125
	Sand Waves in the Geological Record	131

Facies Interpretation 136
General Discussion 136
Facies A/PVR 137
Facies B/PVR 144
Facies C/PVR 146
Facies D/PVR 147
The Rose Hill Formation 152
General 152
Lithologic Description 154
Lithology 154
Sedimentary Structures 155
Biogenic Structures 158
Bedding Relationships 160
Petrography 162
Depositional Environment 164

IV. PALEOCURRENTS 169
Unidirectional Data 170
Bidirectional Data 172
Interpretation of Data 172

V. SUMMARY AND CONCLUSIONS 176

BIBLIOGRAPHY 187

APPENDICES 201
I. DETAILED MEASURED SECTION 202
II. PETROGRAPHIC ANALYSIS 224
III. MEASURED BED THICKNESS IN THE HAGAN SHALE 256

VITA 260

LIST OF TABLES

TABLE		PAGE
1.	Criteria Used to Document Sand Wave Deposits in the Stratigraphic Record	132
2.	Important Characteristics and Interpretations of the Facies in the Rancho Rojo Sand Body	133

LIST OF FIGURES

FIGURE		PAGE
1.	Lithologic Correlation of the Clinch Sandstone With Some of its Stratigraphic Equivalents in the Appalachian Basin.	6
2.	Location of Clinch Rocks at Powell Mountain, Lee and Scott Counties, Southwestern Virginia	17
3.	The Silurian Strata at the Crest of Powell Mountain, Southwestern Virginia	18
4.	Generalized Stratigraphic Section of the Clinch Sandstone and Rose Hill Formations at Powell Mountain, Southwestern Virginia	22
5.	Key to Symbols Used in the Stratigraphic Section. . . .	24
6.	Brief Description of Facies in the Hagan Shale.	25
7.	Facies A/HS, the Basal Sandstone Bed of the Hagan Shale	27
8.	Photomicrograph of the Basal Sandstone Unit, Facies A/HS, Lowermost Hagan Shale	29
9.	Interbedded Lithology of Sub-Facies B1/HS	32
10.	Sedimentary Structures within Sub-Facies B1/HS	33
11.	Photomicrograph of Sample UH2-5	35
12.	The Interbedded Wackestone/Packstone and Calcareous Quartzarenite of Sub-Facies B2/HS	37
13.	Cut-Slab from Sub-Facies B2/HS	39
14.	Sedimentary Structures within Sub-Facies B2/HS	40
15.	Gutter Casts Showing Internal Structures in Sub-Facies B2/HS	42
16.	Bedding Geometry of Sub-Facies B2/HS	43

FIGURE PAGE

17. Photomicrograph of a Typical Biosparite Commonly Found within Sub-Facies B2/HS. 45

18. Small Blocks Liberated by Weathering from the Shale of Facies C/HS 48

19. Sketch of the Anomalous and Isolated Units Comprising Facies D/HS. 49

20. Internal Structure within a Cut-Slab of a Ferruginous Bryozoan Packstone, Facies D/HS 51

21. Photomicrograph of the Ferruginous Bryozoan Packstone. 52

22. Photo of the Fossiliferous Quartzarenite Unit Occuring at 18.2 m above the Base of the Hagan Shale 54

23. Photomicrograph of Thin Section UH8-2 55

24. Cut-Slab of the Upper Sandstone Conglomerate Unit of Facies D/HS 57

25. Photomicrograph of Thin Section UH10-2 58

26. Brief Description of Facies in the Poor Valley Ridge Sandstone. 60

27. Master Bedding of Facies A/PVR 62

28. Internal Compound Cross-Stratification of Facies A/PVR. 63

29. Cut-Slab of a Quartzarenite from Facies A/PVR. 65

30. Intricate Traces of Arthrophycus Exposed as Semi-Relief at the Bases of some Quartzarenite Units within Facies A/PVR. 66

31. Photomicrograph Showing the Representative Petrographic Character of Facies A/PVR. 68

32. Heavily Bioturbated Sandstone of Facies B/PVR. 70

33. Upper Motttled Surface of a Sandstone in Facies B/PVR. . 72

FIGURE PAGE

34. Granule Lag Zones of Phosphatic Lingula Brachiopods and Quartz Granules. 73

35. Photomicrograph Showing the Representative Petrographic Character of Facies B/PVR. 75

36. Shale of Facies C/HS Found Sporadically Interbedded within Facies A/PVR. 76

37. Lower Contact of Facis D/PVR with the Underlying Hagan Shale. 78

38. Upper Contact of Facies D/PVR. 79

39. Sedimentary Structures within the Basal Unit of Facies D/PVR 81

40. A Problematic Gastropod Trace on a Upper Surface of a Sandstone Bed, Facies D/PVR 82

41. Photomicrographs of Thin Sections P1-1 and P2-1 84

42. Paleoenvironmental Comparisons 86

43. Internal Structures of Bouma Sequences 92

44. Evidence for a Paleosol. 93

45. The Characteristic Lateral Progression of Sedimentary Structures Which are Found with Increasing Distance from the Shoreline 102

46. Vertical Sequence of Sedimentary Structure Association within a Single Bed. 103

47. Geometry of Transverse and Longitudinal Bedforms Found on Continental Shelves 118

48. Block Diagram Illustrating the Sequence of Bedforms Generated on a Normal Continental Shelf. 120

49. Changes in Sand Wave Internal Structure Spaced Along a Line of Net Sand Transport-Deposition. 124

50. Regime Diagram of Dune and Sand Wave Internal Structure. 127

FIGURE PAGE

51. Internal Changes of a Ripple During the Four Stages of a Tidal Cycle. 128

52. Complex Internal Structures of Sand Waves with Megaripples Migrating Upon their Slopes. 130

53. Outcrop Sketch of Facies A/PVR 139

54. Conformable Contact Between the Poor Valley Ridge Member of the Clinch Sandstone and Overlying Maroon Mudstone and Shale of the Rose Hill Formation. 153

55. Regional Variation in the Rose Hill Shale. 156

56. Wave and Interference Rippled Upper Bedding Surfaces, Rose Hill Formation. 157

57. Mudcracks in the "lower" Rose Hill Formation 159

58. Cut-Slab of a Rose Hill Siltstone. 161

59. Photomicrograph of Thin-Section P19-A 163

60. Photomicrograph of Thin-Section P22-UA 165

61. Rose Diagram of Paleocurrent Data. 171

62. Summary of Paleocurrent Studies of the Clinch Sandstone and its Stratigraphic Equivalents. 173

63. Summary Model of a Sand Wave Shelf Setting 181

64. Relative Sea-Level Changes Inferred for the Clinch Sandstone 184

CHAPTER I

INTRODUCTION

Background

The Lower Silurian Clinch Sandstone is one of the most prominently exposed ridge forming units in the Valley and Ridge Province of northeastern Tennessee and southwestern Virginia. This quartzarenite is generally white to light yellow-gray and fine- to medium-grained with some lenses and thin beds of conglomeratic sandstone. Major outcrop belts of the Clinch Sandstone occur along Clinch Mountain, Wallen Ridge, Short Mountain, House Mountain, Pine Mountain, Stone Mountain and Powell Mountain, the latter being the area of this study.

Safford (1869) originally named the Clinch Sandstone the Clinch Mountain Group which he described as all the sandstones from the base of the red shale to the base of the overlying black Chattanooga Shale (Devonian). Safford and Killebrew (1900) further described this unit and noted the Clinch Red Shale to be highly calcareous, measuring up to 400 feet thick in some parts of east Tennessee. Safford's Red Shale of the Clinch Mountain Group was later named the Juniata or Sequatchie Formation (Upper Ordovician).

Butts (1933; 1940), working in southwestern Virginia, decided to restrict the term Clinch to Lower Silurian (lower Llandoverian) rocks and assigned the overlying "Middle" Silurian (upper Llandoverian)

strata to the Clinton Formation. Rogers (1953) noted that in strike belts west of Powell Mountain, the classic sandstones of the Clinch grade laterally into an interbedded sandstone and shale sequence which is highly ferruginous and locally fossiliferous. These rocks were named the Rockwood Formation by Hayes (1891) to replace Safford's term Dyestone Group of 1869 (in Milici and Wedow, 1977). The Rockwood Formation was named for exposures near the town of Rockwood, Roane County, Tennessee (Wedow, 1960). The Clinch Sandstone and the Rockwood Formation are contemporaneous lithologies of the Lower and Silurian, and in areas intermediate between the two, they grade laterally into each other (Rodgers, 1953).

Miller and Fuller (1954) divided the Clinch Sandstone into two members, the lower Hagan Shale Member and the overlying Poor Valley Ridge Member. Both names come from northeast of the Rose Hill mining district, in extreme southwestern Virginia. At Hagan, Virginia, the Hagan Shale is composed mainly of nonresistant, green-gray shale with numerous thin silty to sandy beds of limestone. To the east and southeast, the thin limestone grades laterally to calcareous fine-grained sandstone and siltstone. Dennison and Boucot (1974), divided the original Clinch Mountain Group of Safford (1869) into four units. They kept the lower two units of resistant quartzarenite as Clinch Sandstone, however, the upper units contained glauconite, calcite and an abundance of Lower Devonian fossils. These were assigned to the Wildcat Valley Sandstone. Wagner (1980) extended the two member subdivision of the Clinch southwestward from

Clinch Mountain into areas previously mapped as the Rockwood Formation.

On Clinch Mountain, Safford and Killebrew (1900) described the Clinch as a hard, gray sandstone. To the north in southwestern Virginia, Butts (1940) characterized it as a pure quartz sandstone, white to light gray and extremely dense due to silica cementation. According to Rodgers (1953), the Clinch is a thick-bedded to massive, white or lightly iron-stained, nearly pure quartz sandstone with a silica cement. The sand is generally medium, well-sorted and well-rounded. In Lee County, southwestern Virginia, Miller and Brosge (1954) noted that the Hagan is a gray, fissile shale with some thin interbeds of fine-grained sandstone and locally very few beds of thin, impure limestone. The Poor Valley Ridge, however, contains medium-grained, massively bedded sandstone which becomes thinner upward with occasional interbeds of gray shale. Approximately 30 km east of Powell Mountain at Hagan, Virginia, the sandstone shows an increasing amount of sericite and carbonate matrix. Most beds are uniform throughout, but show parallel laminations, cross-bedding or ripple marks (Miller, 1954).

When Safford (1869) first named the Clinch Sandstone, no specific type locality was designated. It was not until the work of Dennison and Boucot (1974) that a type section on Clinch Mountain was finally proposed. An exposure displaying excellent Clinch lithology crops out along Tennessee Route 70 at Little Water Gap, (Kyles Ford quadrangle), Hawkins County, Tennessee. Their measurements indicate a total

thickness of 311 ft (94.8 m). This section was subsequently designated as the type section for the Clinch. Miller (1976) alternately designated a reference section along U.S. Highway 19 at Little Moccasin Gap through Clinch Mountain in southwestern Virginia. This section is eight miles north-northwest of Abingdon, and is located in Washington County (Brumley quadrangle). Miller measured a total thickness of 294 ft (89.6 m).

Purpose

Clastic strata of the Lower and "Middle" Silurian undergo complex changes in lithology, geometry and overall facies patterns in northeastern Tennessee and extreme southwestern Virginia. Several generalized studies and a handful of more detailed analyses deal with the sedimentology of the Clinch. However, little work has been done at Powell Mountain in southwestern Virginia. The purpose of this investigation is to integrate previous accounts of the Clinch Sandstone into a broader synthesis of information, in conjunction with a detailed sedimentologic study of the Silurian outcrop on Powell Mountain, Lee and Scott Counties, Virginia. Objectives include: (1) a detailed lithologic description of the Clinch Sandstone and overlying Rose Hill Formation exposed on Powell Mountain, (2) to reconstruct the paleoenvironments of the Clinch at this location, and (3) a comparison of this data to that of previous studies by re-examining conclusions of Schoner (1985 a,b) and Fisher (1987) who analyzed the sedimentology and sedimentary petrography of the Clinch

Sandstone at several locations along the Clinch Mountain belt in northeastern Tennessee.

The overall goal of this study is to provide additional information to a research program focusing on the broad regional synthesis of paleoenvironments and depositional processes of Lower Silurian rocks which is presently under supervision by Dr. Steven G. Driese, Department of Geological Sciences, The University of Tennessee (see Driese, 1985; 1986 a, b; Driese et al., 1986 a, b; Driese et al. in press).

Stratigraphic Position and Age

The use of the name Clinch Sandstone today is restricted primarily to east Tennessee and southwest Virginia (Fig. 1). In northern Virginia, Pennsylvania, West Virginia and Maryland the Clinch is termed the Tuscarora Formation, (Darton, 1896), after sandstone cropping out in the Tuscarora Mountains of Pennsylvania. There seems to be no general agreement as to the geographic location of the nomenclatural boundary between the Clinch and Tuscarora Sandstones. The James River was used by Cooper (1944) as a dividing line between the two. Butts (1940) preferred to name sandstone south of the 38 degree parallel Clinch, while applying the name Tuscarora to sandstone north of that line. The Clinch Sandstone extends southwestward into east Tennessee where it disappears due to fault truncation, but farther to the south, equivalent beds in Alabama and northwest Georgia are represented by the Red Mountain Formation

Northwest Georgia	East Tennessee (Westerly Belts)	East Tennessee (Easterly Belts)	Southwest Virginia	Central Pennsylvania
Chattanooga Sh. (Dev. - Miss.)	Chattanooga Sh. (Dev. - Miss.)	Wildcat Valley Fm. (Lower Devonian)	Rose Hill Fm. ("Middle" Silurian)	Rose Hill Fm. ("Middle" Silurian)
Red Mountain Fm. (Lower and "Middle" Silurian)	Rockwood Fm. (Lower Silurian)	Clinch Sandstone (Lower Silurian): Poor Valley Ridge Mbr. / Hagan Shale Mbr.	Tuscarora/ Clinch Sandstone (Lower Silurian)	Tuscarora Fm. (Lower Silurian)
Sequatchie Fm. (Upper Ordovician)	Sequatchie Fm. (Upper Ordovician)	Juniata Fm. (Upper Ordovician)	Juniata Fm. (Upper Ordovician)	Juniata Fm. (Upper Ordovician)

Figure 1. Lithologic Correlation of the Clinch Sandstone with some of its Stratigraphic Equivalents in the Appalachian Basin (data from Chowns, 1972; Dennison and Boucot, 1974; Miller, 1976; Milici and Wedow, 1977; Cotter, 1983). Diagram from Fischer (1987).

(Chowns, 1972). In eastern Ohio and parts of Kentucky, the Lower Silurian sandstone thins and finally disappears grading into the Brassfield Limestone (Amsden, 1955). To the east in eastern Pennsylvania and New York, Clinch equivalents pass into a great thickness of quartz pebble conglomerate and sandstone of the lower part of the Shawangunk Conglomerate (Swartz and Swartz, 1930).

Farther to the southwest and west, the Clinch, in combination with the overlying Rose Hill, laterally grades into the Rockwood Formation. This Formation is described in more detail under the section entitled "Previous Studies."

At most localities in northeastern Tennessee and southwestern Virginia, the Clinch Sandstone conformably or disconformably overlies the Upper Ordovician Juniata Formation. The Juniata is principally a dark maroon, non-calcareous shale, siltstone and fine-grained silty sandstone (Butts, 1940). Toward the southeast, the Juniata becomes sandier and of lighter color. In extreme southwestern Virginia, the Juniata grades laterally into the more marine units of the Sequatchie Formation (Hayes, 1974). To the west and southwest, the Sequatchie Formation becomes a light pink, blue and green, argillaceous limestone. According to Rodgers (1953), Dennison and Boucot (1974), and Miller (1976), the Juniata and Sequatchie Formations intergrade laterally with an arbitrary boundary between the two. The Juniata, however, represents the less calcareous, perhaps littoral or even terrestrial phase of the more normal-marine Sequatchie (Rodgers, 1953; Thompson, 1970).

The Rose Hill Formation conformably overlies the Clinch in northeastern Tennessee and southwestern Virginia. Named by Swartz et al. (1923) after exposures at Rose Hill near Cumberland, Maryland, it generally consists of maroon or olive-gray shale with a few beds of fine-grained sandstone, siltstone and isolated hematitic iron ore up to 0.6 meters thick. Locally, it may contain thick quartzarenite beds such as those found in the Clinch (Miller, 1976). The fossils found within the Rose Hill indicate predominantly marine, shallow-shelf conditions (Hayes, 1974). Folk (1960) concluded that these maroon, fine-grained, highly ferruginous sediments were deposited in a calm, moderately deep-water, open-marine and slightly reducing environment with little macroscopic life. Such an environment was probably offshore from a low-relief coastal plain punctuated by large turbid rivers (Folk, 1960).

Due to the paucity of well-preserved body fossils within the Clinch Sandstone (Cooper, 1939), geologic age is based primarily on lateral and vertical stratigraphic relationships. Berry and Boucot (1970) assigned the Tuscarora of Pennsylvania and Virginia to the lower and middle part of the Llandovery Series. At Cumberland Gap, Tennessee, Butts (1940) correlated marine fauna of the Rockwood Formation (offshore Clinch equivalent) to the Brassfield Limestone of Ohio and the Albion Sandstone of New York, both Early Silurian in age. The Clinton guide fossil Pentamerus oblongus was collected from Brassfield strata at Anderson Hill, Tennessee by Milici and Wedow (1977). In Georgia, the Red Mountain Formation has been dated

lower, middle and upper Llandoverian based on brachiopod zonation. Species of Pentamerus and Eocoelia were found at high stratigraphic levels in the Formation (Butts and Gildersleeve, 1948; Berry and Boucot, 1970).

The Sequatchie Formation has yielded some marine fossils placing it in the uppermost Ordovician, (Butts, 1940; Berry and Boucot, 1970). Rodgers (1953) explained that Sequatchie fossils are of Richmond Age, Late Ordovician.

The Rose Hill is designated as the oldest formation in the Clinton Group and directly overlies the Clinch Sandstone (Swartz, 1923). Butts (1940) found trilobites, brachiopods and ostracodes of Clinton Age. Berry and Boucot (1970) assigned the Rose Hill to the uppermost Llandovery. Three fossils of time-stratigraphic importance were recognized by Lampiris (1975). The brachiopod Eocoelia, ostracodes and conodonts place the Rose Hill in Upper Llandovery C_3 through C_6 time (Lampiris, 1975).

Previous Work

Most previous studies of the Silurian terrigenous clastic strata in the Valley and Ridge have been of a reconnaissance nature. It has only been with more recent studies that attempts have been made to determine the paleoenvironments of the Clinch and its stratigraphic equivalents (the Tuscarora Formation in northern Virginia, Pennsylvania, Maryland, and New York; the Rockwood Formation of

eastern Tennessee; and the Red Mountain Formation of northwestern Georgia and Alabama).

The Clinch Sandstone of northeastern Tennessee and southwestern Virginia was first described from a purely lithologic and stratigraphic standpoint (Safford, 1969; Safford and Killebrew, 1900; Butts, 1933, 1940; Cooper, 1939; Rodgers, 1953; Miller and Brosge, 1954; Miller and Fuller, 1954; Dennison and Boucot, 1974; Miller, 1976). In addition, several geologic quadrangle maps were printed by the U.S.G.S. (Harris and Miller, 1958 and 1963). Nicholson (1978) was the first to interpret the paleoenvironments of the Clinch. His regional study included sections from Clinch Mountain, Powell Mountain, Wallen Ridge and Poor Valley Ridge. The Clinch was inferred to have been deposited by the westward progradation of a beach complex and associated subtidal, fluvial and estuarine deposits (Nicholson, 1978). At most outcrop localities, the lower Hagan Shale Member was inferred to represent an eastward marine transgression following the shallow marine deposits of the Sequatchie Formation. The Poor Valley Ridge Member was interpreted as a beach complex followed by another marine transgression.

Studies by Schoner (1985 a, b) involved a more detailed paleoenvironmental interpretation of the Clinch Sandstone at Beans Gap, Clinch Mountain, Tennessee. The lower part of the Hagan Shale Member with its extremely fine-grained lithology, was interpreted as a transgressive sequence in which rapid deepening occured. This basal lithology was followed by a shoaling-upward trend within the Hagan.

This trend is represented by a constant upward increase in grain-size, bed thickness, large-scale sedimentary structures, and bioturbation by suspension-feeders (Schoner, 1985). Deposition of the Poor Valley Ridge Member was believed to have been initiated by an uplift in the source area (the Taconic Highlands) which caused a progradation of the shoreline. As a result, an extensive barrier system including shoreface, lagoonal and tidal channels covered the earlier Hagan lithology resulting in the coarse-grained, Poor Valley Ridge Member of the Clinch Sandstone. Unimodal paleocurrents were inferred to represent a strong ebb tidal flow (see also Driese et al., 1986 a).

Another detailed sedimentological investigation of the Clinch Sandstone was by Fischer (1987) who studied outcrops along Clinch Mountain, northeastern Tennessee. He interpreted the strata of the Hagan Shale to represent deposition within a back-barrier lagoonal setting. The barrier may have developed in response to transgression during Early Silurian time (Fischer, 1987). An abrupt change in texture and mineralogy was recognized at the contact of the overlying Poor Valley Ridge Sandstone. These upper units are not only coarser-grained, but also contain virtually no detrital feldspar. The absence of feldspar may have been produced by preferential sorting in the high energy paleoenvironments during Poor Valley Ridge deposition, or as Fischer postulates, may be the result of differing source areas for Hagan and Poor Valley Ridge sands. The foreign sands of the Poor Valley Ridge may have been introduced into northeastern Tennessee by

southward advancing sandlobes from a northern Virginia depocenter. Despite the mineralogical problem of Poor Valley Ridge Sandstone, Fischer interpreted them to have been deposited in a combined storm- and tide-dominated, sand-ridge shelf setting. He postulated two modern analogs, the North Sea and the North American Atlantic Shelf.

Other studies deal with the Tuscarora Formation, a Clinch Sandstone stratigraphic equivalent found in Pennsylvania, northern Virginia, parts of New York and Maryland. Its petrography and sedimentology have been discussed in great detail.

Folk (1960) inferred the origin of the Tuscarora with overlying Rose Hill and Keefer Formations largely from a petrographic standpoint. By dividing the Tuscarora of eastern West Virginia into two facies, Folk concluded that the lower subgraywacke to graywacke was deposited in a submerged deltaic-estuarine environment, and the upper supermature orthoquartzite deposited as a beach sand. The source area for the Tuscarora sediments consisted largely of older sedimentary and low-rank metamorphic rocks to the southeast. As erosion proceeded to Rose Hill and Keefer time, these older source sedimentary rocks were stripped off as underlying plutonic material became increasingly important (Folk, 1960). The Rose Hill Formation was believed to have been deposited in an open-marine, brackish-water environment.

In the Central Appalachians, Yeakel (1962) mapped sediment dispersal patterns in the Tuscarora and Upper Ordovician Bald Eagle Formations. After measuring regional variations in cross-bedding,

thickness, lithofacies, fossil data and maximum pebble-size, Yeakel concluded that the Tuscarora was deposited by largely fluvial processes. Isopach maps suggested that two major depocenters merge to form a large detrital apron decreasing in thickness to the northwest, west and southwest. On this northwesterly-inclined paleoslope, conglomerate deposition dominated in the east whereas finer-grained marine sediments were laid down in what is now western Ohio, West Virginia, and Kentucky.

Diecchio (1973) studied the paleoenvironmental significance of ichnofacies within the Tuscarora, Rose Hill and Keefer Formations. Working in the Appalachian Basin of West Virginia and Virginia, Diecchio envisioned a fluvial origin for the Tuscarora sandstone. Fluvial sands became more marine to the northwest (basinward), and formed a delta in the vicinity of Eagle Rock, Virginia. A subsequent transgression of the Rose Hill sea resulted in marine deposition over the entire area (Diecchio, 1973). Overlying Keefer Sandstone strata were believed to have been deposited in a beach or barrier island environment.

In southwestern Virginia, Hayes (1974) recognized shoreface, barrier, lagoon, tidal flat and coastal plain facies in the Tuscarora. The whole marginal marine sequence prograded seaward during its early history but stalled during a transgressive phase leading to the deposition of the overlying nearshore marine, Rose Hill shales (Hayes, 1974). Hayes also recognized a northeast-southwest trending source with a northwest-dipping paleoslope.

The stratigraphy of the Rose Hill and Keefer Formations in central western Virginia and adjacent West Virginia was investigated by Lampiris (1975). In general agreement with earlier workers, he concluded that the Tuscarora was deposited mainly by fluvial processes. Lampiris, however, focused primarily on the paleoenvironments of the Rose Hill and Keefer Formations.

Whisonant (1977) studied the dispersal patterns of the Tuscarora in western Virginia. Again, a northwest-dipping paleoslope feeding on an eastern linear source area was confirmed. Whisonant recognized several features which suggested highly variable flow conditions such as would be expected in fluvial deposits.

Cotter (1983 a, b) analyzed the paleoenvironments of the Tuscarora and Clinton Formation in Pennsylvania. In the earliest Silurian, a glacioeustatic sea-level rise accompanied by uplift of the Taconic source terrain led to clastic deposition on an eastward retrograding (transgressing) shoreline (Cotter, 1983). It was postulated that braided alluvial streams carried sediment northwestward off alluvial fan complexes located in the east. After transport across coastal alluvial plains, sediment was deposited along the beach-strandplain and subsequently moved offshore by storms and then fashioned into shelf sand wave complexes.

The Rockwood Formation of eastern Tennessee and the Red Mountain Formation of northwestern Georgia are additional facies equivalents of the Clinch Sandstone (Fig. 1, p. 6). The Lower Silurian Rockwood Formation (Driese, 1985, 1986; Driese et al., 1968 a, b;

Easthouse, 1987) is interpreted as a subtidal, shallow marine deposit. Easthouse (1987) conducted a paleoenvironmental interpretation of the Rockwood at Green Gap, Whiteoak Mountain, southeastern Tennessee. Deposition was inferred to have taken place above and below fairweather wave-base. Nearshore on the shelf, mega-rippled and rippled sand shoals were deposited above fairweather wave base. This environment was characterized by fairweather and storm wave flows with conditions favorable for the concentration of iron (Easthouse, 1987). Below fairweather wave base, deposition was interpreted to have taken place in quiet oxygen-limiting environments experiencing only occasional effects of storms.

The Red Mountain Formation, the Clinch equivalent in Georgia and Alabama, has been more extensively studied. Sandin (1960) inferred deposition to have taken place in a shallow marine epicontinental sea frequented by turbidity currents and other gravity phenomena. In Alabama, Sheldon (1970) interpreted the Red Mountain Formation to represent lagoonal, barrier island, and nearshore marine deposits. Chowns (1972) concluded that in Georgia, a wide range of sedimentary environments ranging from littoral (lagoon and barrier) to open marine (platform and slope) were responsible for Red Mountain deposition. All the environments comprise a large molasse wedge of clastic sediment which migrated to the west as material was deposited seawards down the promolasse slope (Chowns, 1972).

Study Area

The area of investigation is along U.S. Highway 58 at the crest of Powell Mountain, Lee and Scott Counties southwestern Virginia (Fig. 2). This site is found on the Duffield and Stickleyville 7½' quadrangles and is located at 36°42'30" north latitude by 82°52'15" west longitude. Powell Mountain is one of the northeast to southwest trending linear ridges within the Valley and Ridge Physiographic Province (Raisz, 1957).

The section studied is along a roadcut orientated east-west that exposes the (Upper Ordovician) Juniata Formation, the (Lower Silurian) Clinch Sandstone, and the Late Silurian Rose Hill Formation. Excellent exposures with several additional bench-cuts were studied on both sides of the road (Fig. 3). The south wall consists of the entire Juniata Formation, in addition to the Hagan Shale (23.25 meters) and Poor Valley Ridge Members of the Clinch Sandstone. Only the first two meters of the overlying Rose Hill are exposed due to erosion along the ridge crest. These north-facing cliffs are relatively unweathered but extremely unstable, commonly yielding to downslope movement.

On the north side of the road, the upper four meters of the Hagan, the entire Poor Valley Ridge (27.85 meters) and 17.40 meters of the overlying Rose Hill Formation are exposed. These south facing lithologies are more weathered resulting in the enhancement of bedding surfaces and internal sedimentary structures within the sandstones.

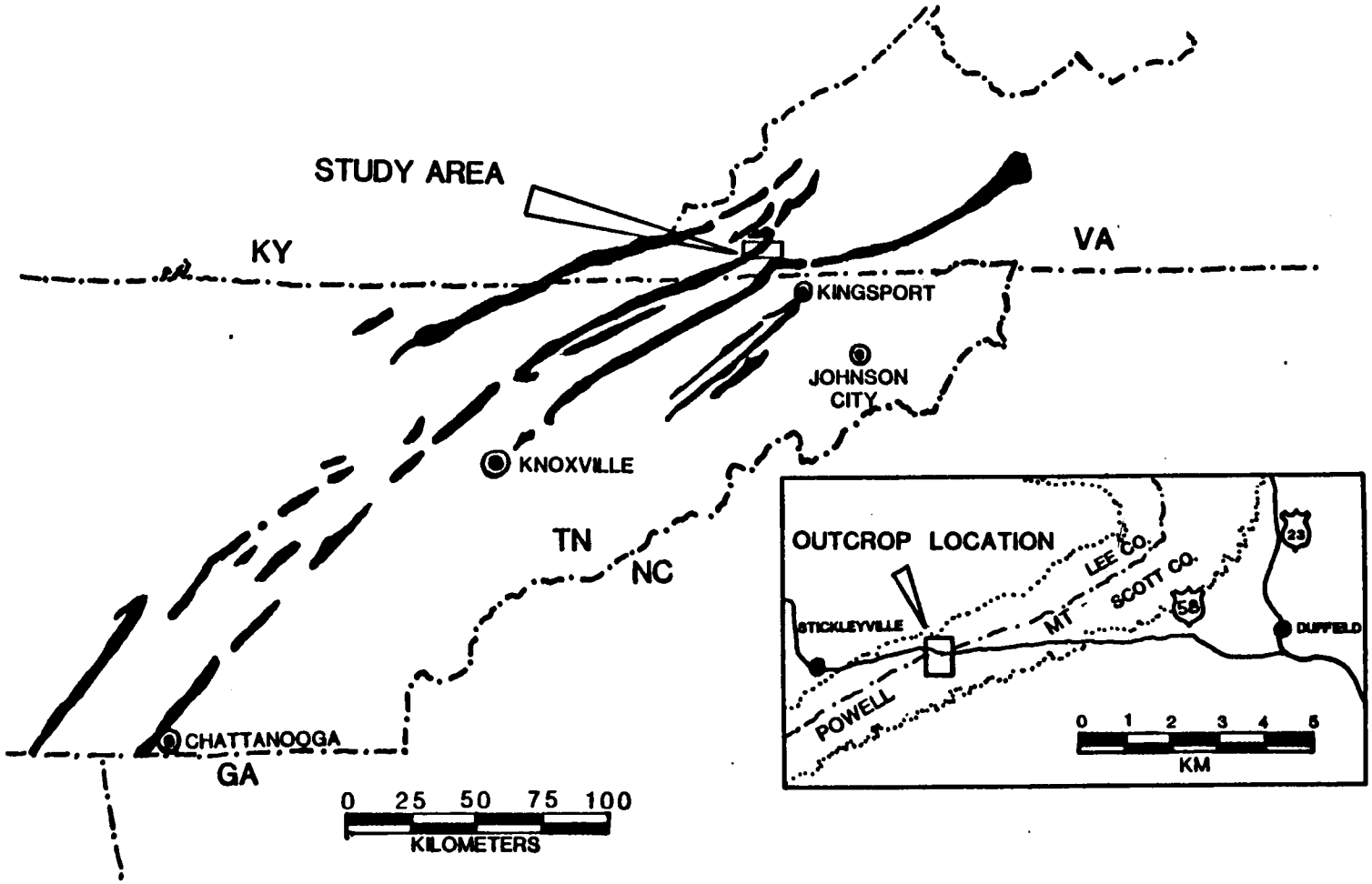


Figure 2. Location of Clinch Rocks at Powell Mountain, Lee and Scott Counties, Southwestern Virginia.

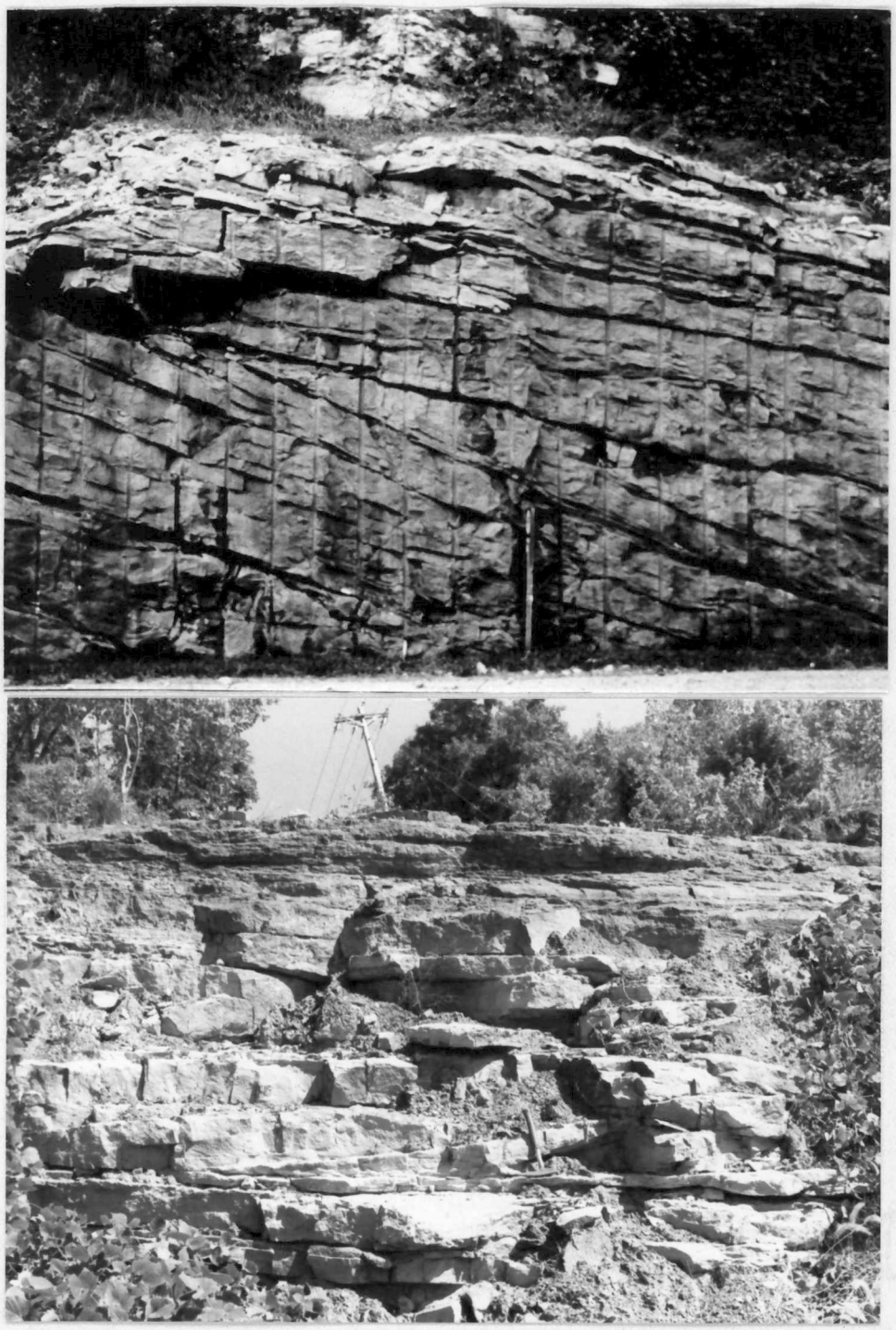


Figure 3. The Silurian Strata at the Crest of Powell Mountain, southwestern Virginia. Upper photo: shows the roadcut on the south side of State Route 58 exposing both members of the Clinch Sandstone along with underlying Ordovician rocks (to the right of the photo). The lower photo: shows the north exposure containing the Clinch and Rose Hill Formations.

Several dip-slopes developed especially within the Rose Hill Formation enabled the examination of upper bedding surfaces.

Methods

The preliminary field investigation, from July through October, 1986 consisted of measuring and describing the entire Silurian outcrop at Powell Mountain, southwestern Virginia. Cross-bedding, ripple marks and other types of primary sedimentary structures were observed and recorded. Body fossils and ichnofossils were collected, categorized and compared with primary sedimentary structures in order to relate biologic, lithologic and physical changes in the environment. A graphic log was constructed in the field. Measured and described sections are in Appendix I.

Chips were broken from the rock at approximately one-half meter intervals within vertically consistent units or at distinct changes in lithology. Estimates of mean grain-size were made through a hand lens and compared to a grain-size chart. In addition, estimates were made of textural maturity, friability, density and the effects of diagenesis.

Hand specimens were systematically collected at one meter intervals or at distinctive lithologies with the intent of studying the variability within each member. The collected rocks were later slabbed and polished in the laboratory yielding 90 finished hand specimens and 35 thin sections. Hand specimens were described and compared with field data.

Thin sections were examined megascopically and petrographically. Point-counting was performed on 17 thin sections with 350 grains-counted per slide. Other features including grain-shape, grain-size, fabric, sorting and diagenetic alterations were also noted. Grain-size was accurately measured and compared with field measurements. Petrographic descriptions and modal percentages are listed in Appendix II.

Paleocurrent orientation data were collected in both members of the Clinch Sandstone and the overlying Rose Hill Formation. The 93 measurements were later corrected for regional dip and plunge using the Schmidt equal-area stereonet. Circular and spherical statistics were calculated and together with the vector data, were plotted on Rose diagrams for comparisons with other observations.

Although each change in composition, texture, color and bedding was described and recorded as a separate unit, lithologies were grouped into facies. Based on recurring associations of similar rock type, sedimentary structures and texture, separate facies were related to one another and then incorporated into a paleoenvironmental scheme of depositional history.

CHAPTER II

FACIES DESCRIPTION

Introduction

The delineation of the Silurian rocks at Powell Mountain into lithofacies was made according to the criteria set forth by Walker (1984). Distinctive combinations of lithology, bedding geometry, texture, biological features, mineral content and physical sedimentary structures were analyzed both in the field and laboratory. The scale of subdivision used by this author was governed by the objectives of this study, the time available and the abundance of physical and biological structures in the rocks.

For additional information not included in this chapter, a more detailed lithological description is presented in Appendix I, and a complete petrographic description for 35 thin sections is given in Appendix II.

The Hagan Shale Member

General

The Hagan Shale Member of the Clinch Sandstone conformably overlies the Upper Ordovician Juniata Formation at Powell Mountain. The interbedded shale, sandstone and wackestone/packstone is divided into four facies based on the aforementioned criteria. Figure 4 presents a generalized stratigraphic section of the Powell Mountain

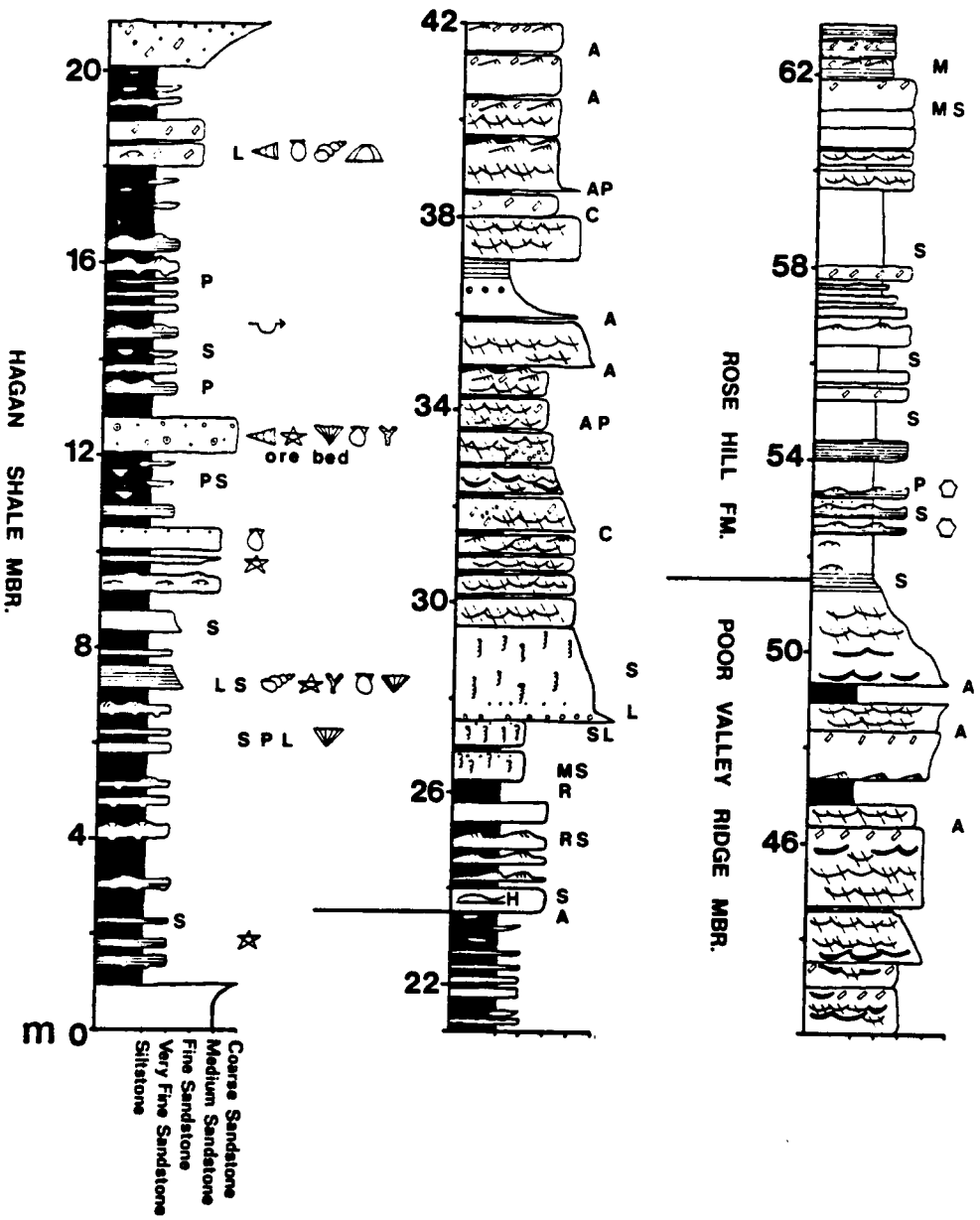


Figure 4. Generalized Stratigraphic Section of the Clinch Sandstone and Rose Hill Formations at Powell Mountain, Southwestern Virginia. Key to symbols shown in Figure 5.

outcrop, and a detailed measured section is described in Appendix I. Figure 5 lists a key to the symbols used in the stratigraphic column. Figure 6 summarizes the lithology, sedimentary structures and distinguishing characteristics of each of the facies found within the Hagan Shale.

Facies A/HS Basal Sandstone

The basal unit of the Hagan Shale is assigned to Facies A/HS which conformably overlies the subaerially exposed, tidal-flat deposits of the Juniata Formation and underlies sub-facies B2/HS of the Hagan Shale. In general, the rocks of this facies can be sub-divided into calcareous quartzarenite, siltstone and shale.

At the base of the Hagan Shale Member occurs a dense, calcareous, quartzarenite bed measuring 0.3 meters thick (Fig. 7). This unit is medium-gray but weathers to a light red-brown-gray. The overlying interbedded thin sandstone units (0.6 meters) are similar in lithology and color to the basal sandstone. The mudstone between all sandstone/siltstone units is medium- to dark-gray and slightly fissile to blocky.

The dominant sedimentary structures in the basal sandstone are horizontal laminations and possible small-scale trough cross-stratification, although the latter is extremely hard to recognize due to heavy diagenetic alteration. Parallel laminations are rare in the overlying thin sandstone units which are massive or normally graded. Near the Juniata/Hagan Shale Member contact,

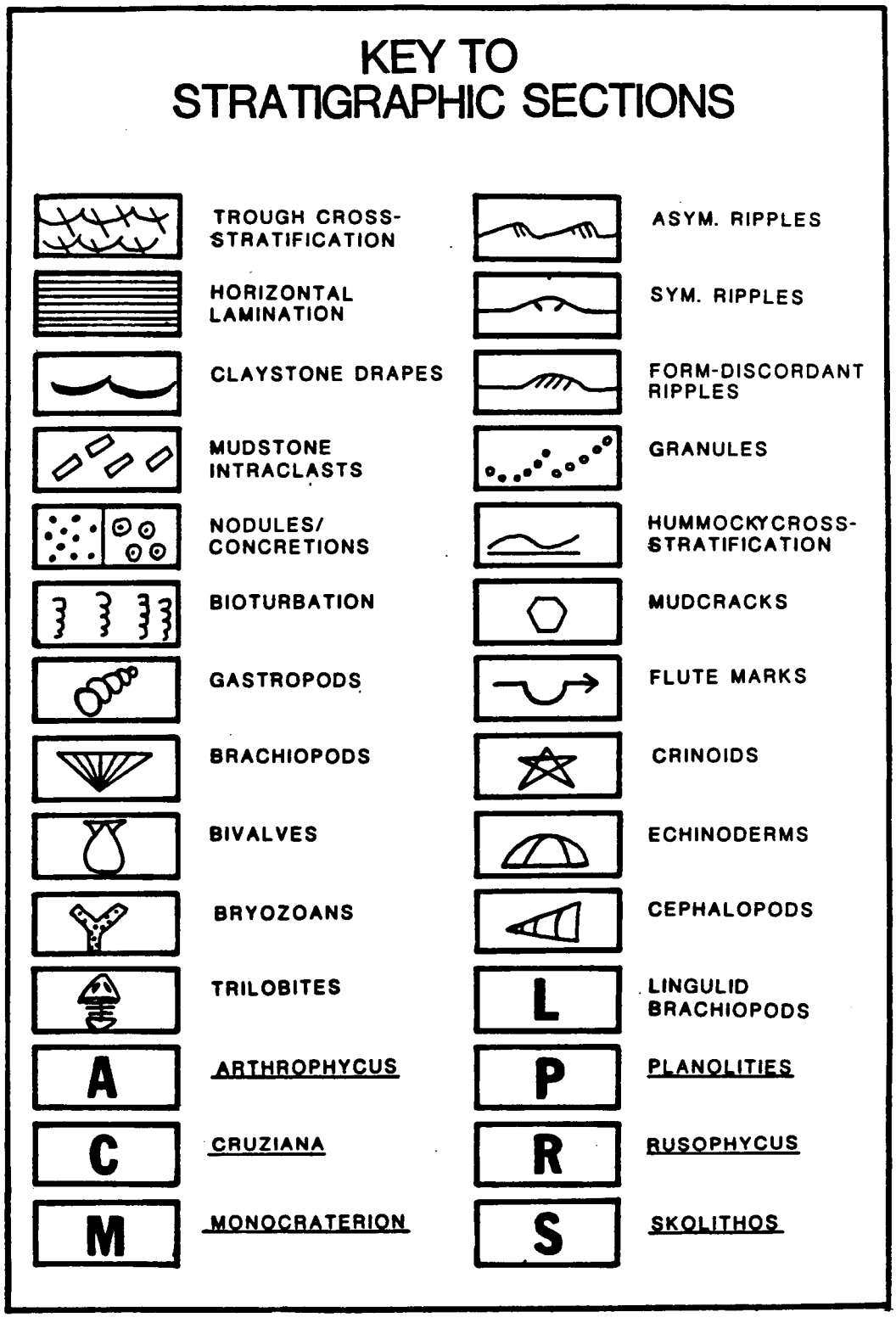


Figure 5. Key to Symbols Used in the Stratigraphic Section (Figure 4).

Facies	Lithology	Sedimentary Structures	Other
A/HS-Basal Hagan	-Interbedded sandstone siltstone -Thick basal unit of calcareous quartzarenite	-Horizontal laminations (basal unit) -Inverse grading (basal unit) -Massive bedding (upper units) -Rare wave ripples (near Juniata contact)	-Skolithos (upper units) -Fragmented brachiopod debris
B/HS-Interbedded Sandstone and Shale			
B1/HS	-Interbedded quartzarenite, calcareous quartzarenite and shale	-Horizontal laminations -Wave ripples -Form-discordant wave ripples -Rare current ripples -Extremely rare micro-hummocky cross laminations.	-Rare Skolithos -Rare Planolites -Rare echinoderm debris -Units more laterally persistant than in sub-facies B2/HS
B2/HS	-Interbedded wackestone/packstone calcareous quartzarenite and shale	-Horizontal laminations -Current ripples -Form-discordant wave -Graded bedding -Massive bedding -Gutter casts	-Rare Skolithos -Rare Planolites -A wide array of fragmented body fossils -Units commonly pinchout, lenticular bedding common

Figure 6. Brief Description of Facies in the Hagan Shale.

Facies	Lithology	Sedimentary Structures	Other
C/HS-Shale	-Shale	-Rare gutter casts -Rare flat-lens lenticular bedding	-Rare Skolithos -Rare Planolites -Rare horizons of fragmented body fossils
D/HS-Isolated Quartzarenite and Iron-Rich Packstone	-Ferruginous bryozoan packstone -Fossiliferous quartzarenite -Ferruginous sandstone conglomerate	-Horizontal laminations -Rare trough cross-stratification -Graded bedding	-Abundant body fossils -Heavy iron mineralization -Units are isolated and pinchout laterally.

Figure 6 (continued)



Figure 7. Facies A/HS, the Basal Sandstone Bed of the Hagan Shale. Rocks below the contact (hammer tip) comprise the Upper Ordovician Juniata Formation. (Hammer for scale.)

isolated wave ripples (height = 2 cm, wavelength = 7.5 cm) occur in rare instances. Wave ripple lamination was also found in some areas in the overlying thin bedded sandstone. Inverse grading occurs in the basal sandstone (top 2 cm) as a thin lag deposit of reworked material. The lag is composed of coarse quartz grains, glauconite pellets, hematite-replaced skeletal debris and phosphate grains.

Discontinuous vertical burrows of Skolithos (measuring up to 0.8 cm in diameter) occur in a few layers within the overlying thinly bedded sandstone and siltstone units. The burrows are slightly oblique to bedding and are vertically continuous for only a few cm. The underlying basal sandstone unit contains no trace fossils; however, fragmented brachiopod shells aligned parallel to bedding occur in the overlying thin bedded sandstone.

As mentioned earlier, thickness of the basal calcareous quartzarenite measures 0.3 m and is laterally persistent over several tens of m along the outcrop face. The lower contact of this unit is planar, but transitional over 3 cm with the underlying Juniata Formation. The overlying thinly bedded sandstone and siltstone average 2 cm thick and pinch-out laterally over 5-9 m. Bedding contacts are planar to wavy and somewhat diffuse.

Thin-sections BH-1 and BH-2 represent the petrographic sample suite of sub-facies A/HS. Sample BH-1 was taken from the lowermost unit of the Hagan at the contact with the underlying Juniata Formation (Fig. 8). This sample is extremely fine-grained with large amounts

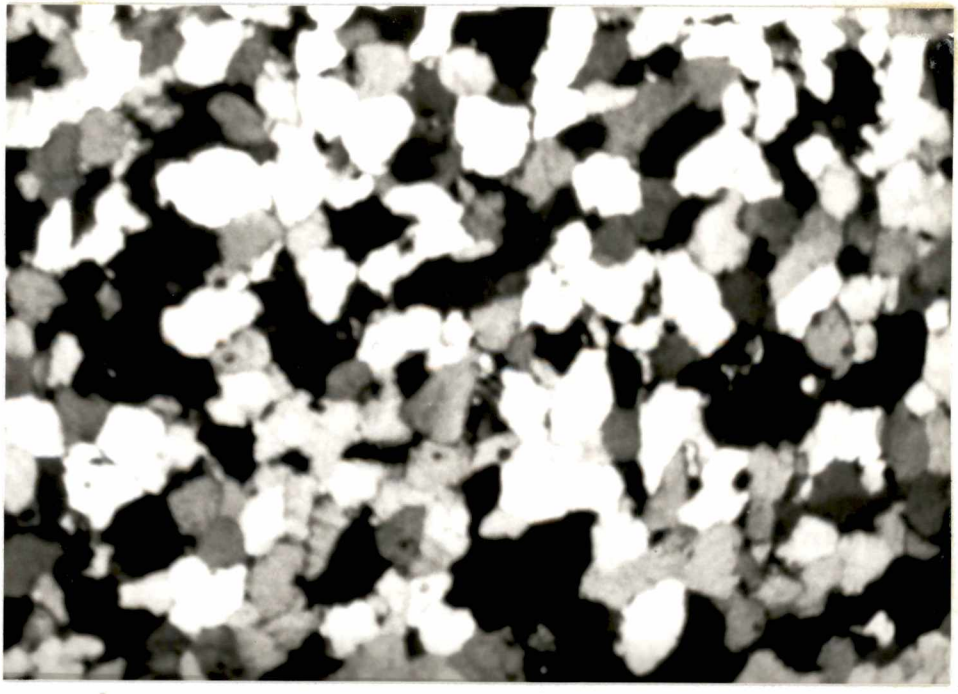


Figure 8. Photomicrograph of the Basal Sandstone Unit, Facies A/HS, Lowermost Hagan Shale. Field of view from left to right is approximately 2 mm.

of carbonate cementation (see Appendix II). The rock is well sorted, mature and is classified as a calcareous quartzarenite. Of the total modal analysis, framework quartz content is extremely low (54 percent) with grains subangular and showing low sphericity. Other framework minerals include plagioclase, microcline, orthoclase and opaques. Muscovite, chlorite, tourmaline and zircon occur as trace amounts. Calcite cement (32 percent) occurs as large, amorphous poikilotopic crystals between framework grains. Thin-section BH-2 was sampled from a thin sandstone unit within the overlying interbedded lithology of A/HS. This slide shows a similar mineralogy to BH-1, although grains are larger and less well-sorted. In addition, a variety of sedimentary rock fragments, fragmented brachiopod shells and minor amounts of phosphate and glauconite were observed.

Facies B/HS-Interbedded Sandstone and Shale

Facies B/HS, a heterolithic interbedded sandstone and shale, comprises the majority of the Hagan Shale Member at the crest of Powell Mountain, Virginia. This facies is further divided into two sub-facies, B1/HS and B2/HS. Although hard to detect, the delineation of these two sub-facies is based primarily on subtle differences in primary sedimentary structures, fossil content, thickness, and mineralogical composition of the sandstone beds.

Sub-facies B1/HS

The interbedded sandstone and shale assigned to sub-facies B1/HS occurs predominantly near the base of the Hagan Shale Member at Powell

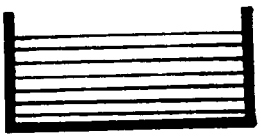
Mountain. Underlying this sequence of rocks is the basal sandstone of Facies A/HS. Overlying and partly intercalated with this sequence is sub-facies B2/HS occuring in the middle and upper parts of the Hagan Shale.

Sub-facies B1/HS consists of interbedded, calcareous quartzarenite and featureless shale (Fig. 9). The shale is generally medium-to dark-gray, fissile to blocky and contains only very sparse trace fossils of Planolites (8 mm in diameter) and Skolithos (4-8 mm in diameter). The quartzarenite is generally light to medium gray, weathers to a light maroon-gray and is very fine-grained. (See Appendix I for more complete descriptions.)

The dominant sedimentary structures in sub-facies B1/HS are horizontal laminations, wave-ripple marks and laminations, wavy-parallel horizontal laminations, form-discordant wave ripples and extremely rare current-ripple crests and laminations. Several combinations of these structures commonly occur as stacked associations within a single bed (Fig. 10). Two of the more common bedding sequences observed in sub-facies B1/HS are as follow: (1) sharp-based, planar beds → horizontal laminations → wave ripple cross-laminations or rippled upper surfaces with no visible internal stratification (Fig. 10), and (2) sharp-based, planar beds → horizontal laminations or non-parallel, discontinuous horizontal laminations → form-discordant wave ripples → capping shale. Graded beds are present, although not as abundant as in



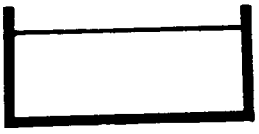
Figure 9. Interbedded Lithology of Sub-Facies B1/HS. Notice the sharp, flat bases of units and horizontal laminations. (Hammer for scale).



QUENCE 1
Horizontal laminations trending throughout the entire unit.



SEQUENCE 2
Horizontal laminations overlain by wave ripples.



SEQUENCE 3
Massive or structureless unit.



SEQUENCE 4
Horizontal laminations overlain by form-discordant wave ripples.



SEQUENCE 5
Non-parallel-discontinuous horizontal laminations.



SEQUENCE 6
Horizontal laminations overlain by rare current ripples.

Figure 10. Sedimentary Structures within Sub-facies B1/HS. Sequences are listed in order of decreasing abundance.

sub-facies B2/HS. Sole markings (flutes, grooves, and tool marks) were found in only one thin sandstone bed occuring at 7.25 meters above the base of the Hagan.

The amount of biogenic reworking overall within sub-facies B1/HS is low compared to other facies in the Clinch Sandstone. Trace fossils found within the intervening shale are discussed above. Sandstone of this sequence shows rare vertical burrows of Skolithos (4-8 mm in diameter) disrupting internal laminations, in addition to semi-flattened horizontal cylinders of Planolites occuring as sinuous trails at the bases of beds. There is also a general paucity of body fossils in this heterolithic sequence. Rare crinoid columnals were found in only two samples. Petrographic examination revealed very limited occurrences of fragmented trilobite and echinoderm debris in several sandstone units.

Bedding geometry shows little change throughout the entire thickness of sub-facies B1/HS. Generally, the strata are thinly bedded with thicknesses of sandstone layers ranging from 2-8 cm. Lower and upper bedding surfaces exhibit ripple marks. Most beds show a consistent lateral thickness which is traceable over the entire outcrop extent.

Thin-sections UH2-3, UH2-5 and UH5-5 represent the petrographic sample suite of sub-facies B1/HS. These rocks are dominantly very fine-grained (in some cases silt), well-sorted, horizontally laminated, calcareous quartzarenite (Fig. 11). Of the total modal analysis, framework quartz content is extremely low (as little as 60

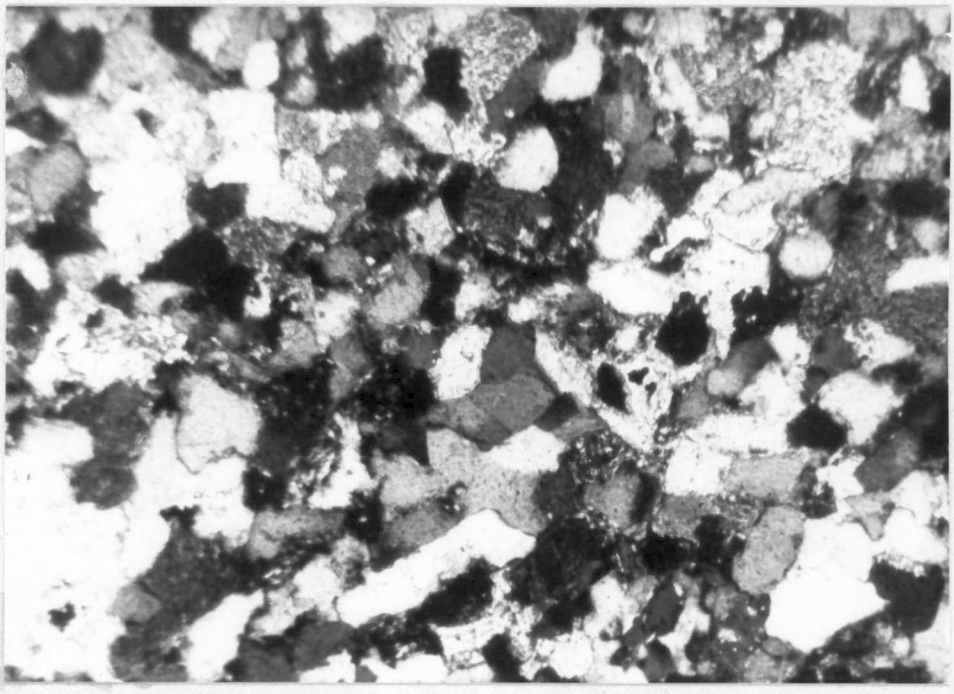


Figure 11. Photomicrograph of Sample UH2-5. Thin section exhibits the representative petrographic character of sub-facies B1/HS. Field of view from left to right is approximately 2 mm.

percent) with grains subangular and showing low sphericity. The monocrystalline quartz variety dominates. Other framework minerals include: chert fragments, opaques, plagioclase, microcline and orthoclase. Muscovite, biotite, chlorite, glauconite, tourmaline and zircon are present in trace amounts. Interstitial matrix material consists of extremely fine-grained opaques, phyllosilicates and quartz (fine silt). Cementing agents, which may constitute up to 30 volume percent, include calcite, dolomite, and silica in decreasing order of abundance. Calcite cement may occur in rather large masses or in combination with rare skeletal debris (echinoderm) which is preferentially located along horizontal laminations. The fabric of these samples is tightly packed; recrystallized quartz forms an interlocking mosaic, precluding the recognition of specific quartz types. (See Appendix II for more complete descriptions.)

Sub-facies B2/HS

Strata assigned to the thinly interbedded sandstone and shale of sub-facies B2/HS occur predominantly in the middle and the top of the Hagan Shale Member. Underlying and gradational with this sequence is the more thickly interbedded sandstone and shale of sub-facies B1/HS (previously discussed). Two additional facies in the Hagan (C/HS and D/HS) are found interbedded within B2/HS. The Poor Valley Ridge Member of the Clinch Sandstone conformably overlies this sub-facies.

Sub-facies B2/HS is a thinly interbedded wackestone/packstone and calcareous quartzarenite with generally featureless shale (Fig. 12).



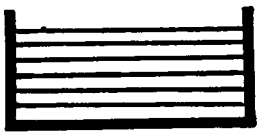
Figure 12. The Interbedded Wackestone/Packstone and Calcareous Quartzarenite of Sub-Facies B2/HS. Note lenticular nature of some units. (Hammer for scale.)

The shale is medium to dark maroon-gray, fissile to blocky and contains some trace fossils of Planolites (various dimensions) and Skolithos (generally 4-8 mm in diameter). Bioturbation within the intervening shale is more extensive here than in sub-facies B1/HS. The wackestone/packstone and calcareous quartzarenite strata are light to medium gray, but also weathering to a light maroon-gray and are very fine-grained. (For a more detailed description, see Appendix I).

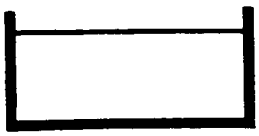
Primary sedimentary structures in sub-facies B2/HS are as complex and varied as in the first sub-facies showing both single occurrences and stacked associations. As was the case for sub-facies B1/HS, horizontal laminations are the dominant feature, however, current-ripple marked upper surfaces and structureless beds are more common in this facies. Also found in greater abundance than in the first sub-facies are form-discordant wave ripples and graded beds (Fig. 13). Two of the more common bedding sequences observed in sub-facies B2/HS are as follow: (1) sharp or scoured bases ⟶ normal grading of fine skeletal debris ⟶ horizontal laminations ⟶ current ripple cross-laminations or rippled upper surfaces with no visible internal stratification, and (less common), (2) sharp or scoured bases ⟶ horizontal laminations ⟶ form-discordant wave ripples ⟶ capping shale (Fig. 14). Soles of beds commonly exhibit scour and gutter casts but rarely display load casts and flute and groove cuts. Gutter casts are abundant in sub-facies B2/HS and commonly occur as isolated features surrounded by mudstone (analogous to starved ripples).



Figure 13. Cut-Slab from Sub-Facies B2/HS. Sample shows graded bedding overlain by horizontal laminations and form-discordant wave ripples. Marks on scale equal 1 cm.



SEQUENCE 1
Horizontal laminations trending throughout the entire unit.



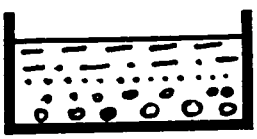
SEQUENCE 2
Massive or structureless unit.



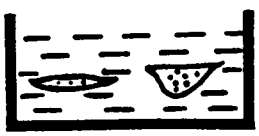
SEQUENCE 3
Horizontal laminations overlain by form-discordant wave ripples.



SEQUENCE 4
Horizontal laminations overlain by current ripples.



SEQUENCE 5
Graded bedding.



SEQUENCE 6
Lenticular bedding and gutter casts.



SEQUENCE 7
Wavy-parallel horizontal laminations (not to be confused with HCS).

Figure 14. Sedimentary Structures within Sub-facies B2/HS. Sequences are listed in order of decreasing abundance.

However, gutter casts are also associated with thin (1-2 cm) sandstone beds, lenticular bedding, or found with much thicker sandstone units (>2 cm). Internal structures show horizontal laminations and low-angle cross-laminations but are more commonly featureless (Fig. 15).

Although the amount of biogenic reworking in sub-facies B2/HS is greater than in B1/HS, it is still very low. Trace fossils found within the interbedded shales are discussed above. Sandstone and wackestone/packstone units may exhibit semi-flattened, horizontal cylinders of Planolites (up to 17 mm in diameter) occuring as sinuous trails at the bases of beds. Skolithos (4 to 8 mm in diameter) and a small problematic vertical burrow (3 mm in diameter, up to 40 mm in length) are also found within these units. Body fossils are more abundant in this sub-facies and are commonly found fragmented. Fossils are concentrated within lag zones and graded intervals in the wackestone/packstone units. Trilobites, bryozoans, brachiopods, rare bivalves, gastropods and echinoderm fragments were observed in the field.

Bedding geometry of this sub-facies shows a slight vertical change from thin units (1.5 cm-5 cm) near the base, to extremely thin (<2 cm), wavy or lenticular beds near the top (Fig. 16). Basal scours and gutter casts are also more common in the middle and upper portions of B2/HS. However, several individual upward-thickening sandstone packages were found near the base of B2/HS. Beds within these sequences average 0.5 cm at the bottom and



Figure 15. Gutter Casts Showing Internal Structures in Sub-Facies B2/HS. Note internal laminations within the lower gutter cast. (Coin for scale.)

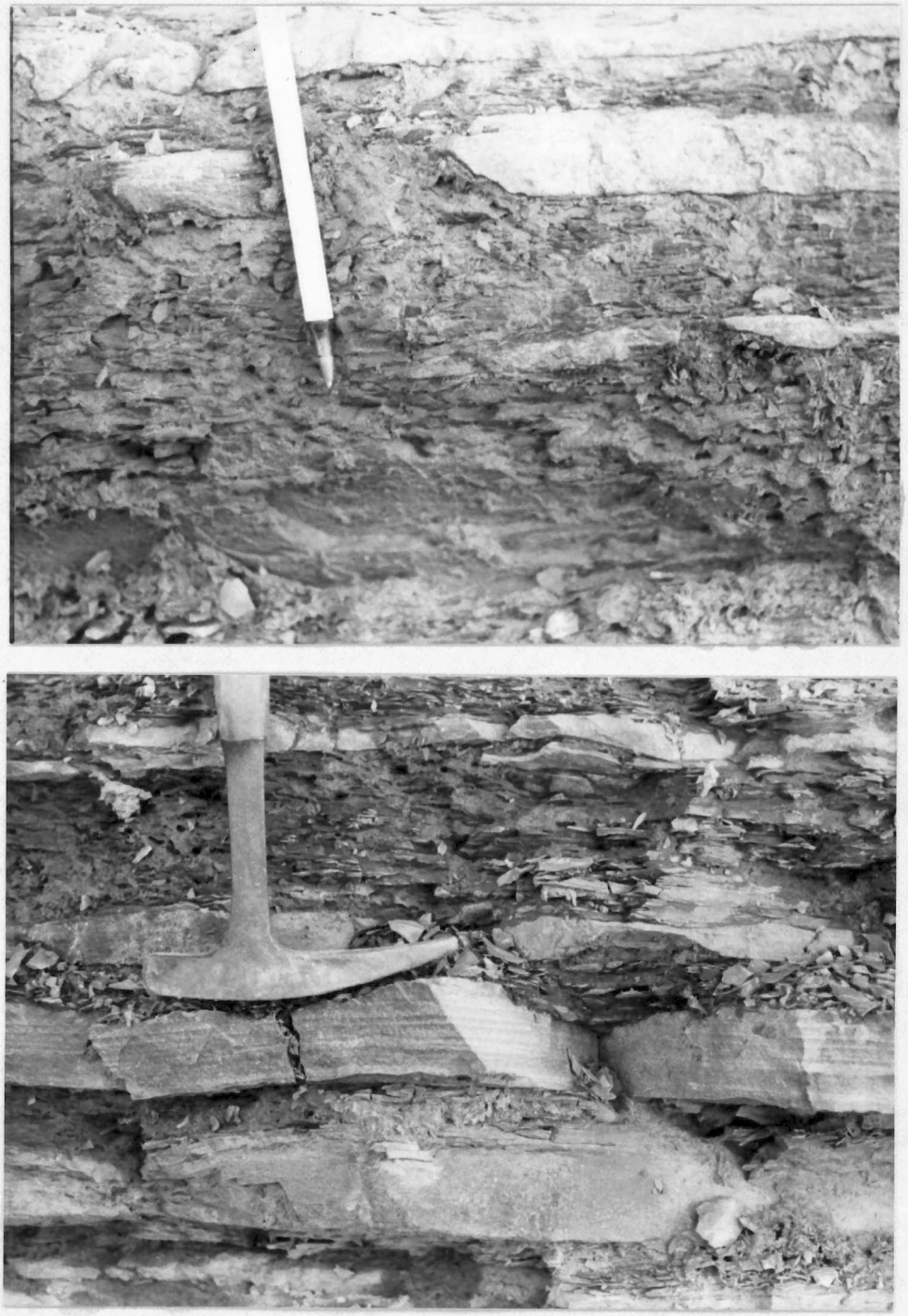


Figure 16. Bedding Geometry of Sub-Facies B2/HS. Upper photo shows the thin, wavy and lenticular bedding of upper B2/HS contrasting with more laterally continuous bedding of lower B2/HS (lower photo). Note the pinch-out of the packstone unit at the pen tip (upper photo). (Pen and hammer for scale.)

increase upward to 5 cm in width. Most units in B2/HS show an inconsistent lateral thickness, many of which pinch-out in one direction (predominantly west) or both directions (east-west). Upper and lower bedding surfaces are generally sharp/wavy.

Thin-sections UH5-7A,B; UH5-8; UH5-10; UH6-13 and UH11-1 constitute the petrographic sample suite of sub-facies B2/HS (see Appendix II). The calcareous quartzarenite beds are very fine-grained (in some cases silt), moderately to well-sorted and sporadically iron-stained. Limestone within this sub-facies was petrographically classified as quartz-rich, fossiliferous biosparite using Folk's classification scheme. Fossils are highly fragmented, poorly sorted and show staining by hematite and/or limonite (Fig. 17). Modal analysis of the quartzarenite shows a higher quartz percentage than for the sandstone strata of sub-facies B1/HS. Grains are generally monocrystalline, subangular and low in sphericity. Sedimentary rock fragments, feldspars, opaques and fossils (echinoderm and trilobite debris) make up other dominant framework grains. Feldspars show little alteration. Trace constituents include chert, chlorite, muscovite, biotite, glauconite and zircon. Matrix material consists of fine-grained opaques, hematite and phyllosilicates between framework grains. Calcite, dolomite, hematite and silica are the major cementing agents. Heavy recrystallization of quartz forms a tight, interlocking fabric which precluded the identification of specific quartz types. Petrographically, major differences between these rocks and the sandstone of sub-facies B1/HS are the higher

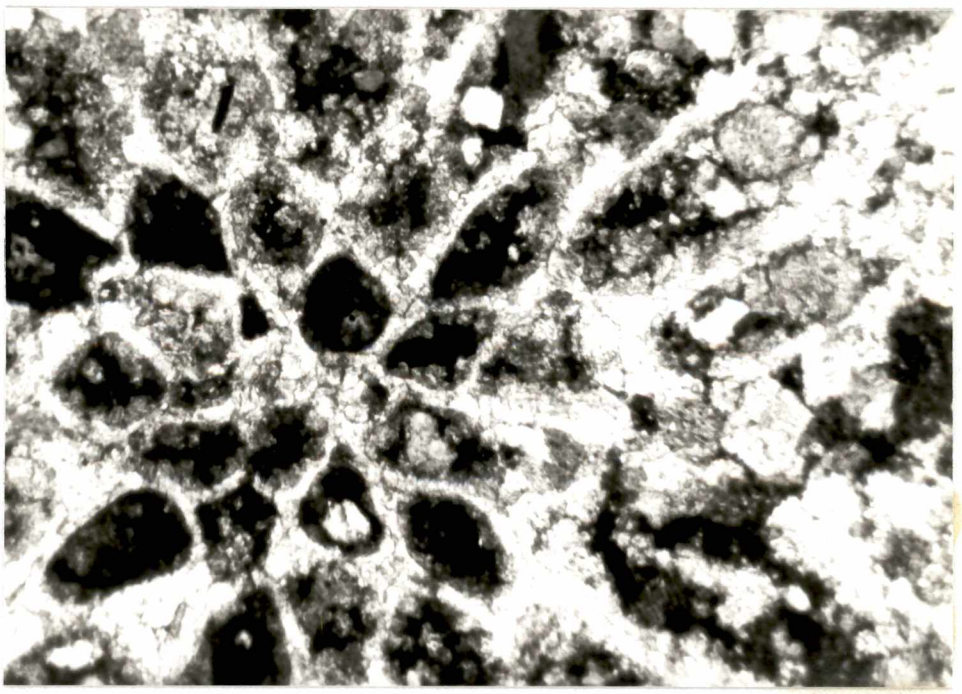


Figure 17. Photomicrograph of a Typical Biosparite Commonly Found within Sub-Facies B2/HS. Field of view from left to right is approximately 1 mm.

fragmented fossil content (usually forming iron-stained horizontal laminations), the increase in framework quartz (up to 92.5 percent), and the abundance of hematite and/or limonite staining (coating both fossils and matrix material). The quartz-rich fossiliferous biosparite beds contain a wide variety of fragmented fossil allochems (mentioned earlier), also with fenestrae, orthoclase feldspar, opaques, and trace amounts of muscovite, hornblende, chlorite, glauconite and plagioclase feldspar (see Appendix II). Matrix material, which is usually no greater than one percent, consists of phyllosilicates and fine-grained opaques. Dolomite is the dominant cementing agent in most samples (as high as 55 percent), although subordinate amounts of calcite and traces of hematite cement were also observed.

Facies C/HS-Shale

Shale of Facies C/HS occurs in the lower, middle and upper sections of the Hagan. This facies is most commonly found, however, intercalated within sub-facies B2/HS (previously described). Delineation of this facies was made by visual estimates in the field and on the graphic log based on the paucity of interbedded sandstone or siltstone. Sandstone-to-shale ratios ranged from 1:20 to 1:30.

The shale of Facies C/HS is generally medium to dark gray, rarely black, or light maroon-gray, and weathering to light red-brown. Locally, iron-staining by hematite produces limited maroon-mottled zones. The texture is fissile to slightly blocky. Small blocks liberated by weathering commonly measure 1 cm in length by 0.5 cm in

width by 0.25 cm in height (Fig. 18). Sporadically found are mud or silt-filled burrows of Planolites (7 mm in diameter) and Skolithos (2 mm in diameter). Burrows exhibit sharp contacts with the enclosing rock. Faint, extremely thin, horizontal laminations were found only at a few locations within the shale. The rare sandstone and siltstone found within this facies is very thin-bedded (0.5-1 cm) and occurs mainly as wavy or flat-lensed lenticular bedding. Thin wisps or streamers of silt and small silt-filled gutter casts were also observed.

Body fossils within Facies C/HS were generally absent with the exception of a fossiliferous shale interval located at 5.8 meters above the base of the Hagan. Crinoid columnals, brachiopods and bivalves were found in low to moderate abundances. Most shale intervals show a semi-consistent lateral thickness, however, thin sandstone and siltstone layers within this facies commonly pinch-out laterally. No petrographic or x-ray analyses was performed on these shale sequences.

Facies D/HS-Isolated Quartzarenite and Iron-Rich Packstone

Only four individual beds comprise Facies D/HS, however, because of their anomalous characteristics, these units cannot be fitted into the aforementioned sequences. These beds, which are intercalated within sub-facies B2/HS, occur mainly in the upper Hagan Shale at 11.9, 12.2, 18.2 and 20.2 meters respectively (Fig. 19). The lithology of facies D/HS is of three types. Ferruginous, bryozoan



Figure 18. Small Blocks Liberated by Weathering from the Shale of Facies C/HS. (Lens cap for scale.)

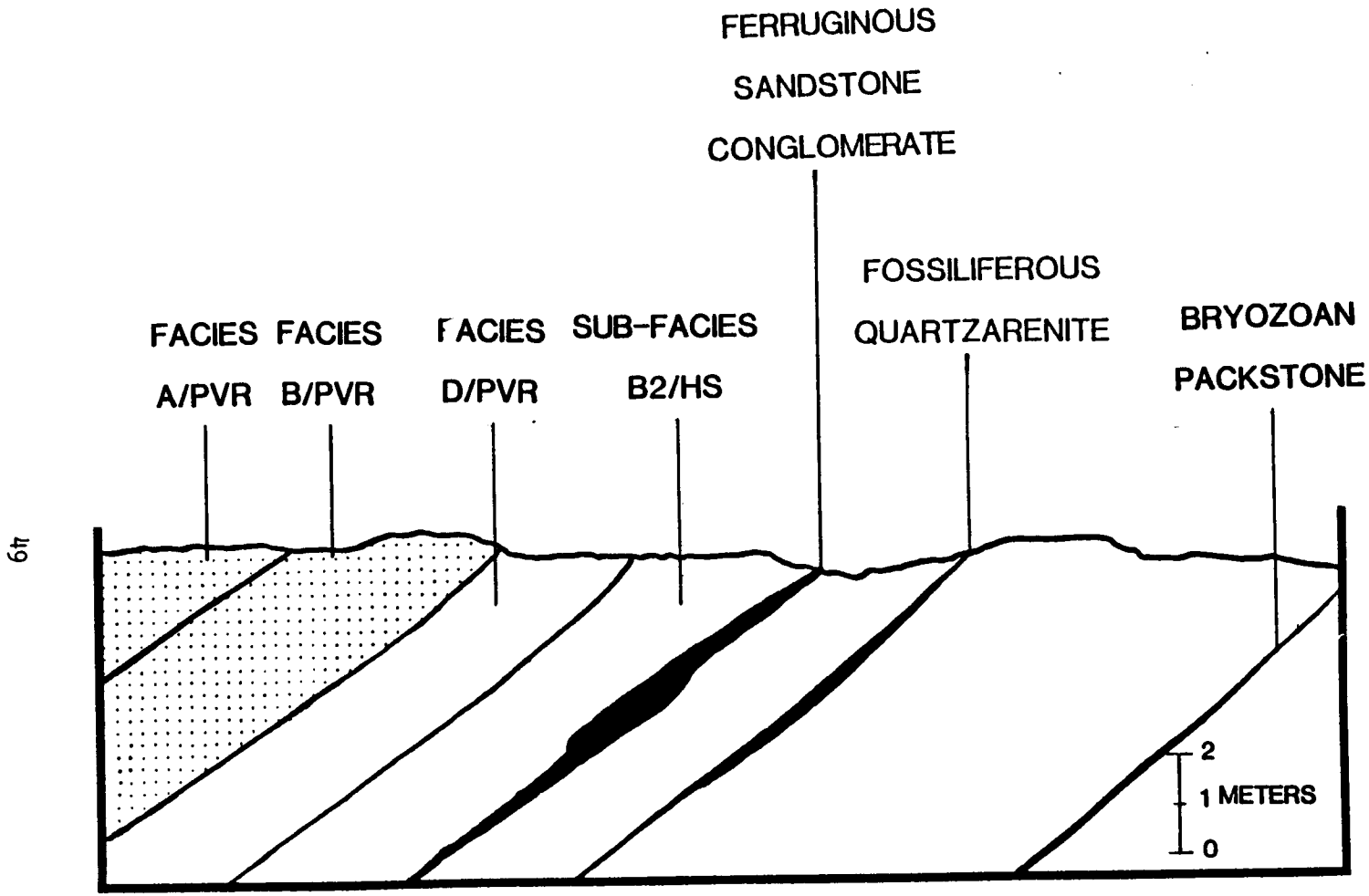


Figure 19. Sketch of the Anomalous and Isolated Units Comprising Facies D/HS.

packstone occurs at 11.9 and 12.2 meters, a fossiliferous quartzarenite is found at 18.2 meters and a ferruginous sandstone conglomerate is located at 20.2 meters.

The ferruginous bryozoan packstone units are 12 and 3 cm thick, the larger one occuring at 11.9 meters. It is light-brown to medium-gray with maroon mottling. Discontinuous and continuous, wavy horizontal laminations are produced by maroon mud intraclasts (Fig. 20). Fragmented fossils show their long axes parallel to bedding and include ramose bryozoans, trilobites, crinoids, echinoderm plates, high-spiraled gastropods and rare bivalves. Fossils are heavily iron-stained. Bed boundaries are extremely sharp and planar with the whole unit displaying a consistent lateral thickness. Petrographic examination of both the thick and thin units shows them to be poorly sorted, quartz-rich, dolomitic biosparite. Fossil allochems are more abundant in the thick basal unit (thin-section UH6-5) and constitute 42 percent of the rock (Fig. 21). Approximately 28% trepostome bryozoans and 5% quartz grains occur in the basal unit. The upper unit (thin-section UH6-6), however, has only 7% trepostome bryozoans but over 25% quartz. Quartz grains in both units are subangular to angular, low in sphericity and exhibit a tight interlocking mosaic due to recrystallization. Other grains which occur in small or trace amounts include sedimentary rock fragments, microcline, plagioclase, chlorite, opaques, and zircon. Interstitial matrix is more abundant (15.5 %) in the basal unit and includes fine-grained micrite mud, opaques and phyllosilicates. The upper

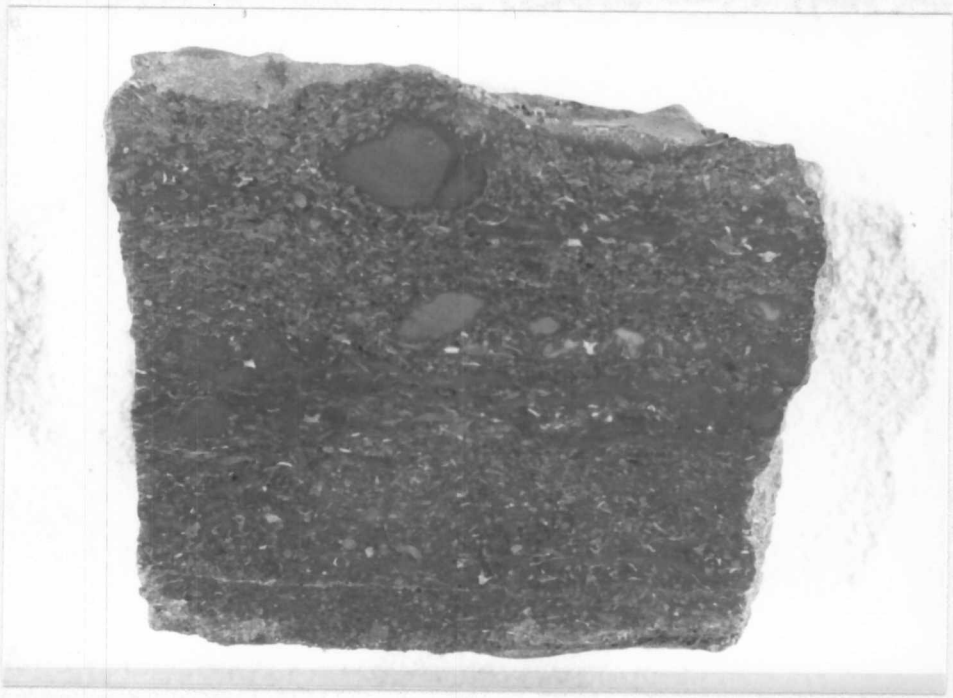


Figure 20. Internal Structure within a Cut-Slab of a Ferruginous Bryozoan Packstone, Facies D/HS. Notice the internal laminations. Marks on scale equal 1 cm.

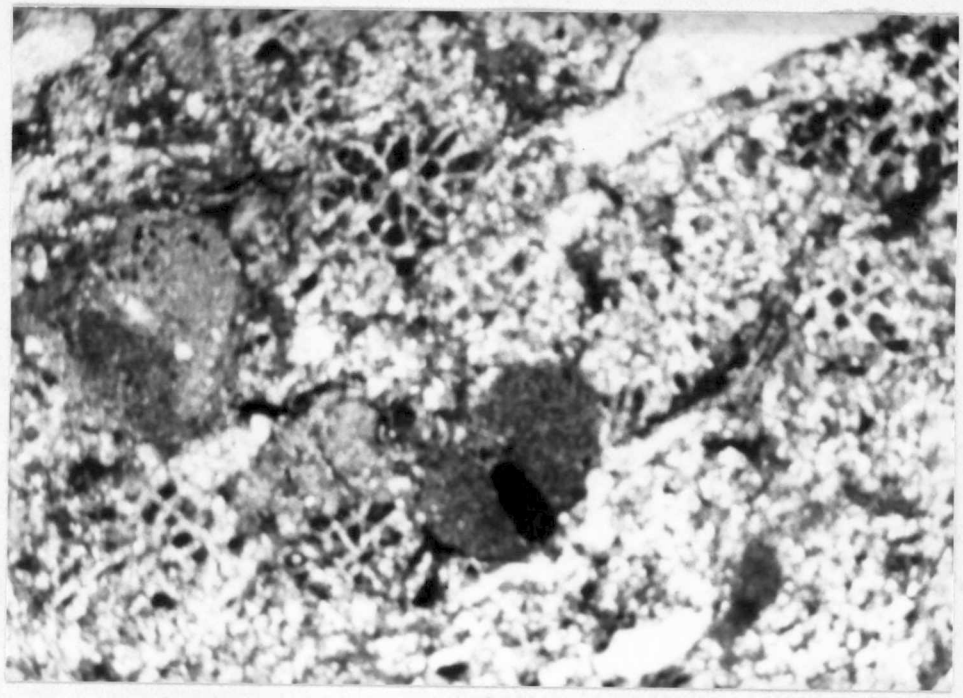


Figure 21. Photomicrograph of the Ferruginous Bryozoan Packstone. Notice the bryozoan cross-sections, echinoderm plates and gastropod fragments. Field of view from left to right is approximately 2 mm.

unit, however, contains more cement with dolomite predominating (48%), but calcite, hematite and silica occur in subordinate amounts. The lower unit contains 30% dolomite, and 6% calcite, with hematite and silica found as traces. (See Appendix II for additional information.)

The second lithological type comprising Facies D/HS is a fossiliferous quartzarenite occuring at 18.2 meters above the base of the Hagan Shale (Fig. 19). This sandstone is medium-gray, weathering to a light red-brown and fine- to medium-grained. Form-discordant wave ripples are found capping the bed with internal small-scale trough cross-stratification. Large body fossils occuring predominantly at the base include echinoderms debris, gastropods, cephalopods and ramose bryozoans. Overall, this unit has a flat, semi-lens-shaped geometry measuring over nine meters in length and 0.2 meters at its widest part (Fig. 22). Bedding planes are sharp. Petrographic analysis reveals several similarities to the calcareous quartzarenite beds in sub-facies B2/HS, however, fossils in this unit are larger, show greater variability and abundance, and less abrasion (Fig. 23). Thin section UH8-2 reveals small amounts of orthoclase, plagioclase, microcline, opaques, chert and trace amounts of biotite, chlorite and zircon. Calcite cement predominates (9%) with smaller amounts of dolomite, hematite and silica. (See Appendix I and II for additional data on this unit.)

The final and upper-most unit of Facies D/HS is an iron-rich, sandstone conglomerate found approximately 2 m below the overlying contact with Poor Valley Ridge Sandstone (Fig. 19). Coloration



Figure 22. Photo of the Fossiliferous Quartzarenite Unit Occuring at 18.2 m above the Base of the Hagan Shale. (Note hammer for scale.)

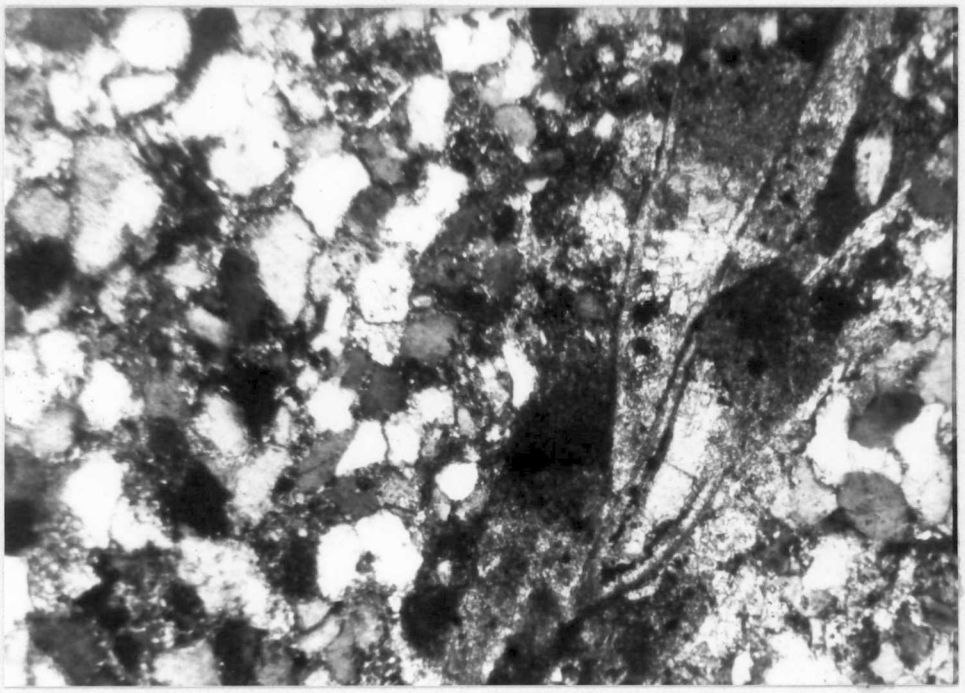


Figure 23. Photomicrograph of Thin-Section UH8-2. This sample represents the typical petrographic character of the fossiliferous quartzarenite bed, Facies D/HS. Field of view from left to right is approximately 2 mm.

within this bed is varied showing several shades of dark gray, red, brown, green and black. Grain size varies from medium sand grading upward to gravel (inversely graded). Rounded, disc-shaped mud intraclasts show imbrication and hematite oxidation rims (Fig. 24). Current ripple crests found at the top of the bed were the only primary sedimentary structures observed. The overall geometry of this unit is somewhat lens-shaped measuring 20 m in length by 1.1 m in width. The bed exhibits sharp/planar lower and sharp/wavy upper bedding surfaces. Thin sections UH10-1 and UH10-2 show quartz (76%) and sedimentary rock fragments (20%) as the major grain types (Fig. 25). Quartz is dominantly monocrystalline, subangular and shows low sphericity. Five major varieties of sedimentary rock fragments are as follows: (1) structureless micritic mudstone, (2) clay-rich siltstone clasts with minor opaques, (3) structureless, terrigenous mudstone, (4) fine-grained sandstone, and (5) horizontally laminated mudstone. Most of these clasts are pebble-sized, highly rounded and shows oxidation rims of hematite. Trilobite fragments and orthoclase feldspar were found in small percentages whereas microcline, plagioclase, hornblende, opaques, chert and zircon occur only in trace amounts. The major cementing material (only 1%) consists of hematite, silica, and dolomite. Petrographic examination also revealed large areas of iron-mineralization forming irregular patches of pyrite and hematite. (See Appendix II for additional information.) Weak iron-mineralization occurs sporadically throughout much of the Hagan

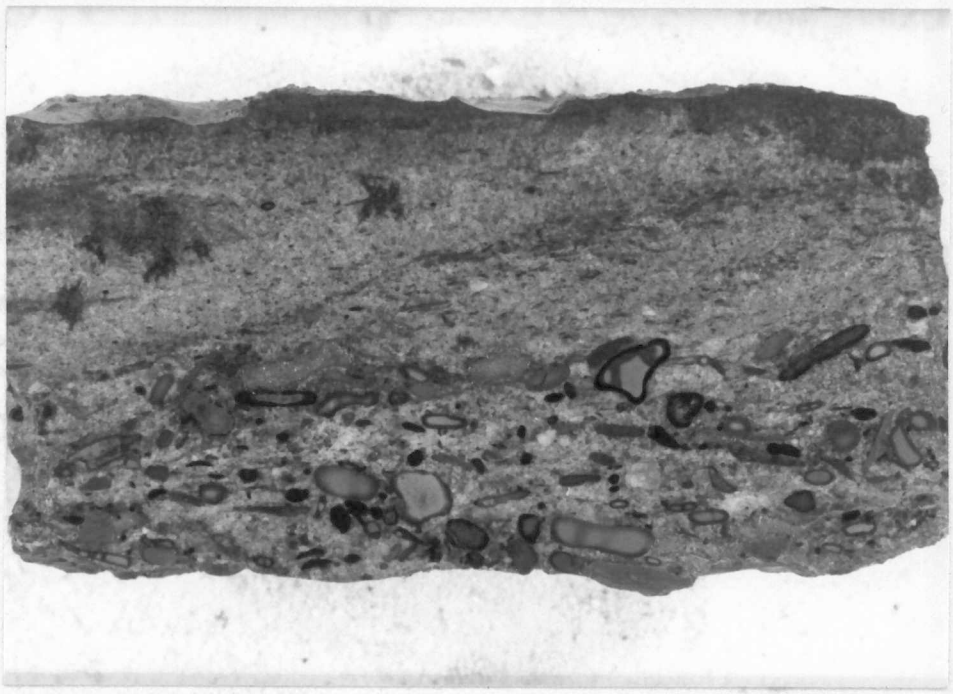


Figure 24. Cut-Slab of the Upper Sandstone Conglomerate Unit of Facies D/HS. Marks on scale equal 1 cm.



Figure 25. Photomicrograph of Thin Section UH10-2. This sample exhibits the various sedimentary rock fragments found within the upper conglomerate unit of Facies D/HS. Field of view from left to right is approximately 2 mm.

Shale but is concentrated in Facies D/HS. Of this facies, the highest percentage of iron-minerals was found in this unit.

Poor Valley Ridge Member

General

The Poor Valley Ridge Member of the Clinch Sandstone conformably overlies the Hagan Shale Member. At Powell Mountain, Virginia, the Poor Valley Ridge (PVR) is generally finer-grained and more thinly bedded than stratigraphic equivalents at Clinch Mountain to the east. Still classified as a quartzarenite, these rocks are well indurated and exhibit abundant cross-stratification, rounded mud intraclasts and bioturbation (Fig. 4, p. 22). The PVR Member can be divided into four major facies based on primary sedimentary structures, texture, bedding geometry and biological structures (Fig. 26).

Facies A/PVR-Compound Cross-Stratified Quartzarenite

Facies A/PVR is a fine-grained, compound cross-stratified quartzarenite sequence. This facies, which is approximately 22 m thick, is the best represented lithofacies at Powell Mountain (Fig. 4, p. 22). Conformably overlying Facies A/PVR is the maroon sandstone, siltstone and mudstone lithology of the Rose Hill Formation (described later in the chapter on Rose Hill deposition) and underlying Facies A/PVR is the massively bedded and heavily bioturbated sandstone of Facies B/PVR.

Facies	Lithology	Sedimentary Structures	Other
A/PVR-Compound Cross-Stratified Quartzarenite	-Quartzarenite -Thin intercalated mudstone and shale	-Compound cross-stratification -Small- to medium-scale trough cross-stratification -Current ripples -Reactivation surfaces	-Arthrophycus -Cruziana -Abundant mud intraclasts -Clay drapes
B/PVR-Bioturbated Sandstone	-Clay-rich quartzarenite	-Structureless beds -Possible faint horizontal laminations	-Skolithos -Lingulid brachiopods -Phosphate nodules -Granule lag zones
C/PVR-Shale	-Shale	-Few current ripples -Horizontal laminations	-Arthrophycus -Pyrite concretions
D/PVR-Interbedded Sandstone and Shale	-Subarkose -Quartzarenite -Interbedded shale	-Current ripples -Horizontal laminations -Structureless beds -Micro-hummocky cross-laminations	-Skolithos -Planolites -Rusophycus

Figure 26. Brief Description of Facies in the Poor Valley Ridge Sandstone.

Facies A/PVR consists of a light- to medium-gray, very fine- to rarely medium-grained quartzarenite displaying an extremely complex internal geometry. The dominant internal structure is a master bedding consisting of long, slightly convex-upward bounding surfaces which dip to the east (Fig. 27). These second-order surfaces are 4-50 cm thick, are parallel to subparallel, somewhat evenly spaced and commonly dip from 5-15°, but average about 8°. Individual units measure up to 3.25 m thick, but average 2 m thick. This type of bedding is similar to the epsilon cross-stratification proposed by Allen (1963).

These second-order bounding surfaces contain internal trough cross-bedding of small- to medium-scale with sets averaging 0.75 m thick. Several compound set bundles are also observed throughout Facies A/PVR. This internal bedding occurs as co-sets of two or more thin sets, or less frequently, a single set may make up the total thickness of the master unit (Fig. 28). The cross-bedding generally dips in the same direction as the master bedding and is interrupted occasionally by third-order erosional surfaces. These reactivation surfaces are irregular and have low dips in comparison to those of the second-order bounding surfaces. Some reactivation surfaces are developed over almost the whole set length, whereas others are developed only in the upper parts. The forsets of the internal trough cross-stratification have dip-angles which average 28° and terminate tangentially. Set thickness averages 0.30 m and are laterally



Figure 27. Master Bedding of Facies A/PVR. Notice how units pinch-out in both lateral directions.

persistent for up to 10 m with some greater in length. This type of bedding is similar to Allen's (1963) pi-cross-stratification.

Small scale, asymmetrical current ripple marks cap some sandstone beds in Facies A/PVR. In addition, horizontal laminations are also found within a few thin units, however, this feature is somewhat rare. Also concentrated along the upper surfaces of some beds and within internal troughs, are coarse-granule lag and/or mud intraclast zones. Coarse-granule lag zones, which consist of rounded clasts of vein quartz, are more commonly found as lag streamers within internal trough forsets but may comprise the upper 2 cm of the sandstone bed (Fig. 29). Mud intraclasts are medium gray, subrounded to rounded, somewhat disc-shaped and assume various shapes. No occurrences of complete megaripple (dune) bedforms preserved in their entirety were observed at Powell Mountain. In addition, the conspicuously bundled forsets (double-clay-drape couplets) forming the tidal bundle sequences found in the more eastern Clinch strike belts by Driese (1987) were not found at this location.

Although no body fossils were observed in Facies A/PVR, abundant trace fossils, especially concentrated at bed boundaries, were found throughout the interval. Much of the bioturbation is in the form of two trace fossils: Arthrophycus, and less commonly Planolites. Arthrophycus (12 mm in diameter) appears as sinuous, horizontal, slightly flattened cylinders, isolated or in radiating networks expose in convex semi-relief on the botton of sandstone beds (Fig. 30). Individual cylinders commonly show transverse ridges. Planolites

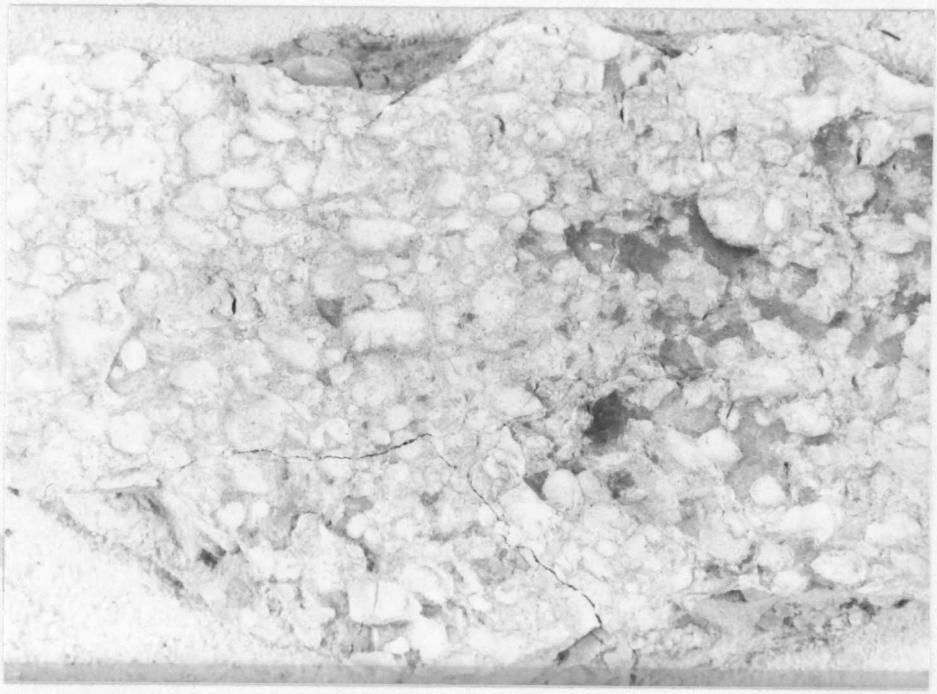


Figure 29. Cut-Slab of a Quartzarenite from Facies A/PVR. Notice the heavy concentration of mud intraclasts occuring near the top of the sample. Marks on scale equal 1 cm.



Figure 30. Intricate Traces of Arthrophycus Exposed as Semi-Relief at the Bases of some Quartzarenite Units within Facies A/PVR. (Lens cap for scale.)

occur in semi-relief, and are found as isolated, sinuous, horizontal and slightly-flattened cylinders. Planolites, however, are commonly isolated and do not show transverse ridges. Bilobate trails of Cruziana are located generally along tops of sandstone beds. The trails are sinuous, horizontal and semi-continuous. Other trace fossils found within facies A/PVR include Rusophycus, Rhizocorallium and Diplocraterion, all of which are found locally in very limited amounts.

Bedding geometry within facies A/PVR changes slightly as one moves up the sequence. Sandstone units at first show a consistent lateral thickness and are medium-bedded. Towards the middle of A/PVR, units are thin- to medium-bedded and take on a wedge-like geometry with many units pinching-out in both directions. At 2 m below the contact with the overlying Rose Hill Formation, units become less wedge-like and grade upward into sheet-like units, similar to those found near the base of A/PVR. These units are also medium bedded. Most sandstone beds in this facies have sharp/planar lower and sharp/planar or sharp/wavy upper bedding planes.

Samples P9-1, P10-6, P13-A, P14-A, P17-A and P18-B represent the petrographic thin-section suite of Facies A/PVR (see Appendix II). All are fine- to medium-grained, well sorted, quartzarenite with over 95% quartz and subordinate amounts of orthoclase, phyllosilicates, chert, opaques and rare sedimentary rock fragments (Fig. 31). Microcline and plagioclase feldspar are also very rare. Accessory minerals include tourmaline and zircon. Rare rutile needles

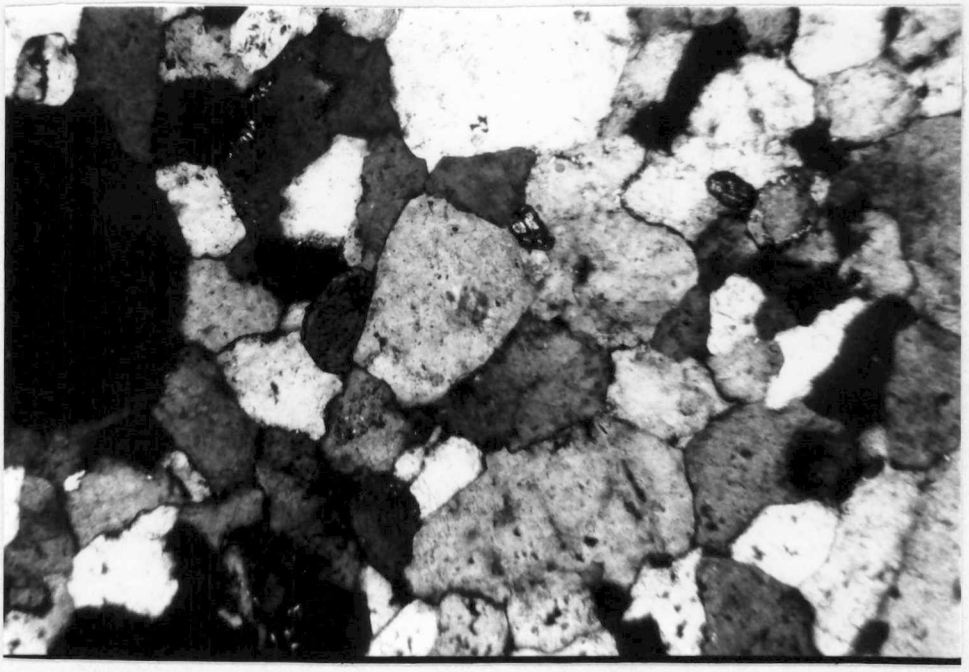


Figure 31. Photomicrograph Showing the Representative Petrographic Character of Facies A/PVR. Most samples are fine-grained, well sorted quartzarenite. Field of view from left to right is approximately 4 mm.

were observed occuring as inclusions enclosed within clasts of vein quartz. Quartz grains are subangular to subrounded and show medium sphericity. The monocrystalline quartz variety predominates. Identification was not made of the specific quartz types for provenance analysis because of the intense recrystallization which formed a tight, interlocking mosaic. Samples P10-6 and P18-B have a bimodal texture. Grains of the coarse mode are generally better rounded and more spherical than the fine mode. Clay matrix almost never exceeds 1% and porosity is very low. The dominant cementing agents are silica and hematite, however, quartz overgrowths (which undoubtedly exist) were extremely hard to observe.

Facies B/PVR-Bioturbated Sandstone

Facies B/PVR is a heavily bioturbated sandstone three meters thick, which directly overlies Facies D/PVR. The contact between the two is gradational over 0.25 m with some coarse sand and Skolithos tubes of B/PVR extending downward into the interbedded sandstone and shale of Facies D/PVR. Overlying Facies B/PVR are the trough cross-stratified, fine-grained, "Clinch-like" sandstones of Facies A/PVR, the contact between which is sharp.

The sandstone of Facies B/PVR, a clay-rich quartzarenite, is medium to dark gray, but weathers yellow-brown or green yellow-brown. The lower unit is fine-grained and the upper unit coarse-grained, but both are clay-rich and thoroughly bioturbated by Skolithos (Fig. 32). Skolithos is generally 3-6 mm in diameter, with tubes anastomosing and

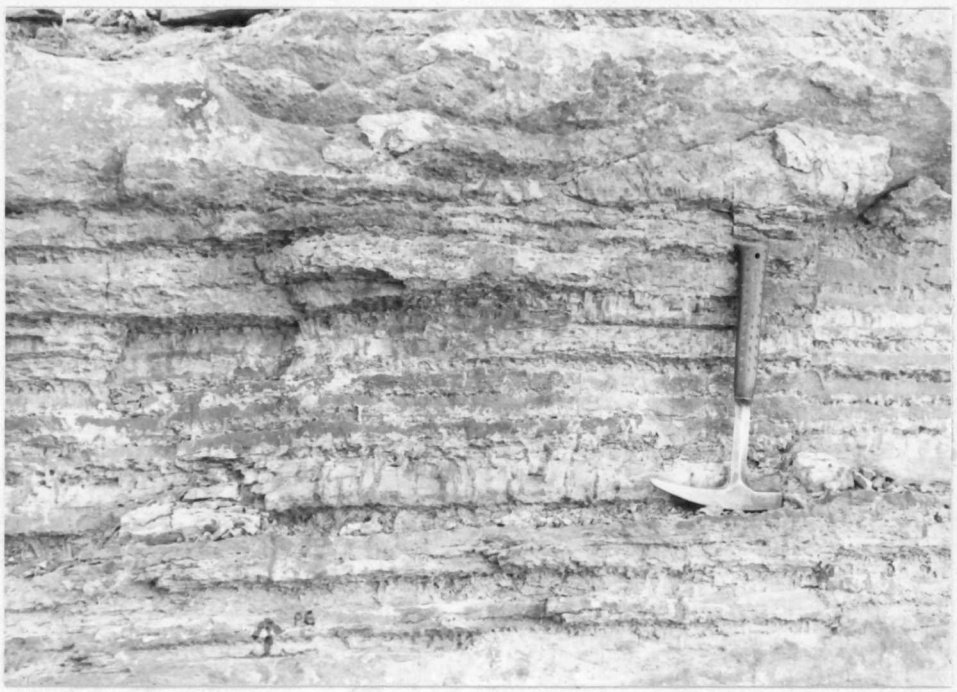


Figure 32. Heavily Bioturbated Sandstone of Facies B/PVR. Notice small vertical tubes of Skolithos punctuating the rock. (Hammer for scale.)

extending vertically for several cm. Few problematic horizontal burrows were also found along some bedding planes. Most trace fossils are preferentially stained by hematite and/or limonite. As a result of the intense bioturbation, the rock takes on a mottled and very friable character which is easily weathered (Fig. 33). No physical sedimentary structures were observed except for a few horizontal laminations. Several granule or even pebble lag zones were found within both the fine- and coarse-grained subunits. These zones are thin (under 2 cm) and discontinuous containing rounded quartz clasts, fragmented Lingula (inarticulate brachiopods) and few phosphate nodules (Fig. 34).

Sandstone beds of Facies B/PVR are medium- to thick-bedded with sharp/planar lower and upper surfaces. The fine-grained subunit at the base of the lithofacies is somewhat gradational with the underlying D/PVR facies. This subunit, which is approximately 1 m thick, grades upward to medium-grained sandstone. The overlying coarse-grained subunit, approximately 2 m thick, inversely grades upward into medium-grained sandstone. The contact with overlying A/PVR-Trough Cross-Stratified Facies (fine-grained) is sharp. Both subunits show a constant lateral thickness over the entire exposure at Powell Mountain.

Petrographically, Facies B/PVR is classified as a fine- to coarse-grained, poorly sorted, clay rich quartzarenite (sample P5-A, Appendix II). The bimodal texture shows scattered, floating, large grains of quartz in a tightly packed, interlocking fine-grained mosaic



Figure 33. Upper Motttled Surface of a Sandstone in Facies B/PVR. Individual tubes of Skolithos are preferentially iron-stained. (Coin for scale.)



Figure 34. Granule Lag Zones of Phosphatic Lingula Brachiopods and Quartz Granules. (Pen for scale.)

(Figure 35). Highly rounded and spherical clasts of vein, metamorphic/stretched, and plutonic quartz were identified. Hematite is the primary cementing agent with up to a five percent phyllosilicate matrix between grains. An unusually high percentage of opaques and trace amounts of feldspar, chert, muscovite, chlorite and zircon were identified in sample P5-A.

Facies C/PVR-Shale

Facies C/PVR is a slightly fissile to slightly blocky shale which is found interbedded with the sandstone of Facies A/PVR. The contacts between the two facies are sharp and planar. These units are differentiated from the thin intercalations of mudstone and shale (less than 3 cm thick) which are commonly found between sandstone beds of Facies A/PVR. Shale of Facies C/PVR is generally thicker than 0.30 m, shows little bioturbation, is more silty and contains some anomalous features not found within the thin mud interbeds and claystone drapes of the former facies.

The shale of Facies C/PVR is light gray to light brown-gray with black and red mottling. It is slightly fissile to slightly blocky and generally homogenous with the exception of thin streamers or thicker zones of silt occuring in a few locations (Fig. 36). Major intervals are found at 11.0, 12.0, 13.25, 23.0 and 25.6 m above the base of the Poor Valley Ridge Member of the Clinch Sandstone.

Trace fossils are generally lacking, however, slightly flattened, horizontal tubes of Arthrophycus (12 mm in diameter) are found in the

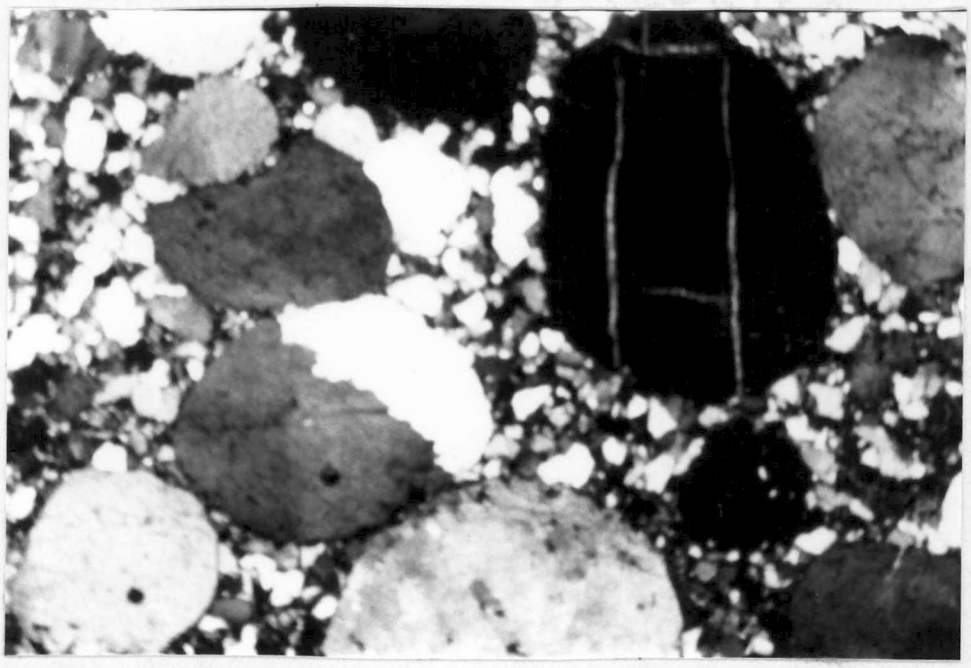


Figure 35. Photomicrograph Showing the Representative Petrographic Character of Facies B/PVR. Field of view from left to right is approximately 4 mm.



Figure 36. Shale of Facies C/PVR Found Sporadically Interbedded within Facies A/PVR. This shale is generally 0.5 m thick and is not to be confused with the thin mudstone or shale partings between sand units of Facies A/PVR. (Hammer for scale.)

siltier portions of the unit located at 12.0 m. This bed is 0.8 m thick, but pinches in the eastward direction. Silt content increases upward, finally grading into thin, flat-lensed lenticular bedding near the base of an overlying sandstone unit (Facies A/PVR). Several concretions of pyrite were also found (measuring 2-3 cm in diameter).

Primary sedimentary structures within Facies C/PVR consist of two major types. Asymmetrical current ripples were located within the siltier portions of the shale at 11.0 meters. Thin, horizontal laminations were also found in several shale units but most abundantly at 12.0 m. These laminations are even-parallel, generally spaced 1 mm apart and defined by concentrations of dark clay minerals and possible organic matter.

Facies D/PVR-Interbedded Sandstone and Shale

Facies D/PVR is found at the Hagan Shale/PVR transition overlying the thin, very fine-grained sandstone and shale strata of the Hagan and underlying the coarse-grained, heavily bioturbated sandstone of Facies B/PVR (Fig. 37 and 38). Facies D/PVR consists of interbedded sandstone and shale. The shale is dark brown-gray and fissile to slightly blocky. It becomes slightly silty about half-way up into the facies. Small (3 mm in diameter) sand-filled vertical tubes of Skolithos are found extending into the shale. The sandstone beds in Facies D/PVR are medium- to dark maroon-gray, very fine-grained subarkose and clay-rich quartzarenite. Lunate current ripples are



Figure 37. Lower Contact of Facies D/PVR with the Underlying Hagan Shale. Notice that with the exception of the basal sandstone, bed thickness increases upward. (Hammer tip denotes contact.)



Figure 38. Upper Contact of Facies D/PVR. The overlying lithology is the massive and heavily bioturbated sandstone of Facies B/PVR. (Hammer tip denotes contact.)

found capping many sandstone units lower in the facies, however, beds become structureless higher up. Some beds also contain wavy horizontal laminations, micro-hummocky cross-laminations (basal unit) and interference ripples (Fig. 39). Several thin units contain scoured bases but flute and groove casts and other sole features are lacking.

Trace fossils within the interbedded sandstone and shale facies are well-represented by Skolithos (averaging 0.5 mm in diameter) whose vertical tubes frequently disrupt internal sedimentary structures but also penetrate into the underlying shale. Thin, discontinuous, horizontal burrows of Planolites (8 mm in diameter) are found on the bottom of sandstone beds. Subordinate occurrences of Rusophycus and a problematic gastropod grazing trail (8 mm in diameter) (Fig. 40), occur higher up in the interval. Skolithos and Rusophycus increase in abundance upward. Most trace fossils exhibit preferential iron mineralization.

The interbedded sandstone in Facies D/PVR shows an overall upward-thickening trend. This trend, however, does not include the lowermost sandstone unit (20 cm thick) at the Hagan/PVR contact. Lowermost beds average 1.5 cm in diameter and are bounded by sharp/planar lower and sharp/wavy upper contacts. Some bedding is wavy-parallel, but overall, beds show a uniform lateral thickness. Uppermost units in Facies D/PVR become thicker, massive and show no scour features or wavy bedding. Bedding surfaces are generally sharp/planar showing a uniform lateral thickness (Fig. 38).



Figure 39. Sedimentary Structures within the Basal Unit of Facies D/PVR. Structures include wavy-parallel horizontal laminations, micro-hummocky cross-laminations and current ripples. (Coin for scale.)

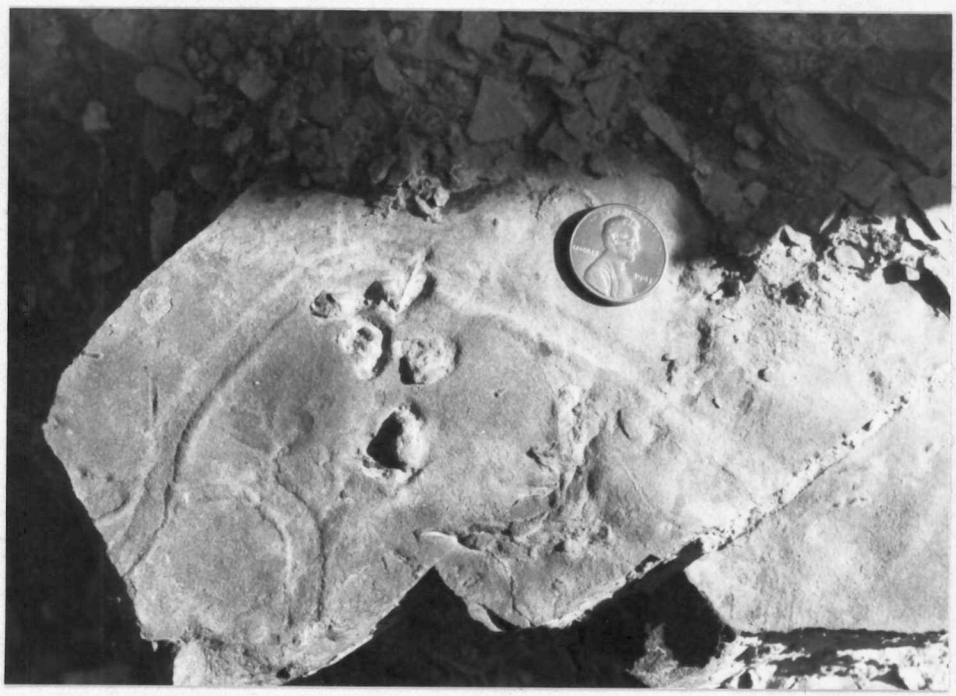


Figure 40. A Problematic Gastropod Trace on a Upper Surface of a Sandstone Bed, Facies D/PVR. (Coin for scale.)

Just as for other features, the petrography of Facies D/PVR shows considerable variation as one moves upward in the sequence. Feldspar content, amount of clay matrix and iron-mineralization decrease, whereas quartz content, grain-size and silica cement increase upward. Samples P1-1, P2-1 and P3-2 are the thin-sections representing Facies D/PVR (Fig. 41). They are classified as subarkose and contain albite, microcline, and orthoclase in amounts greater than in any other rocks examined at Powell Mountain. Quartzarenites are found at the top of D/PVR. Phyllosilicates occur as framework grains and as matrix material, the latter stained by hematite and/or limonite. Although not as apparent in these two samples representing progressively higher stratigraphic positions, the overall clay and iron content decreases upward within Facies D/PVR. Grain-size shows a progressive upward increase in Facies D/PVR. The three thin-sections reveal modes of 0.065 mm for P1-1, 0.10 mm for P2-1 and 0.12 mm for P3-1. Although not analyzed petrographically, sandstone near the top of Facies D/PVR shows mean grain diameters of up to 0.5 mm. Grain-size trends are also accompanied by an increase in silica cement and an overall increase in quartz content upward in the section. It should be noted that although all three upward-increasing trends may be explained by the formation of quartz overgrowths, no such authigenic features were observed in the thin sections.

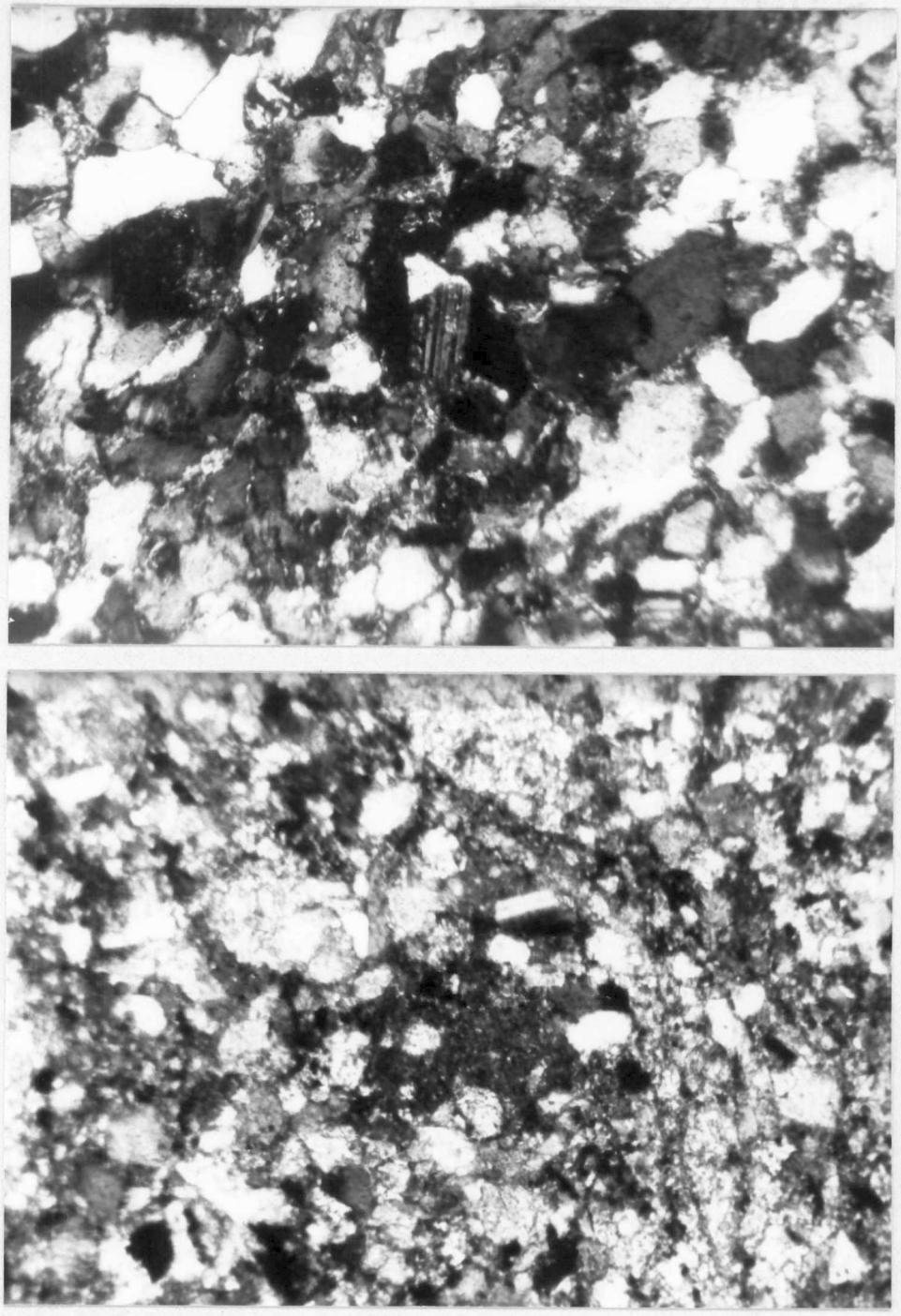


Figure 41. Photomicrographs of Thin Sections P1-1 and P2-1. These samples represent the lower (bottom photo) and middle (upper photo) sandstone units within Facies D/PVR. Field of view from left to right is approximately 2 mm.

CHAPTER III

PALEOENVIRONMENTAL INTERPRETATIONS

Hagan Shale Member

The Hagan Shale Member of the Clinch Sandstone at Powell Mountain is interpreted as a sequence of marine storm deposits emplaced in shallow and moderately deep shelf environments. These rocks were deposited as a result of the transgression during Early Silurian time (McKerrow, 1979) which led to the inundation of the Upper Ordovician tidal flat deposits of the Juniata and Sequatchie Formations (Thompson, 1970; Thompson, 1984). The paleoenvironments of the Hagan shale were then succeeded by the clastic progradational wedge resulting in the marine, sand wave deposits of the Poor Valley Ridge Member (this study). The depositional model of the Hagan Shale envisioned by this author differs from that of Fischer (1987) but is somewhat similar to the interpretation of the Hagan by Schoner (1985 a, b) (Figure 42). Detailed explanations of Poor Valley Ridge depositional systems as well as an overall environmental model for both members of the Clinch are presented in subsequent sections of this report.

Modern Storm Deposits

The effects that storms have on modern shelf sediments are not well understood for a variety of reasons. First, most sediments on modern shelves can at best be classified as palimpsest (slightly

PALEOENVIRONMENTAL INTERPRETATIONS

Schoner (1985 a & b)	Fischer (1987)	Marks (this study)
Hagan Shale - Shelf mud deposition - Transition-zone deposition	Hagan Shale - Back-barrier lagoon	Hagan Shale - Shelf-mud deposition - Transition-zone and middle shelf storm deposition
Poor Valley Ridge Sandstone - Barrier-bar complex cut by a tidal inlet system	Poor Valley Ridge Sandstone - Shelf-sand ridge complex	Poor Valley Ridge Sandstone - Shelf-sand wave complex
Provenance - Local source for both members	Provenance - 1) Local source for both members, or - 2) Local source for Hagan shale, distant source (northern Virginia) for Poor Valley Ridge Sandstone	Provenance - Local source for both members

Figure 42. Paleoenvironmental Comparisons. Interpretations from this study are compared to those of other workers in northeastern Tennessee. (Modified from Fischer, 1987).

reworked relict sediment) (Swift and Niedoroda, 1985), and serve as poor analogues for ancient deposits. Secondly, modern storm deposits laid down above fairweather wave base have a very low preservation potential; the effects of daily tidal, rip- and wind-forced currents as well as the homogenizing effects of burrowing organisms tend to erase all evidence of storm deposition (preservational omission). Third, it is presently impossible to make direct observations of bedform formation, evolution and migration on the seafloor during active storm conditions. And finally, the possibility that modern day storms are not of the same intensity as the "rare event" storm deposits commonly preserved in the stratigraphic record (i.e., no storm has yet occurred in recorded history analogous to the 10,000 to 15,000 year event of Brenchley et al., 1979). These limitations prompt specific questions concerning storm effects, namely:

(1) during a storm, to what extent is sediment stirred up and sorted in place versus transported over appreciable distances?,

(2) exactly how do storms transport sediment?,

(3) are turbidity currents generated by storms in the nearshore zone? and

(4) what are the factors responsible for the initiation of hummocky cross-stratification?

Answers to these questions are beyond the scope of this study, however, a brief summary of transport mechanisms responsible for sublittoral storm deposits is given below.

Goldring and Bridges (1973) and Kelling and Mulling (1975) discussed the problem of episodic emplacement of sand below fairweather wave base. Exactly what mechanism(s) are responsible for breaching the littoral energy fence of Swift et al., (1971)? These authors list several types of currents on modern shelves which may be responsible for moving sand. These include tidal currents, intruding ocean currents, density currents (salinity- or temperature-controlled) and meteorological currents. Of these, meteorological currents (storm-induced currents) seem most likely to transport sediment to the distal reaches of the shelf. Meteorological currents can be subdivided into rip currents, wind-forced currents, incremental storm flows, storm-surge-ebb currents and sediment-density-driven turbidity currents (Walker, 1985).

Rip currents consist of turbulent jets of seaward flow from the beach through the breaker zone, continuing for several hundred meters before they finally dissipate (Swift et al. 1983). These flows result from channeled return flow of water which has been forced onshore by winds and waves. Geologically, their coarse-grained deposits have been described (Leckie and Walker, 1982) but are generally reworked by fairweather processes between storms.

Wind-forced currents result from winds blowing consistently across the ocean surface during strong gales or hurricanes. Surface layers are set in motion and entrain progressively deeper layers generating the Ekman spiral illustrated by Defant (1961). Data on wind-forced currents from modern shelves comes primarily from studies

of hurricanes and tropical storms (Murray, 1970; Swift and Field, 1981). Walker (1985) summarized the bedforms and preservable sedimentary structures resulting from wind-forced currents acting on modern continental shelves. Sand is observed to move incrementally across and along isobaths during successive storms. Current ripples, small sand waves and sinuous crested dunes leave various scales of cross-bedding in the geological record. Sharp-based graded beds and/or hummocky cross-stratification may also be preserved (Walker, 1985).

Swift et al., (1983) envisioned incremental storm flows as being responsible for moving considerable volumes of sand offshore to its final site of deposition. Sand would therefore eventually be introduced into areas of former mud deposition as thin, sharp-based beds enclosed in fairweather mud strata. The types of sedimentary structures produced by incremental storm flows are similar to those produced by wind-forced currents, however, the effects of oscillatory flows may be more important here. If storms produced a combined geostrophic current plus an oscillatory flow, hummocky cross-stratification could form. However, if storm waves do not reach the bottom, unidirectional traction movement of sand would produce current ripple lamination, medium-scale cross-stratification and horizontal laminations.

Hayes' (1967) study of the effects of Hurricane Carla regarded relaxation (storm-surge-ebb) currents a mechanism for rapid and catastrophic movement of sand seaward. A storm of generally hurricane

proportions tends to pile (wind-forced) water along the shoreline, consequently raising the tide (storm-surge). The accumulation of water along the coast is accomplished by wind, waves and the low-pressure area associated with the center of a storm (Swift et al., 1971). Surge tides may be as high as six meters above normal high tide and persist for several hours before storm winds change. After landfall of the hurricane, there is a constant offshore/alongshore flow of water driven by the hydraulic head and the Coriolis force (Walker, 1985). This relaxation discharge may transport sand as bedload or in suspension (turbidity currents). Nelson (1982) suggested that graded beds could be the result of storm surges on the modern Bering Shelf. Nelson compares the classical vertical sequence of the turbidite structures of Bouma (1962) to features he encountered in cores. From bottom to top of his stacked vertical sequence occurs the following: a lower parallel laminated, fine- to medium-grained sand showing a sharp, flat base; finer sand with cross and convolute laminations; upper parallel-laminated very fine sand to coarse silt, terminating in an upper mud cap.

Turbidity currents are density-driven currents of sediment-laden water which flow down a submarine slope or shelf setting. Despite the numerous examples of ancient turbidites (Kelling and Mullin, 1975; Brenchley et al., 1979; Hamblin and Walker, 1979; Aigner, 1982) since the pioneering work of Bouma (1962), there is little direct evidence for turbidity currents on modern shelves. Deposits laid down by turbidity currents represent the "rare-event" of only short duration

with fluctuating but overall waning currents. Turbidites with Bouma sequences are generally 0.5 to 10 cm thick and contain graded bedding, parallel lamination and small scale cross-lamination (Fig. 43).

Individual Facies Interpretation

Facies A/HS

Facies A/HS occurs at the base of the Hagan Shale and conformably overlies the Upper Ordovician Juniata Formation. Milici and Wedow (1977) interpreted the Juniata to represent deposition in a tidal flat to shallow subtidal environment. At Powell Mountain, southwestern Virginia, fossilized soil horizons found in the Juniata are direct evidence of subaerial exposure. Slickensided soil fractures and rare carbonate concretions characteristic of paleosols are located approximately 0.5 and 0.95 m below the contact with the overlying Hagan Shale (Fig. 44). Gray (1984) noted similar convex or concave surfaces in the red mudstone of the Bloomsburg Formation (Silurian), central Pennsylvania. She described these fractures as saucer-shaped with slickenlines radiating away from the base and compared them to similar slip surfaces that occur in seasonally wet/dry modern vertisols. Blodgett (1985) observed that modern vertisols contain over 35 percent smectite clay, carbonate nodules and have a distinctive slickensided ped structure. The optimum development of vertisols is in tropical to subtropical monsoonal climates with precipitation being the main controlling factor. The slickensided ped structure is modified little by changes in climate and subsequent

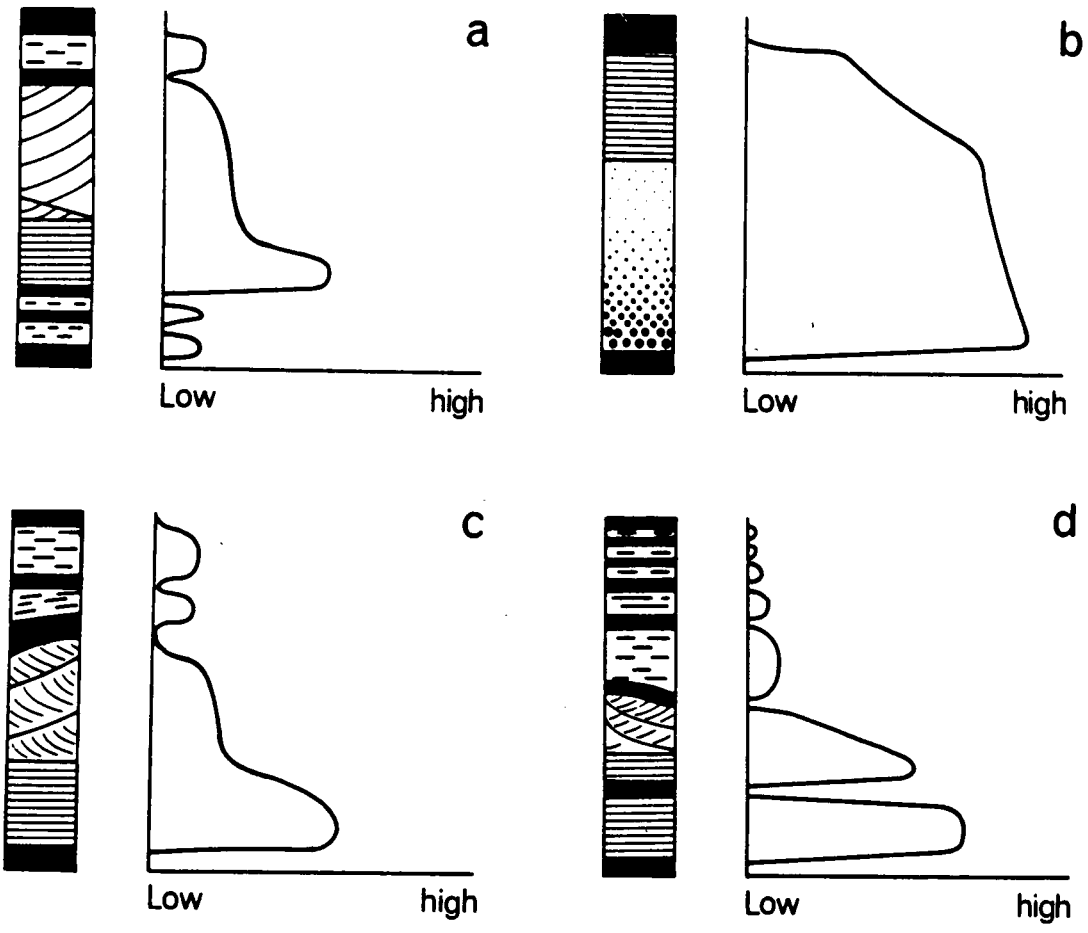


Figure 43. Internal Structures of Bouma Sequences. a) Mud-sand lamination, overlain by planar lamination, cross-lamination and mud-sand lamination. b) Graded to planar laminated bed. c) Planar lamination overlain by cross-lamination and mud-sand lamination. d) Planar lamination with mud interbed, overlain by cross-lamination and mud-sand lamination. (Taken from Brenchley et al., 1979).

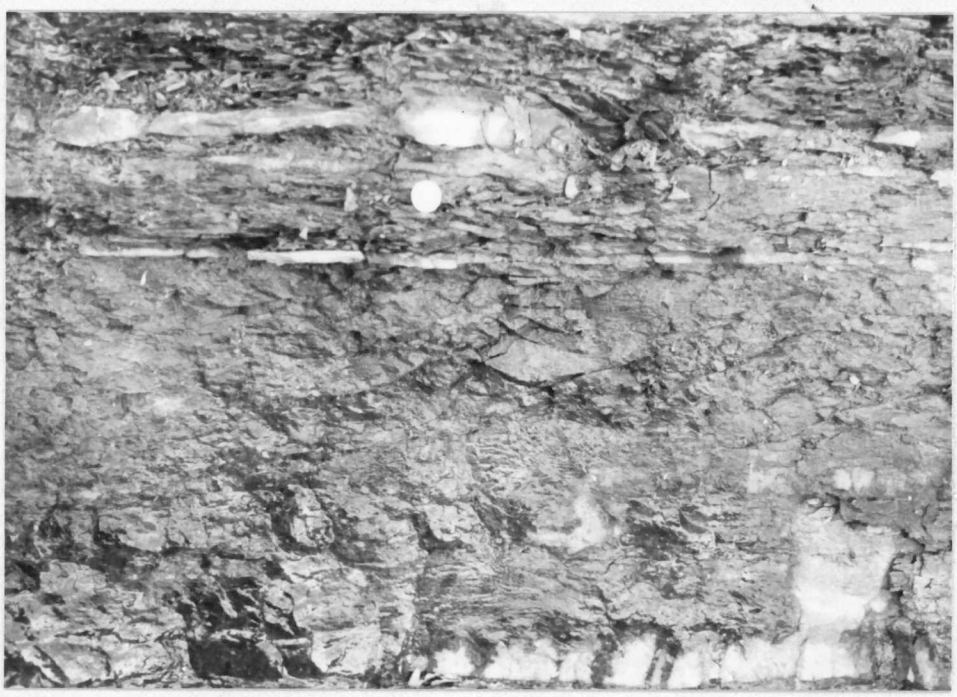


Figure 44. Evidence for a Paleosol. Saucer-shaped, concave-up, slickensided paleosol fractures preserved in the Juniata Formation only 1 m below the contact with the overlying Hagan Shale Member of the Clinch Sandstone.

burial, therefore, having a high preservation potential in the rock record (Blodgett, 1985). The soil fractures and rare carbonate nodules found in the paleosol horizon in the uppermost Juniata Formation indicate subaerial exposure of the sediment prior to the Late Ordovician/Early Silurian transgression.

The juxtaposition of Facies A/HS overlying the tidal flat deposits of the Juniata suggests a possible marine origin. Direct evidence of a shallow-marine origin for Facies A/HS include: (1) Lingulid brachiopod shells, (2) Skolithos trace fossils and (3) minor amounts of glauconite and phosphate. Most of the trace fossils, sedimentary structures, body fossils and phosphate grains were found in the upper, thin-bedded sandstone and siltstone units of this facies. The basal unit of Facies A/HS (calcareous quartzarenite) contains few of the above features with the exception of inverse grading of the upper 2 cm of the bed. In addition, rare wave ripples were found at the Juniata/Hagan contact.

The basal Hagan Shale Member of the Clinch Sandstone is inferred to represent deposition above fairweather wave base by currents and waves associated with the Late Ordovician/Early Silurian transgressing sea. Similar interpretations were given for the basal Rockwood Formation in east Tennessee by Milici and Wedow (1977) and Easthouse (1987). Easthouse (1987) observed Hagan-like sedimentary structures, lithology and mineralogy in the basal Rockwood Formation at Whiteoak Mountain. One minor difference, however, is that the Rockwood section is heavily bioturbated and dominated by Cruziana,

whereas the Hagan at Powell Mountain is only slightly bioturbated and is dominated by Skolithos. This difference can be explained by the more distal (oceanward) paleogeographic position for the Rockwood at Whiteoak Mountain, Tennessee than for the Hagan Shale at Powell Mountain, Virginia. In contrast to the transgressive model proposed here and in earlier studies, Thompson (1984) interpreted the basal Rockwood to represent emergent deposits of shoreline sands and tidal channels prograding out over the underlying Sequatchie tidal flat sequence. Neither mudcracks nor channel deposits were detected in Facies A/HS, therefore, the transgressive model seems more appropriate than Thompson's emergent progradational model. In addition, an important characteristic of the Hagan at Powell Mountain, also observed at the base of the Rockwood by Easthouse (1987), is the presence of a thin basal lag zone and associated bioturbated sandstone. Swift (1968), Swift et al. (1971) and Swift (1975) described similar sand sheets and attributed their formation as a product of erosional shoreface retreat during an erosional or depositional transgression. Also called ravinement surfaces (Stamp, 1922), these condensed sequences usually represent a shoreline lag deposit produced by surf action cutting into underlying marsh, lagoonal, estuarine or tidal flat deposits, along a narrow zone at the foot of the shore face (Swift, 1968). Distinctive characteristics of ravinement surfaces mentioned by Swift include:

(1) generally a single, continuous sedimentation unit of thin to medium thickness;

(2) a sharp, flat, continuous lower bedding contact along this "sheet-like" bed;

(3) intrabasinal megaclasts, pebbles, abraded wood, bone or marine vertebrate fossil fragments commonly displaying textural grading;

(4) innershelf and estuarine or tidal flat lithosomes commonly juxtaposed with no intervening beach sands and

(5) a lack of interfingering between lithosomes in (4).

Facies A/HS shows all of the aforementioned characteristics and could represent a ravinement surface deposited across underlying Juniata sediments during the Late Ordovician/Early Silurian transgression.

Facies B/HS

Both heterolithic sub-facies of Facies B/HS show characteristics of being deposited in marine, sublittoral, storm-shelf settings. The mudstone and shale intercalated with the siltstone, sandstone and wackestone/packstone represent deposition below fairweather wave base but above storm wave base. The sandstone units show several features indicative of formation from initially strong currents which progressively waned over the entire depositional event. The stratigraphic relationships, geometry and internal sedimentary structures of these thin units suggest that they were formed when the quiet-water environment of the Hagan was punctuated by infrequent but

intense storms. The paucity of preserved body or trace fossils within the shale indicates biologic activity was low except during periods shortly after storms when intense surface waves, storm-surge-ebb currents and geostrophic flows oxygenated the offshore waters. According to Levington (1982), the factors controlling the abundance and distribution of marine-benthic organisms include wave energy, salinity, temperature, substrate consistency and oxygen content. Cluff (1980) concluded that of these limiting environmental factors, the most important one restricting organisms is a low dissolved oxygen content. The low levels of bioturbation and preserved body fossils within the water column could be related to reduced oxygen levels within the Hagan Shelf, however, another explanation can be gleaned from studies by Walker and Diehl (1986). These workers concluded that when sediment is initially deposited, the water content may be extremely high (> 60%) but decreases gradually with depth and as more sediment accumulates. This progressive sediment water loss results in an increase in shear strength. Walker and Diehl (1986) explained that these initial, overly soft ("soup-ground") substrate conditions can preclude colonization by most skeletonized as well as many soft-bodied burrowing taxa. However, lithological, and in rare cases, biogenic evidence preserved in the Hagan Shale indicates that the mud was of firm consistency. Pinch-and-swell, load casts, ball-and-pillow and other soft-sediment deformational structures are lacking in the Hagan. In most cases, lower bed boundaries are sharp and erosional or show scouring of the underlying mudstone. Even the thicker beds of Facies

B/HS (up to 7 cm) exhibit sharp/erosive contacts with the underlying shale. In addition, of the rare burrows that were observed within the shale, most contained sharp outlines or shear haloes indicating an initially firm substrate (Walker and Diehl, 1986). Therefore, an oxygen depth-stratification may have prevailed during Hagan deposition (see paleoenvironmental interpretations for Facies C/HS), however, this control is not necessarily mutually exclusive. It is quite possible that the paucity of taxa may be a function of a number of other environmental parameters, which are not always easily interpreted from the rock record.

The stratigraphic relationships of Facies B/HS indicate deposition in a sublittoral, storm-influenced, marine environment with background sedimentation dominated by suspension deposition of fine mud and clay. Shale dominates this facies, therefore a beach or delta-front environment can be eliminated as possible depositional regimes because their typical high energy conditions would tend to keep fine-grained particles in suspension (Walker, 1984). The siltstone, sandstone and wackestone/packstone beds punctuating shale horizons may be interpreted as washover fan deposits found in lagoons, however, this environmental model seems doubtful based on the absence of beach lag deposits, low angle cross-stratification and abundant parallel laminations (Reineck and Singh, 1980). In addition, no signs of subaerial exposure were found in the Hagan Shale Member further precluding any association with a lagoon or tidal flat environment. Conversely, a deep-water pelagic environment also seems unlikely for

Facies B/HS based on the presence of storm-generated sandstone beds (not turbidite deposits), sedimentary structures indicating shallower water (rare micro-hummocky cross-stratification) and the absence of a dark black color characteristic of anoxic mud.

The bedding geometry of both sub-facies in B/HS is not unlike the geometry described for other storm sequences in the rock record. Units in B1/HS are generally thicker and more continuous than in B2/HS, however, both subfacies show many geometrical similarities. In both subfacies, units are always under 10 cm thick and display sharp erosional bases. The bases of beds in B2/HS also commonly show small scours. These units pinch-out in both lateral directions on the outcrop face. Kreisa (1981), Hunter and Clifton (1982) and Mount (1982) described storm-generated bedding geometries similar to those found in the Hagan Shale. They attributed the nearly always sharp, erosional bases to have been formed during high-energy scouring conditions during storms. Kreisa (1981) mentioned that storm-generated oscillatory currents are more effective in eroding bottom sediment than unidirectional currents. His interpretations are based on findings by Madsen (1976) who concluded that oscillatory currents can exert a shear stress on the sediment several times larger than that of unidirectional currents of the same magnitude.

Average unit thickness in sub-facies B1/HS is greater and more continuous than thicknesses in B2/HS. While studying vertical variability trends in the Martinsburg Formation of southwestern Virginia, Kriesa (1981) used storm layer thickness as an indication of

relative water depth. Aigner and Reineck (1982) and Aigner (1985) also used storm layer thickness as an indicator of proximality changes within ancient shelves. Other parameters suggested by these authors include percentage of sand, frequency of storm layers, percentage of wave ripples, percentage of graded beds and amount of bioturbation. Of these indicators, the latter three were uncommon in the Hagan Shale, therefore proximality analysis was not applied by the present author. (Refer to Appendix III for a listing of storm bed thickness and its position above the base of the Hagan Shale). In clastic, carbonate and mixed clastic/carbonate sequences, average storm-layer thickness decreases from shallower to deeper water indicating a slightly deeper-water origin for sub-facies B2/HS than for B1/HS.

The sedimentary structures within the storm-generated units of Facies B/HS attest to their catastrophic origin. Figures 10 and 14 (see p. 33 and 40) illustrate major differences in the frequency of occurrence of the major sedimentary structures within both sub-facies. As with bedding thickness, the sedimentary structures in B2/HS point to a slightly deeper-water origin than for B1/HS.

Graded beds are more commonly found in sub-facies B2/HS than in sub-facies B1/HS. These intervals generally display coarse-grained quartz or fossil lags grading upward into very fine-grained sandstone or coarse siltstone. Aigner (1985) and Swift and Niedoroda (1985) concluded that graded deposits form as a continuous sheet during waning storm conditions. Kumar and Sanders (1976), Kreisa (1981),

Brenchley and Newall (1982), and Walker et. al (1985) also related terrigenous granule and/or fossil lags of a mixed assemblage to storm deposition. The more distal paleoenvironment of sub-facies B2/HS than of B1/HS is confirmed by the abundance of graded beds in the former. Swift and Niedoroda (1985) explained that graded storm units are the product of currents of a combined flow origin rather than a wholely unidirectional flow. Figure 45 incorporates this idea into the resulting sequence sedimentary structures formed on a clastic shelf. Notice that graded bedding is found on more distal reaches on the shelf.

Horizontal laminations are the most common sedimentary structure in both sub-facies. Other structures occurring in association with horizontal laminations include wave ripples, current ripples, form-discordant wave ripples, graded bedding and intraclasts (Fig. 46). Mount (1982) interpreted horizontal laminations in the Andrews Mountain Member of the Campito Formation (Lower Cambrian) to have been deposited by several different processes. First, as a product of high flow-regime, plane-bed deposition, secondly, as deposition from sediment-charged suspension clouds in current velocities lower than those which generate ripples, and, finally, as a plane-bed phase of sediment transport at low current velocities. The horizontal laminations found within Facies B/HS are associated with erosional bases, gutter casts, coarse-grained lag zones and rare flute casts, all which suggest deposition from energetic flows in the upper current regime. Under such conditions of high current-velocity and bottom

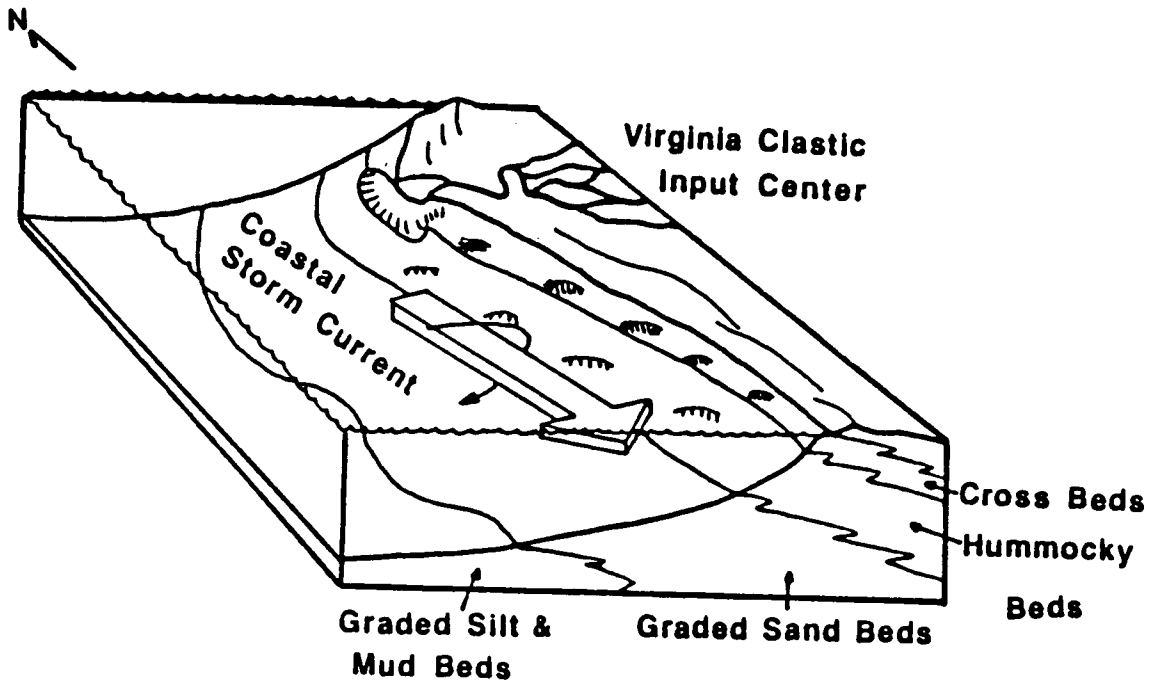


Figure 45. The Characteristic Lateral Progression of Sedimentary Structures Which are Found with Increasing Distance from the Shoreline (Taken from Driese et al., in press).

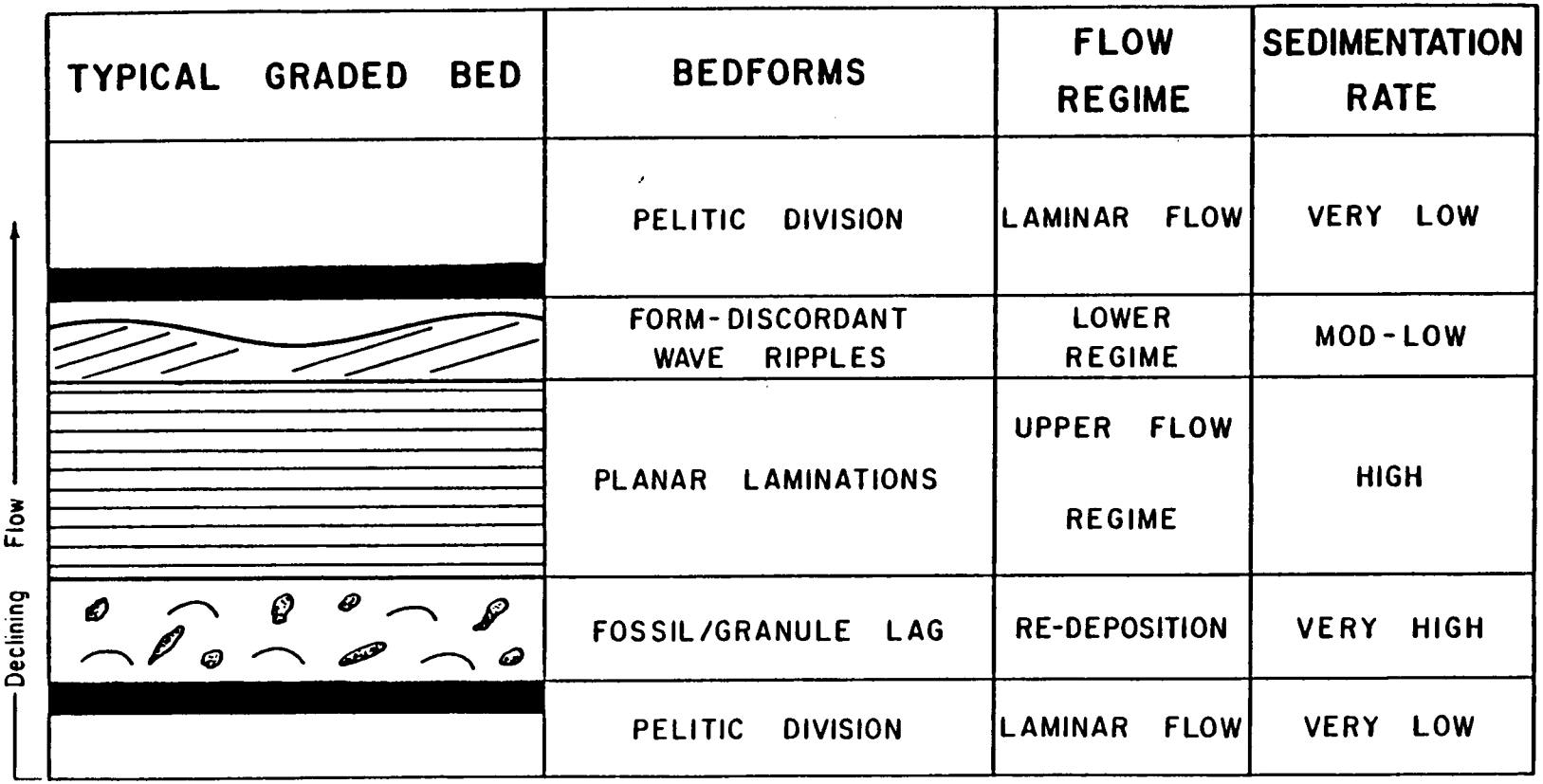


Figure 46. Vertical Sequence of Sedimentary Structure Association within a Single Bed. (Taken from Easthouse, 1987).

shear, the stable bed morphology is a planar surface. Easthouse (1987) arrived at similar conclusions for horizontal laminations and horizontal laminations associated with other sedimentary structures in the Rockwood Formation. These units are presumed to be offshore lateral equivalents of the Clinch Sandstone at Powell Mountain, Virginia.

Ripples are found in both sub-facies of Facies B/HS and occur as wave ripples, form-discordant wave ripples, and to a lesser extent, current ripples. In the case of sub-facies B1/HS wave ripples predominate, whereas in B2/HS form-discordant wave ripples and current ripples are the dominant forms. Most ripples do not exhibit well developed internal laminations.

Wave and form-discordant wave ripples are the dominant ripple varieties in sub-facies B1/HS. Komar (1984) and Brenchley (1985) both stated that the abundance of wave ripples over other forms suggests a proximal position to the shoreline. A zone of wave ripple maximum was defined by Aigner and Reineck (1982) as occurring in 7-15 meters of water for the Helgoland bight region of the North Sea. During storms and fairweather periods, the effects of oscillatory currents predominate in this zone shoreward, whereas at greater depths, the effects of oscillatory currents give way to unidirectional currents. Form-discordant wave ripples are also found in sub-facies B1/HS but are not as common and are generally restricted to higher stratigraphic intervals. These ripples were described by Harms (1969) and Aigner (1985) to be slightly asymmetrical, rounded and have weak

cross-laminations indicating deposition by unidirectional currents. Some ripples may be nearly symmetrical. These ripples indicate that both unidirectional currents and waves influenced the seafloor during storm conditions (Harms, 1969). The relative influence of each current type can be calculated by measuring the average spacing, length, pattern and orientation of the crests (Harms, 1969), however, such measurements may prove to be inaccurate due to their poor preservation and general paucity in the Hagan.

Current ripples are more common in sub-facies B2/HS, implying a strong unidirectional current-flow component predominating over an oscillatory component. Again, using the logic of Komar (1984) and Brenchley (1985) for interpreting wave and form-discordant wave ripples, it would seem evident that rocks in sub-facies B2/HS were deposited oceanward of sub-facies B1/HS. The oscillatory component during storms was weak in this environment which was probably below fairweather wave base. Unidirectional bottom currents originated from storm-surge-ebb effects during high-energy storm periods.

Intraclasts are generally found at the bases of wackestone and packstone units or exist in gutters; both features are common to sub-facies B2/HS. Most intraclasts are small (1 to 4 mm), light to dark gray mudstone and are best recognized petrographically. Petrographic analysis also indicates that these intraclasts are lithologically similar to the intercalated shale of sub-facies B2/HS. Kelling and Mullin (1975) and Aigner (1985) reported that storms commonly rip-up intraclasts of the underlying mud substrate and

transport them as coarse-grained terrigenous material along with allochthonous pebbles and shell debris. The mudstone intraclasts in sub-facies B2/HS are also located at the base of graded sequences (described earlier in this section).

Gutter casts are more commonly associated with the thin, irregular and lenticular sandstone beds of sub-facies B2/HS. These layers of thin and channelform bedding are extremely fine-grained and may be compared to the distal tempestites of Aigner (1985). Therefore, the above features further substantiate that sub-facies B2/HS is indeed a lateral, deeper-water equivalent and thus farther away from the coastal sand source than sub-facies B1/HS (proximal tempestites). Major characteristics and the origin of gutter casts will be discussed in the interpretation of Facies C/HS (next section).

Facies C/HS

Facies C/HS consists of moderately fissile to slightly blocky, medium to dark gray or light maroon-gray, generally homogenous shale. Faint and thin whisps of discontinuous siltstone and rare silt and mud-filled burrows (commonly Planolites) occur in limited areas. The depositional setting inferred for this lithology was a quiet one with low deposition rates. This environment was possibly located a little seaward of the depositional area of Facies B/HS. Brenchley and Newall (1982) envisioned similar lithologies in the Cheney Longville Formation (Ordovician of Wales) to form in an environment where normal conditions of sedimentation were mainly from suspension. A similar

interpretation is assigned to Facies C/HS because little evidence of bottom traction-transport is present.

The shale of this facies exhibits only minor amounts of bioturbation and is generally fissile. Byers (1974) concluded that the fissility of shale is related to the horizontal alignment of micaceous mineral grains in the sediment during suspension settling. The parallel orientation of these minerals is disrupted by the grazing and burrowing activities of benthic organisms, which results in a more blocky shale or mudstone. Only rare stratigraphic intervals were observed to have blocky shale. In addition, burrow traces were few and body fossils were generally limited to only two or so blocky shale beds. These fossils consist mainly of Lingula, and some articulate brachiopods, unfragmented and showing no signs of intense abrasion. Fossils were sparse in these zones and preservation was poor precluding the determination of life positions and taxonomic identification in general. Such rare, blocky and bioturbated horizons indicate that occasionally, environmental conditions were conducive for metazoan life. Overall, however, the substrate lacked organisms, leading to the speculation that oxygen levels were possibly low (Cluff, 1980). However, shales of Facies C/HS did not exhibit the characteristic deep black color, graptolite preservation, or a so-called "deep marine" trace fossil assemblage indicative of wholely anaerobic bottom conditions (Reineck and Singh, 1980). In addition, the shale of this facies is not unlike that which is intercalated with the sandstone of Facies B/HS, some of which occur only a few meters

above the subaerially exposed Juniata Formation. This similarity, combined with the relatively thin nature of C/HS shale, prevents one from assigning a moderately deep-water origin.

Using the biotope oxygen-zonation model for a three-layer basin from Byers (1977), the lithology of Facies C/HS may have been deposited near the base of the dysaerobic zone. In a stratified basin, this zone is situated within the pycnocline between the overlying aerobic zone (high dissolved oxygen content) and the underlying anaerobic zone (no dissolved oxygen). In this middle layer, indigenous, calcareous epifauna are lacking but sediment is bioturbated due to the activities of opportunistic organisms. In the underlying anaerobic zone, all types of metazoan activity (both epifaunal and infaunal) are extremely low to absent. Therefore, it seems likely that the shale of Facies C/HS was deposited near the dysaerobic/anaerobic boundary. No Bouma sequences were observed in Facies C/HS. The thin siltstone wisps and small silt-filled gutter casts rarely found in Facies C/HS indicate that some type of current action rarely reached the more distal depositional setting of Facies C/HS. The thin, discontinuous siltstone wisps could have been formed by the outermost pulses of sediment-charged water carried seaward by a storm-surge-ebb current. The small, separated gutter casts represent horizontal helicoidal flows hugging the seafloor (Whittaker, 1973). Whittaker also mentioned that separated gutter casts indicate low sediment supply, another feature not in disagreement with distal shelf environmental interpretations. It should be noted that the helicoidal

flows responsible for gutter cast formation need not be solely limited to shallow water or nearshore conditions as demonstrated by McBride (1962) and Tucker (1969) who worked in turbidite successions.

To summarize, the dominantly homogenous, thin shale intervals of Facies C/HS were laid down in environments where quiet-water "background" sedimentation prevailed. Mud accumulation was by suspension settling interrupted rarely by the distal reaches of unidirectional storm currents. Biologic activity was limited. The paleographic setting of this facies existed oceanward of Facies B/HS and may represent several minor transgressions or simply periods of diminishing sand supply during Hagan time.

Facies D/HS

Facies D/HS occurs in the middle and upper parts of the Hagan Shale and consists of only four beds surrounded by sub-facies B2/HS. Because of their varied lithologic composition, unique bedding geometry, differing sedimentary structures and moderate iron-mineralization, these units are quite unlike the surrounding thinly bedded, heterolithic lithology and warrant a separate facies classification.

The packstone, fossiliferous quartzarenite and ferruginous conglomeratic units of Facies D/HS represent deposition in the transition zone by a combination of normal tidal and storm-generated bottom-traction currents. The internal trough cross-stratification and form-discordant wave- and current-rippled upper surfaces were

generated by three-dimensional ripples and dunes migrating across offshore shoals or bars which were detached from any shoreline facies.

The lithology of Facies D/HS is markedly different from that of any other facies in the Hagan Shale. Found particularly at the bases of these units are maroon mud intraclasts, coarse-grained sedimentary rock fragments and a wide variety of suspension feeder traces. Most of the coarse-grained sedimentary particles are allochthonous to the proposed sublittoral marine bar environment and were probably introduced by storm processes. The mud intraclasts are flat and disc-shaped. The chert and other sedimentary rock fragments are well-rounded with partial weathering of the enclosed clay and iron-minerals. Body fossils are commonly fragmented and show some signs of abrasion. Goldring and Bridges (1973) discussed the fact that fossils of suspension-feeders are common to abundant in Phanerozoic sublittoral sheet sandstones deposits. Petrographic analysis also reveals a host of accessory minerals including phosphate nodules and glauconite. These two minerals, coupled with the presence of open-marine body fossils and a Cruziana/Skolithos trace fossil assemblage, attest to an offshore shallow-marine site of deposition. It is proposed that storms occasionally scoured the adjacent tidal flats and intershoal areas introducing mud chips and body fossils into this offshore shoal setting. Fairweather tidal processes restored the ripple and dune bedforms to the shoal which further reworked the newly introduced material.

The geometry of the units in Facies D/HS is varied and problematic. Upper and lower bedding surfaces are sharp and either flat or sculptured. The ferruginous bryozoan packstone units (11.9 and 12.2 m) have extremely sharp/flat boundaries and pinch-out laterally.

The sharp erosional lower bed boundaries are inferred to have been formed by the scouring currents of storms (Cotter, 1983a), whereas the rare cross-stratification and rippled upper surfaces represent fairweather reworking. Mount (1982) found similar features in his S2 sub-facies of the Andrews Mountain Member of the Campito Formation (Lower Cambrian). The laterally discontinuous tabular geometry with some evidence for continuous currents is inferred to represent development of some type of shoal or bar. Sculptured upper surfaces are another interesting feature of bed morphology which suggest the influence of storms. Several fluted erosional forms can be observed at the margins of the sandstone where it abruptly terminates against the shale. Cotter (1983b) described similar features in the Tuscarora Formation in Pennsylvania. He attributed the sculptured upper bedding surfaces to have been formed during storm conditions when high-energy currents eroded and entrained sediment of an earlier storm deposit.

The sedimentary structures found within Facies D/HS also support a storm origin for the beds with later reworking by ripple and dune bedforms operating on the offshore shoal or bar. Massive bedding predominates over trough cross-stratification in Facies D/HS. The

packstone units which exhibit massive bedding have gross features consistent with a storm-bed origin, but unfortunately lack internal evidence. Cotter (1983b) reported that this type of bedding is commonly composed of coarse skeletal debris and is therefore unfavorable for the generation of sedimentary structures such as are found in finer-grained rocks. Some units in D/HS, especially the fossiliferous quartzarenite, display small-scale trough cross-stratification. In addition, there are numerous occurrences of form-discordant wave ripples, current ripples, and current ripple cross-laminations. Planar and wavy horizontal laminations were also observed. The cross-stratification along with transported fossils, sedimentary rock fragments and mud intraclasts suggest that some of the tabular sand bodies in D/HS were built by traction transport of sand by dunes and ripples. At times, current velocity must have exceeded the lower-flow-regime (during storms?) as inferred by the interstratified parallel laminations.

The sedimentary structures in Facies D/HS indicate storm and to a lesser degree fairweather conditions, however, evidence for tidal currents is weak in this facies. Paleocurrent data are sparse with the exception of basal scour features and preferential alignment of fossils. Meager data obtained from these paleocurrent indicators shows a west-northwest (offshore) flowing current.

Traces of iron-mineralization occur in some storm units throughout the Hagan Shale, however, the greatest concentrations exist within Facies D/HS. The ferruginous sandstone conglomerate contains

the most iron (up to 5 percent), with subordinate amounts occurring in the packstone and quartzarenite beds. Iron-mineralization in the latter two units occurs as only traces of hematite, both coating as well as partially replacing skeletal grains. In the sandstone conglomerate (located only 2 m below the contact with the overlying Poor Valley Ridge Sandstone) hematite and minor amounts of glauconite and limonite are found replacing fossils, coating sedimentary rock fragments and filling intergrain areas as amorphous cements.

Although at lower concentrations and frequencies of occurrence, the iron mineralization in the Hagan Shale is not unlike the ferruginous rocks described in the Rockwood Formation by Easthouse (1987). Tropical humid areas of low relief and tectonic activity seem favorable for the supply of iron concentrations in surface waters (Blatt et al., 1972). Hunter (1970) studied the iron-ores of the (Late) Silurian Clinton Group (equivalent to the Rose Hill Formation at Powell Mountain) and concluded that the iron and clastic material had a coexisting source, that being the land area to the east of the Silurian depositional basin. Hunter (1970) concluded that the key environmental factors promoting the concentration of iron-minerals in the sediments are restricted circulation in a shallow-marine setting. The amount of clastic sediment input should also be low to prevent mixing of iron-minerals with other sediments. Cotter (1983b) speculated that Clinton iron-mineralization took place when the input of terrigenous clastics to the Appalachian Basin had lessened. In addition, both hydrated iron-oxides and clay minerals had to be in the

proper compositions/concentrations in suspension for the precipitation of iron to have taken place (Cotter, 1983). The iron ores in the Rockwood Formation were interpreted by Easthouse (1987) to have been deposited in shallow, well-aerated seas, where the water was both warm and clean. The following environmental model proposed by Easthouse (1987) will be adopted for the iron units in Facies D/HS. He postulated that rivers flowing off the Tactonic Highlands transported iron in solution to lagoons or other restricted areas where the low clastic load would immediately be dropped. The iron, still in solution, would pass through this zone and eventually mix with the open ocean water. In this environment, iron would then precipitate out of solution as coatings on sand grains and skeletal debris. For a more detailed environmental interpretation as well as an excellent summary of the environmental conditions of iron formation see Easthouse (1987).

To summarize the paleoenvironmental model for Facies D/HS, the effects of minor fairweather processes are combined with the scouring effects of storms. Infrequent but strong bottom-traction currents generated by storms introduced terrigenous and skeletal material onto a shelf experiencing low depositional rates. These thicker, more proximal units of Facies D/HS are stratigraphically enclosed amongst the deeper water deposits of sub-facies B2/HS, a relationship possibly indicating minor regressions superimposed on the overall Early Silurian transgression. Substantial amounts of iron-mineralization attest to lower sedimentation rates and a possible minor regression

during these periods. The sublittoral sand and skeletal sheets were occasionally reworked by fairweather (tidal?) processes justified by the small-scale trough cross-stratification and form-discordant wave ripples.

Poor Valley Ridge Sandstone Member

General

Most of the nearly 28 meter-thick succession of Poor Valley Ridge quartzarenite is interpreted to have been formed in a combined storm- and tide-dominated innershelf setting by the migration of large asymmetrical sand waves. Sand deposition took place when ebb tidal currents were enhanced by storm processes. The compound cross-bedding was produced by the migration of dune bedforms superimposed on the stoss and lee sides of large sand waves. Frequent current reversals caused dunes to occasionally migrate to the flood direction. The geometry of second-order bounding surfaces (giant forsets) and the tabular and wedge-shape bodies they enclose resemble the Class V sand wave model proposed by Allen (1980a).

The remainder of this chapter will document the probable marine shelf sand wave-complex origin of the Poor Valley Ridge Member of the Clinch Sandstone. First, however, the known characteristics of modern sand waves will be explained. In the discussion that follows, evidence will be given for the recognition of sand wave features in the rocks at Powell Mountain. Each separate facies within the Poor Valley Ridge Sandstone represents a unique paleoenvironment associated

with the sand wave complex. A section will be included listing reasons why the Powell Mountain outcrop does not fit the sand ridge (or sand bank) model proposed by Fischer (1987) for the Clinch Sandstone at Clinch Mountain. Finally, a model of another documented ancient sand wave deposit is presented in an attempt to further elucidate the recognition of these complex sand bodies.

Modern Sand Waves

Definition. There seems to be some confusion in the literature regarding the loose terminology used for bedforms found on continental shelves. Houbolt (1968) differentiated two major classes of bedforms, those longitudinal to current flow and those whose crestlines are orientated transverse to flow. He uses the word "ridge" for an elongated rise on the seafloor, either straight or curving, several meters high with the longitudinal axis (crestline) situated parallel to current flow (storm and/or tide). Synonyms used are tidal current ridge, sand bank or rug. Transverse bedforms, namely megaripples, are usually smaller. Synonyms used are sand wave, under-water dune or large sand ripple. Brenner (1980) placed quantitative limits on his terms for both longitudinal and transverse bedforms. His longitudinal bedforms include sand ribbons, which are low-amplitude sand strips on a coarse substrate; longitudinal furrows, which consist of strips of coarse sand or coarser material; and sand ridges, larger features which attain heights of 10 m or more above the surrounding seafloor with wave lengths in the range of kilometers. Transverse bedforms,

however, include ripples (wave lengths up to 60 cm) and sand waves (wave lengths greater than 60 cm) (Fig. 47). Boersma and Terwindt (1981) differentiated between sand waves and dunes (megaripples). They stated that sand waves have a high length-to-height ratio with continuous, straight to smooth-undulating crestlines and a general absence of scour pits. They occur in moderate current velocities. Dunes, however, have a low length-to-height ratio, sinuous-discontinuous crests and commonly show deep scours in the troughs. Dunes exist under velocities exceeding those of sand waves (Boersma and Terwindt, 1981). Nio and Nelson (1982) found that sheet-like sand bodies consist of a complex vertical development of two major bedforms, sand banks and sand waves. They classified both features based on their dimensions, heights and wavelengths. Sand banks are larger than sand waves and may reach to up 120 kilometers in length and 30 kilometers in width. Sand waves are generally smaller, and may occur either climbing up both flanks of the sand bank, on the crest, or in the depressions between two successive sand banks. Furthermore, they may also occur as isolated features not directly associated with sand banks. Isolated varieties are of larger-scale and commonly attain heights of 6 m but may reach 15 m. Wavelengths in general are at least 10 times that of the heights. This variety of isolated large-scale sand waves are inferred to have formed the bulk of the Poor Valley Ridge Sandstone on Powell Mountain, southwestern, Virginia.

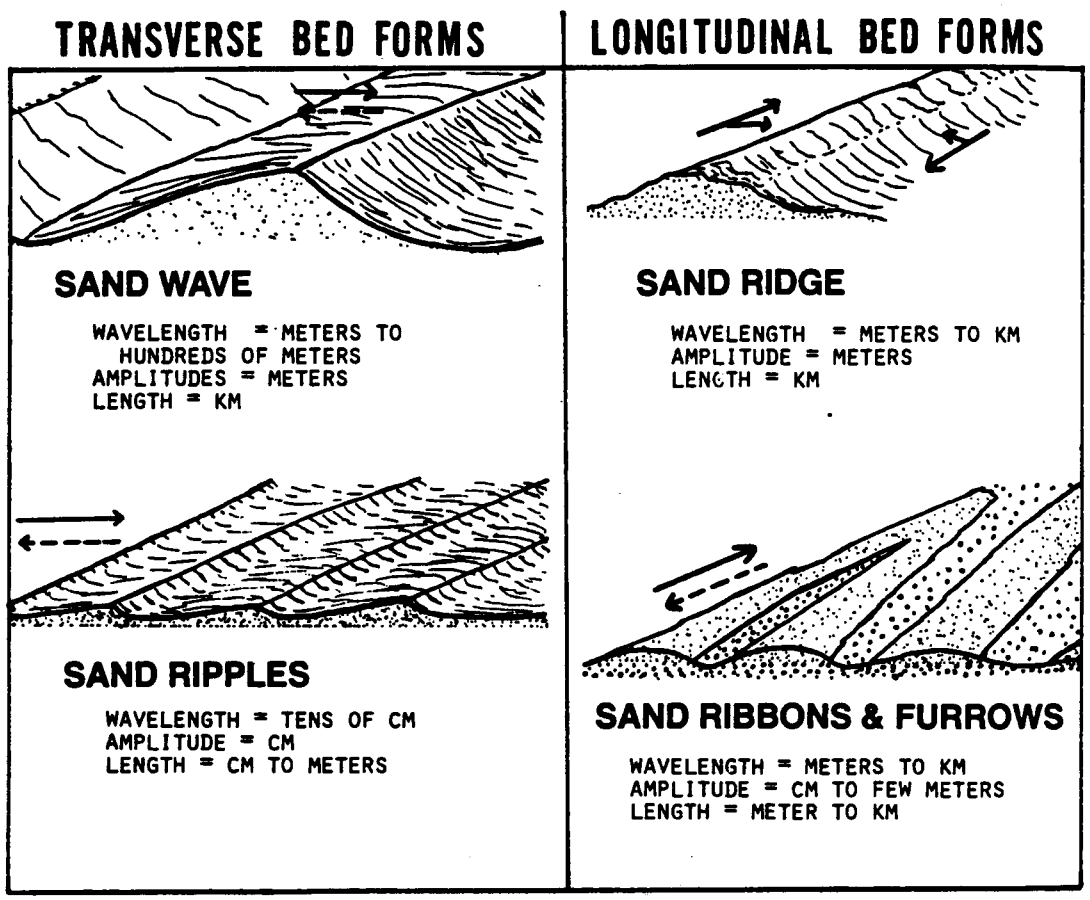


Figure 47. Geometry of Transverse and Longitudinal Bedforms Found on Continental Shelves. (Taken from Brenner, 1980).

Occurrence

Both large- and small-scale sand waves have been recognized in several kinds of modern environments since the pioneering work in the Netherlands by Van Veen (1935). These bedforms are found in complex channels of sandy coastal barriers and estuaries, restricted tide-swept seas, the approaches to major rivers and on shelf environments or shallow-marine platforms. Modern sand waves and related structures have been documented extensively in the North Sea (Stride and Tucker, 1960; U.N.D. Caston, 1965; Houbolt, 1968; Boersma, 19169; Stride, 1970; Kenyon and Stride, 1970; Belderson et al., 1971; McCave, 1971; Terwindt, 1971; Langhorne, 1973; Allen, 1980a; Boersma and Terwindt, 1981; Stride, 1982 and Nio and Nelson, 1982). Work on the Atlantic shelf includes that of Jordan, 1962; Steward and Jordan, 1964; Drapeau, 1970; Swift, 1975; and Hunt et al., 1977. The sand waves which are the focus of this study occur on the continental shelf or shallow sea setting, generally in tens to a hundred or so meters of water with heights of several meters and wavelengths of hundreds of meters. Allen (1980a) stated that wavelengths range from the order of 25 m under intertidal and shallow subtidal conditions to 1000 m in the deeper subtidal (100 m depth). The heights of these sand waves vary from 1-25 m.

Sand waves form on the continental shelf in current velocities slightly less than those necessary for the formation and maintenance of the larger sand banks and sand ribbons (Belderson et al., 1977; Hunt et al., 1977). Figure 48 is a block diagram illustrating the regular

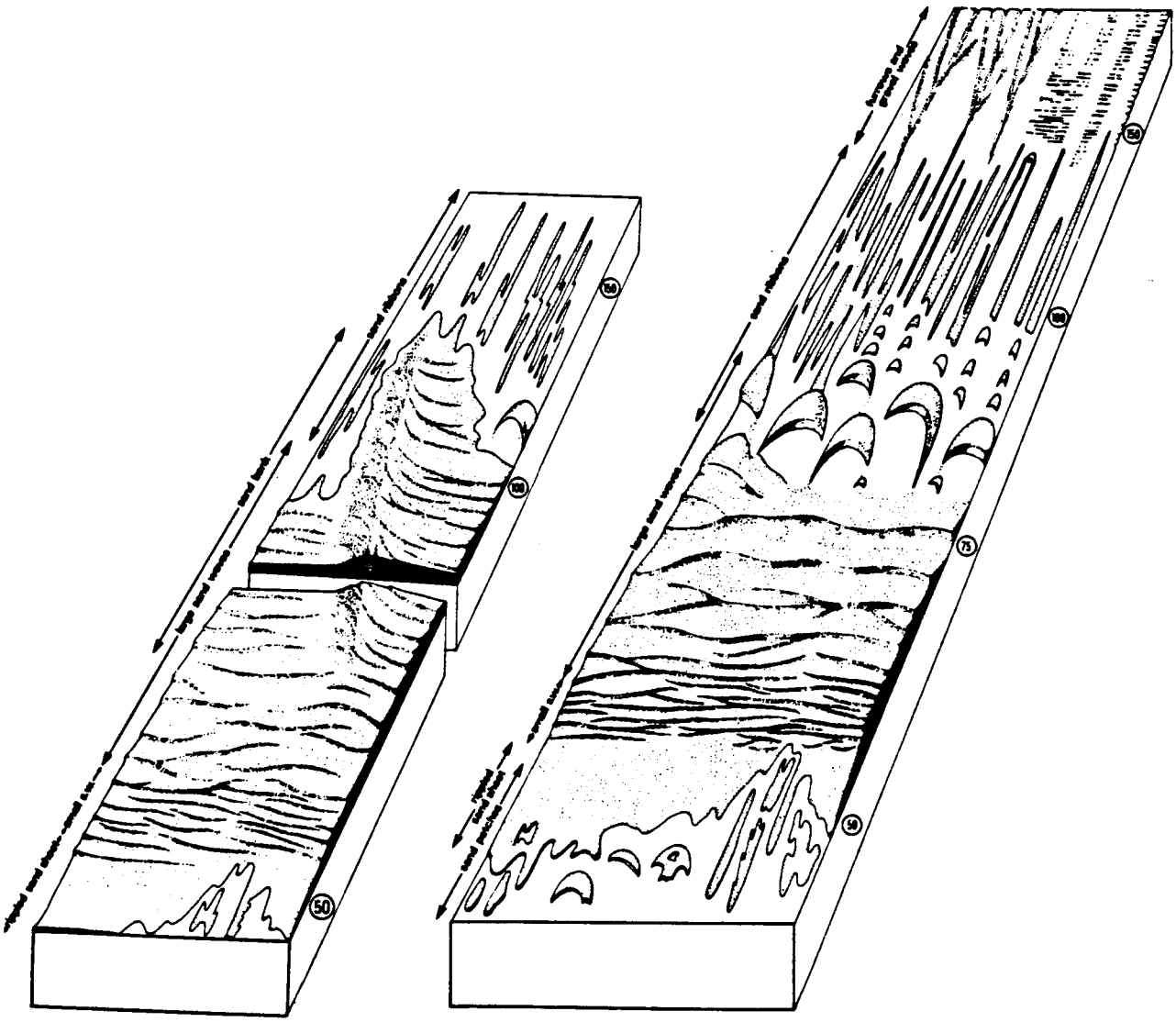


Figure 48. Block Diagram Illustrating the Sequence of Bedforms Generated on a Continental Shelf. Numbers indicate the mean spring near-surface tidal current velocity in cm/s. (Taken from Stride, 1982).

sequence of bedforms generated by tidal currents on continental shelves. Note that the sand waves occur seaward of the sand ridge (bank) facies. A slight shifting in their geographical position as well as changes in overall bedform geometry can be induced by storm currents or wind shear superimposed upon tidal currents, however, this generalized sequence of large scale tidal bedforms can be used for the purposes of this study.

Formation

The conditions governing the transition from ripples to sand waves have rarely been studied in flume work (Stride, 1982). However, it is well known that as current speed increases, smoothing of the sand ripples begins to take place at about 50 cm/sec. Longer wavelength bedforms (very low-height sand waves) begin to appear soon afterward over a very narrow velocity range of only a few centimeters per second (Middleton and Southard, 1984). The large-scale, well developed sand waves are maintained at higher current velocities usually exceeding 1 m/sec. Allen (1968) suggested that ripples are the consequence of transverse flow perturbations within the boundary layer whereas large sand waves form by transverse perturbations over much of the entire flow. Sand wave deposition is controlled mainly by the dominant current in the tidal ellipse (in most documented cases, generally the ebb current) which may also be enhanced by storm-return bottom flow (Belderson et al., 1977). These authors attributed wind-driven

currents and waves during the yearly maximum of the spring tide to be responsible for much of the sand wave construction.

Lateral Variations

Shelf sand waves forming closer to the shoreline are generally under the influence of strong reversing tidal currents, which commonly change the bedform's overall asymmetry during each ebb and flood current (Allen, 1980a). Moreover, these reversing currents are capable of generating and maintaining regularly spaced sand waves. Despite such vigorous currents (speeds of 1.5 m/sec are not exceptional) the resulting bedforms are very slow moving and symmetrical in form (Terwindt, 1970; McCave, 1971; Langhorne, 1973; Allen, 1980a) and net sand transport in these regions is almost zero. These intertidal/shallow subtidal sand waves commonly contain coarse sand and are mantled by megaripples (large ripples or small dunes) climbing both ebb and flood flanks. Sand wave height in this region may reach 5 m, but is generally smaller.

The symmetrical profile grades to more asymmetrical forms in the offshore direction (Stride, 1970; Terwindt, 1970; McCave, 1971; Brenner, 1980). As the water depth increases in the offshore direction, mean grain size, amplitude and wavelength of the sand waves decrease. These generalizations are seldom without variations in modern shelf environments. Quite commonly, the small, symmetrical intertidal sand waves may grade seaward to extremely large scale asymmetrical ones with heights of 8-12 m and wavelengths of several

hundred or thousands of meters. Even farther offshore, large sand waves stay asymmetrical but only obtain heights of a meter or so. Stride (1965) suggested that the asymmetry of their cross-sectional profiles suggested that they are moved forward (offshore) by removal of material from the gentle slope (facing shoreward) for deposition on the steeper lee slope. His study area was in a section of the North Sea where the ebb current was stronger than the flood current. Belderson and Stride (1969) reasserted that the direction of bed-load transport in tidal seas is determined by an asymmetry in the current elipse (peak current velocity in one direction greater than that reached in the other). However, the degree of tidal asymmetry need not be great for net sand transport in the direction of strongest flow (Belderson and Stride, 1969). The estimated average net rate of advance of large sand waves (about 6 m high) was calculated by Langeraas (1966) off the Dutch coast to be much less than 60 m/y.

Sand waves forming in the outermost reaches of continental shelves generally have a very low amplitude and wavelength. Grain size continues to decrease to very fine sand and the megaripples tend to disappear off the backs of the bedforms. Stride et al. (1982) constructed a hypothetical model of the changes in sand wave internal structure spaced along a transport path in the offshore direction (Fig. 49). Tidal rhythmic bedding (found closer to shore), wave and current ripple bedding and mud laminae (mud chips in offshore areas) are not illustrated on the diagram. Changes in sand wave morphology due to decreased current strength were noted by Terwindt (1971) and

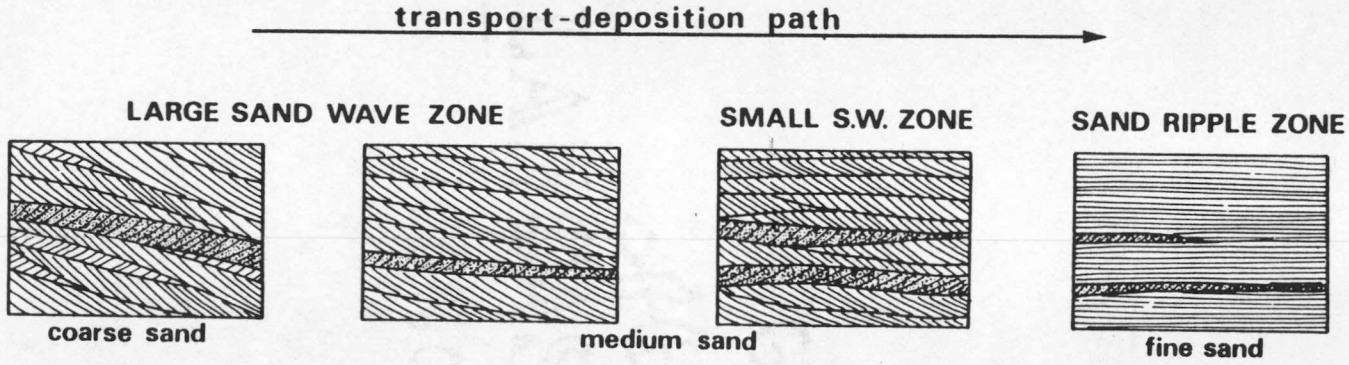


Figure 49. Changes in Sand Wave Internal Structure Spaced Along a Line of Net Sand Transport-Deposition. Tidal rhythmic bedding and wave and current ripple-bedding as well as probable mud laminae are not shown, but are commonly present. The amount of cross-bedding produced by storms increases in the offshore direction. (Taken from Stride, 1982).

Stride (1970). These authors concluded that in the southern bight of the North Sea, there is a relation between the maximum tidal current strength and sand wave height. Therefore the highest sand waves are not necessarily encountered in areas with the highest current velocities. Jordan (1962) working on Georges Bank, also found no correlation, however, he discovered an apparent correlation in the ratios of height to wavelength. In addition, he observed temporal changes in sand wave morphology based on measurements several months apart. The major changes were bifurcation or branching of sand wave crestlines (similar to that found in wave ripples) caused by unequal pulses in the ebb current. Langhorne (1973) surveyed sand waves in the outer Thames Estuary 14 months apart using side scan sonar. He also noted that the most pronounced temporal changes in sand wave character are associated with crestline branching in which the point of bifurcation moves laterally along the crests.

Internal Structures

Although much is known concerning the morphology and distribution of modern sand waves, their internal structures and controlling hydrodynamics have been neglected. According to Allen (1980a), two factors are obstructing the progress toward understanding the internal sedimentary features:

(1) the great financial cost and technical difficulty of sampling under strong tidal conditions, and

(2) the tendency amongst investigators to study sand waves with results derived from bedforms produced solely from unidirectional flows and ignoring the complexity of oscillatory boundary layers common in sand wave environments.

Most studies use observations of smaller intertidal sand waves, or are based on predictions from the movement and configuration of smaller superimposed bedforms migrating across the backs of larger sand waves (Blakey, 1984). Therefore, direct observations of the internal geometry of modern, large-scale sand waves have not yet been possible. Allen (1980a) found that the character of the sand wave's internal structure depends on the strength and degree of asymmetry of the governing currents. Sand waves formed in currents of low asymmetry contain small-scale herringbone or climbing cross-bedded sets. Asymmetrical currents produce a sand wave of asymmetrical profile, resulting in flow separation over the lee side of the bedform. The predominant internal structure is then expected to be long avalanche bedding divided into sets by mud drapes and bioturbated zones (Classes I through III, Fig. 50). These sets are commonly bundled and have been documented by many workers including Visser (1980) and Driese (1987). Couplets are formed by individual ebb, flood and slack-water events and are diagnostic of tidal environments and facies (Fig. 51). Driese (1987) observed bundled forsets in the Clinch Sandstone strike belts east of Powell Mountain, which he classified as the double clay drape variety consisting of: laminated sandstone, tens of centimeters thick ⟶ clay drape, mm thick ⟶ thin sandstone

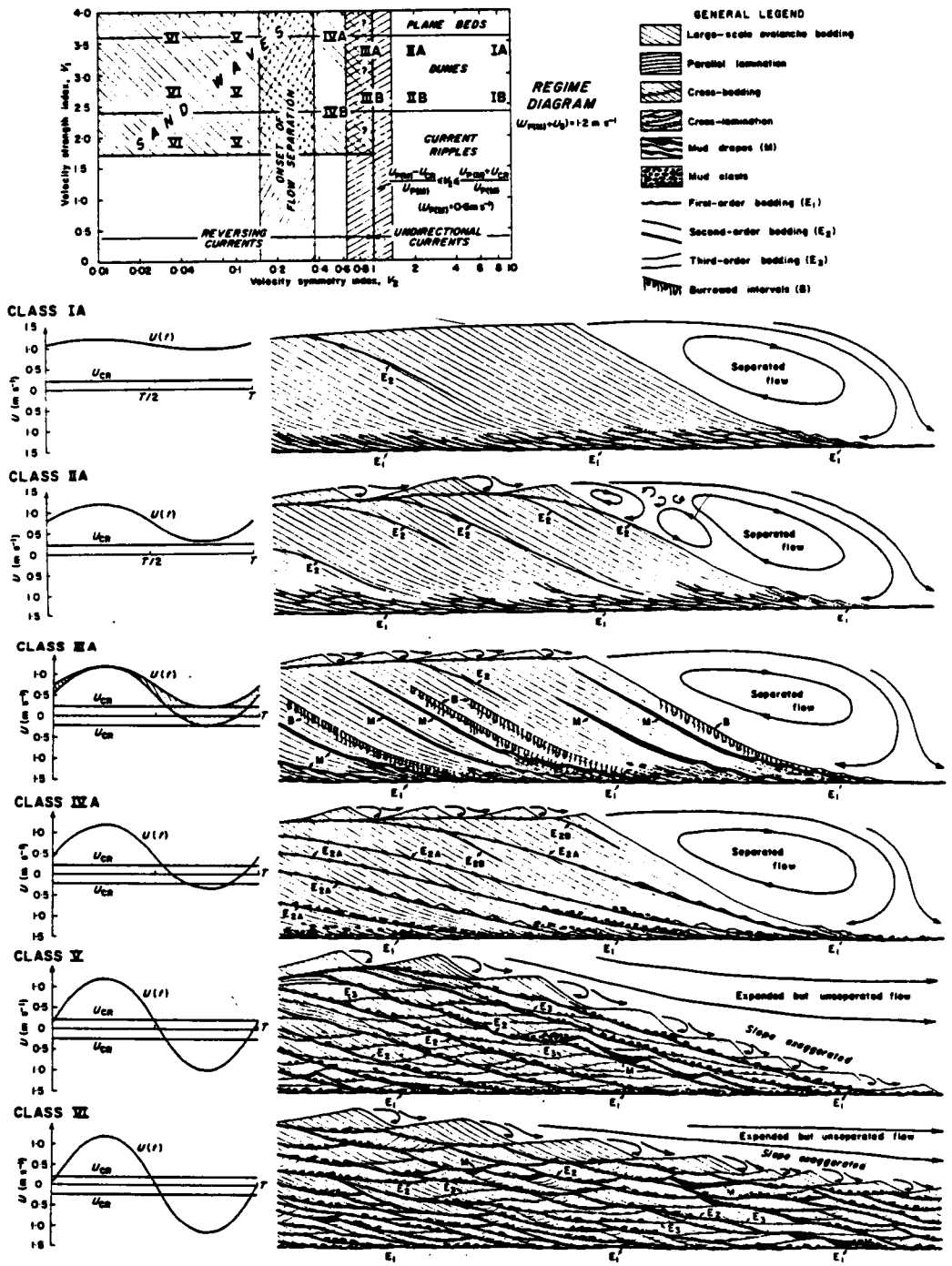


Figure 50. Regime Diagram of Dune and Sand Wave Internal Structure. The sand waves responsible for the deposition of the Poor Valley Ridge Member of the Clinch Sandstone may have had an internal geometry resembling that of Class V. (Taken from Allen, 1980a).

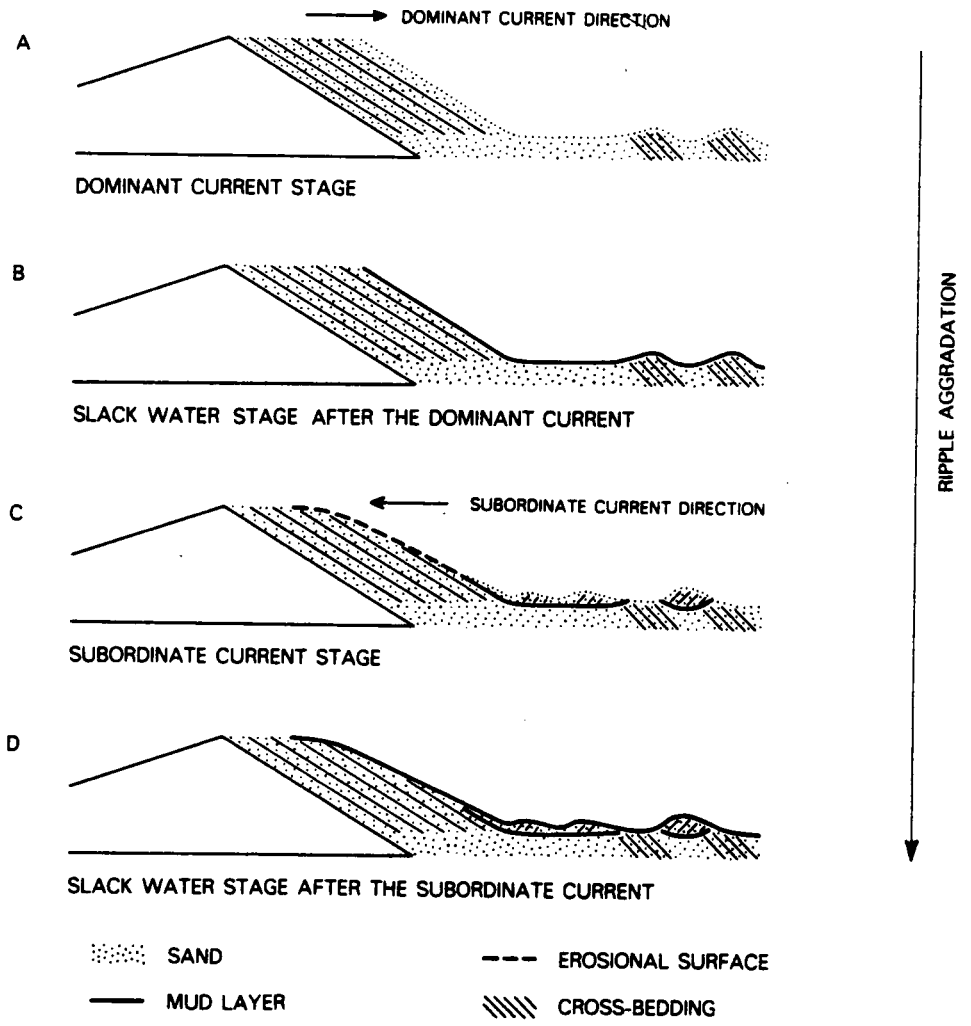


Figure 51. Internal Changes of a Ripple During the Four Stages of a Tidal Cycle. The small-scale cross-bedding generated by the subordinate current strongly resembles, but is not caused by back flow. (Taken from Visser, 1980).

with ripple forms, less than two cm thick → clay drape, mm thick (Driese, 1987). Mud chips commonly replace the more continuous drapes in offshore areas influenced by storms.

In the majority of offshore, large-scale sand waves, the preserved internal structure is the result of migration of superimposed dunes eroding the sand wave's stoss side and depositing material on the lee flank during tide and/or storm flows. The resulting internal structure resembles Allen's Classes IV, V and VI sand wave models. The dominant internal structure consists of compound cross-bedding of trough or planar sets. Master bedding generally consists of large-scale foresets on the order of several tens of cm thick and tens of m in length, dipping from 5-25° from the horizontal. These large-scale foresets and the internal cross-bedding they enclose generally dip in the same direction and the latter may sometimes occur in climbing sets divided by third-order erosional surfaces. Similarly Stride et al. (1982) found that the majority of the sand wave's internal cross-bedding was produced by smaller megaripples passing over them. These workers add that the sinuosity of sand wave crests, together with the oblique orientation of the superimposed megaripples and the presence of small current ripples (commonly produced at the base of the lee slope during backflow) will result in a three-dimensional and extremely complex array of compound cross-bedding (Fig. 52). Ripples and megaripples have also been observed on modern sand waves by several other workers (Drapeau, 1970;

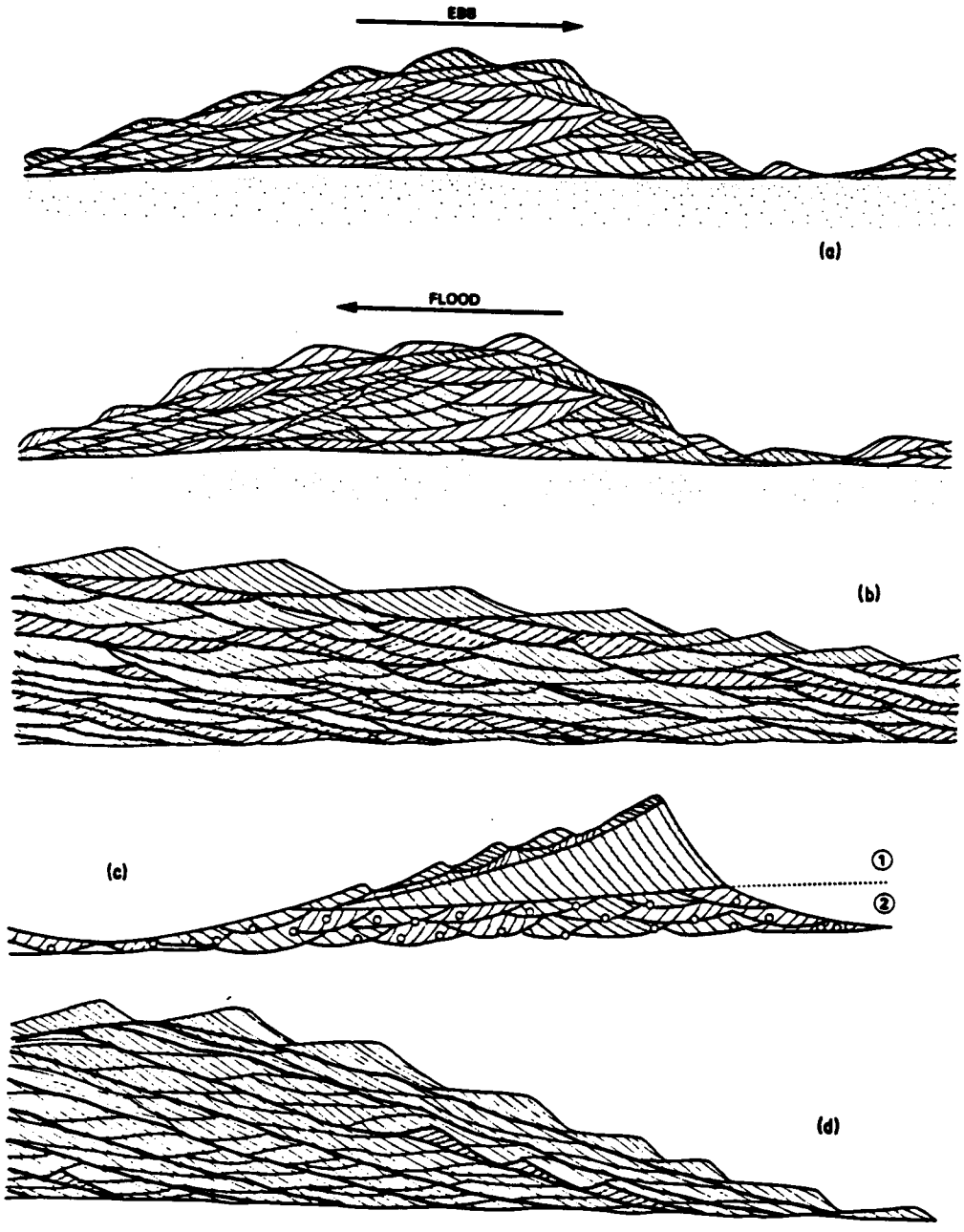


Figure 52. Complex Internal Structures of Sand Waves with Megaripples Migrating Upon their Slopes. (a) Internal structure from a region of strong ebb and flood tidal currents (after Reineck, 1963). (b) Internal structure of a symmetrical sand wave (after Allen, 1980a). (c) Hypothetical cross-section to show internal structure of a large asymmetrical sand wave with small sand waves climbing up both slopes (after McCave, 1971). (d) Internal structure of an asymmetrical sand wave as visualized by Allen (1980a). (Taken from Stride, 1982).

Terwindt, 1970; Langhorne, 1973; Hunt et al., 1977; Allen, 1980a; Brenner, 1980).

Sand Waves in the Geological Record

Some of the criteria used to substantiate a sand wave origin for the Clinch Sandstone at Powell Mountain have been used by other workers (Table 1). However, there still exist few documented examples of sand wave deposits in the literature. In addition, examples with a structure fully in accord with that of Allen's (1980a) Class V sand wave model (proposed for the Poor Valley Ridge Sandstone at Powell Mountain) have rarely been described from the stratigraphic record. Serving as a comparison, the Permian Rancho Rojo Member of the Schnebly Hill Formation (Blakey, 1984) shows features similar to the Clinch. An "identical fit" between the Poor Valley Ridge and Rancho Rojo Members is precluded by minor differences in their genesis.

Blakey (1984) interpreted the large-scale cross-stratification in compound sets several meters thick to be formed by a submarine sand wave complex. He based his conclusions on the geometry, stratigraphic sequencing and sedimentary structures preserved in the rocks. The Rancho Rojo was subdivided into five facies, three of which will be discussed (Table 2). The facies are sequentially ordered representing increasing stratigraphic height. The lowermost Planar-Tabular Foreset Facies consists of laminated and cross-laminated sets of planar-tabular cross-stratified sandstone.

Table 1

Criteria Used to Document Sand Wave Deposits in the Stratigraphic Record

Author(s)	Unit and Age	Location	Important Criteria
Baars and Seager 1970	White Rim Sandstone, Permian	Southern Utah	Geometry and sedimentary structures.
Pryor and Amaral 1971	St. Peter Sandstone, Ordovician	Southern Wisconsin	Large-scale compound cross strata.
Hobday and Reading 1972	Skallneset Sandstones, Precambrian	North Norway	Mineralogy, texture, erosion surfaces; coarsening upwards sequences.
Johnson 1975	Ekkeroy Formation, Precambrian	North Norway	Commonly cited tidal criteria and absence of emergent features.
Anderton 1976	Jura Quartzite, Precambrian	Scotland	Erosion surfaces; "best fit."
Nio 1976	Roda Sandstone, Eocene Lower Greensand, Cretaceous Swiss Molasse, Miocene	Spain Southern England Switzerland	Arguments based on stratigraphic succession.
Johnson 1977	Tanafjord Group, Precambrian	North Norway	Process analogs with modern sand waves.
Hobday and Tankard 1978	Peninsula Formation, lower Paleozoic	South Africa	Partial analogs with modern sand waves; facies relations.
Brenner 1980	Jurassic-Cretaceous	Western U.S.	Partial analogs with modern sand waves.
Visser 1980	Holocene	The Netherlands	Bundles of mud-layer couplets—their relation to tidal processes.
Banarjee 1980	Eze-Aku Formation, Upper Cretaceous	Nigeria	Sedimentary structures, vertical sequences, geometry.

Source: Blakey, 1984.

Table 2

Important Characteristics and Interpretations of the Facies in the Rancho Rojo Sand Body

Facies	Major Characteristics	Distribution	Interpretation
Planar-tabular foreset facies	Westward-dipping internal bedding planes with dips of 12–21°. Laminae between foreset planes are parallel or slightly inclined to the surfaces. Thin even to wavy laminae, slightly thicker, homogeneous sand layers and structureless sand with mud chips are dominant stratification types.	Most abundant near base of lower unit.	Deposited as relatively steep-faces, straight-creasted large sand waves that lacked superimposed dunes on lee slopes. Grain fall, grain avalanche, and storm-surge suspension deposits dominate.
Intraset cross-stratified facies	Westward-dipping internal bedding planes with dips of up to 9°. Complex intrasets between bedding planes; herringbone pattern common. Both planar and trough cross-stratification common. Rare *Planolites*like trace fossils.	Most abundant near middle of lower unit.	Deposited by sand waves with lower lee slopes and possibly less asymmetrical. Internal laminae formed by migrating dunes on lee slopes.
Trough cross-stratified facies	Trough-shaped erosional features dominate. Low angle of dip on surfaces. Trough laminae dominate between trough erosion surfaces. Major westward-dipping surfaces typically obscured by troughs. Rare *Skolithos*like trace fossils.	Most abundant at top of lower unit.	Deposited by sand waves with low-angle lee slopes. May have been nearly symmetrical. Sand waves totally mantled by undulatory dunes. Dunes shifted in response to complex, tidal currents.
Ripple-laminated sand facies	Faintly ripple-laminated sandstone probably partially bioturbated.	Base of upper unit.	Formed by shoaling waves or other irregular currents following decline of active sand waves.
Homogeneous sand facies	Mostly structureless sandstone with faint ripple laminae and burrows.	Top of upper unit, top of Rancho Rojo.	Period of low sedimentation. Sediments reworked by small waves and sediment burrowers.

Source: Blakey, 1984.

These large foresets are enclosed by first-order erosional surfaces (giant megasets) which dip from 12-21° to the west. They measure 7.5 m thick and 1-3 km across. The laminae and bounding surfaces between foresets are parallel or slightly inclined to them. The sandstone may contain numerous, 1-3 mm long, red mudstone chips. Locally abundant are ripple cross-laminations and trough cross-stratification is uncommon. Bedding is even-parallel to wavy and uniform. This facies is interpreted to have been formed by deposition on the lee side of a large, westward migrating, straight crested sand wave. Blakey mentioned that the lee slopes of these bedforms were probably featureless with the exception of back-flow ripples at the base producing the small-scale cross-stratification found within some bottomsets. Grainfall, sandflow avalanching and traction deposition dominated on the lee slopes. Characteristics of this facies compare to those predicted by Allen (1980a) for Class IV sand waves, although there is probably some gradation with Class III (Fig. 50, p. 127).

The second facies, found near the middle of the Rancho Rojo, is the Intraset Cross-Stratified Facies. These rocks exhibit compound cross-bedding consisting of intricate smaller sets situated between larger, westward dipping second-order bounding surfaces. Similar to the previous facies, these second-order surfaces are identified as giant forsets which are characteristically parallel to subparallel and evenly spaced. Planar-tabular and trough cross-stratification, as well as herringbone stratification are preserved. Several third-order erosional surfaces transect the sets and vary significantly in shape

and size. Red mud chips and thin mud drapes (rarely 3 mm thick) are associated with some second-order surfaces. Trace fossils are also common. Blakey interpreted the sedimentary structures of the Intraset Cross-Stratified Facies to represent deposition resulting from the migration of dune bedforms superimposed on the lee side of westward-facing, straight-crested sand waves. The preserved planar-tabular cross-stratification is inferred to have been formed by the migration of straight-crested dunes, whereas trough cross-stratification was formed by the migration of sinuous-crested dunes. Paleocurrent observations indicate that the dunes migrated in many oblique directions to the paleoshoreline, and at times, migrated shoreward due to infrequent current reversals. Large-scale grain-fall deposits are totally absent from this facies, suggesting that there was no flow separation across the sand wave. Blakey assigned the sand wave deposits of this facies to Class V of Allen's (1980a) sand wave model, however, some gradation exists with Class IV.

The third facies of Blakey's that will be discussed is the Trough Cross-Stratified Facies. These strata exhibit complex trough sets measuring 6 m across and 0.6 m thick. Second-order bounding surfaces dip at a lower angle (7°) than those of the previous facies. These surfaces are irregular and commonly define troughs, wedges and less commonly tabular cosets. The cosets contain an internal array of trough sets separated by third-order bounding surfaces. Mud chips are much less common but Skolithos-like trace fossils are widespread. The distinguishing feature which sets this facies apart is the curving,

irregular second-order bounding surfaces which Blakey attributed to the deposition of sinuous-crested dunes migrating across both flanks of a sand wave. The sand wave was of low profile and probably subjected to complex tidal currents. Blakey assigned this facies to the Class VI sand wave model of Allen (1980a).

Facies Interpretation

General Discussion. As stated earlier, the compound cross-bedding recognized in the Poor Valley Ridge Member of the Clinch Sandstone at Powell Mountain resembles features illustrated in the Class V sand wave model of Allen (1980a). Furthermore, these rocks display several features consistent with the various subenvironments found within modern sand wave complexes. The dominant sedimentary features within the Poor Valley Ridge Sandstone suggest that deposition took place near fairweather wave base by a combination of storm and tidal flows. Paleocurrent data from Powell Mountain are in accord with this hypothesis showing a strong ebb-tide predominance of current flow (to the west and northwest). Also supporting a storm influence for these rocks are the paleocurrent data collected from the Rockwood Formation (the westward equivalent of the Clinch Sandstone). These measurements indicate a west to northwest storm-wave approach and a southwesterly geostrophic flow (Driese, 1985; 1986a, b; Driese and others, in press; Easthouse, 1987). Consequently, the paleocurrent data collected at Powell Mountain may indeed reflect more than just fairweather ebb-tidal flow but rather, offshore-directed

storm-surge-ebb flow and/or storm flows superimposed on a dominant ebb-current flow during spring tide maximums.

Facies A/PVR

Sandstone of Facies A/PVR consists of compound cross-bedding and trough cross-stratification. This facies is interpreted to have been deposited by an offshore sand wave complex. The intricate internal cross-stratification and other sedimentary structures were formed by the migration of superimposed, sinuous-crested dunes on both flanks of giant sand waves.

The characteristics of Facies A/PVR are similar to those of Allen's (1980a) Class V sand wave model, however, some gradation exists with Class IV (Fig. 50, p. 127). Listed by Allen, distinguishing features of Class V include:

1. an underlying and persistent first-order bounding surface created by the winnowing and scour in the troughs between sand waves;
2. a dominant internal structure consisting of gently inclined, closely spaced second-order erosional surfaces generated by scour on the lee slope;
3. strata interrelated between second-order surfaces consisting of cross-lamination (current ripple regime) or cross-bedding (dune regime) dipping in the same general direction as master bedding;

4. third-order erosional surface running through the cross-bedding but inclined at lower angles than the second-order bounding surfaces; and
5. extremely thin, discontinuous mud drapes and/or mud intraclasts.

Facies A/PVR shows all the above characteristics with the possible exception of the first one. However, the limited dimensions of the outcrop and low restored dip-angles made the distinction between first- and second-order bounding surfaces difficult. Field measurements of the major erosional surfaces revealed that some were indeed near horizontal after restoration. Truncation of underlying strata and granule lag zones concentrated at the bases attest to the erosional character of these surfaces. Second-order surfaces (lee slopes of the sand wave) have dip angles of approximately 7°-15° and are commonly mantled by mudstone or shale. It would be difficult to explain the genesis of the second-order bounding surfaces from any other mechanism than that of a large bedform (sand wave) (Fig. 53). Climbing ripples or dunes may produce similar bounding surfaces but climbing ripple cross-stratification was not observed.

Trough cross-stratification is the dominant internal deposit between second-order bounding surfaces within Facies A/PVR. This bedding is interpreted to have been deposited by the foresets of sinuous-crested dunes migrating on the backs of sand waves. These small-scale bedforms were activated during seasonally strong ebb currents with a high oscillatory component. During storms, the dunes

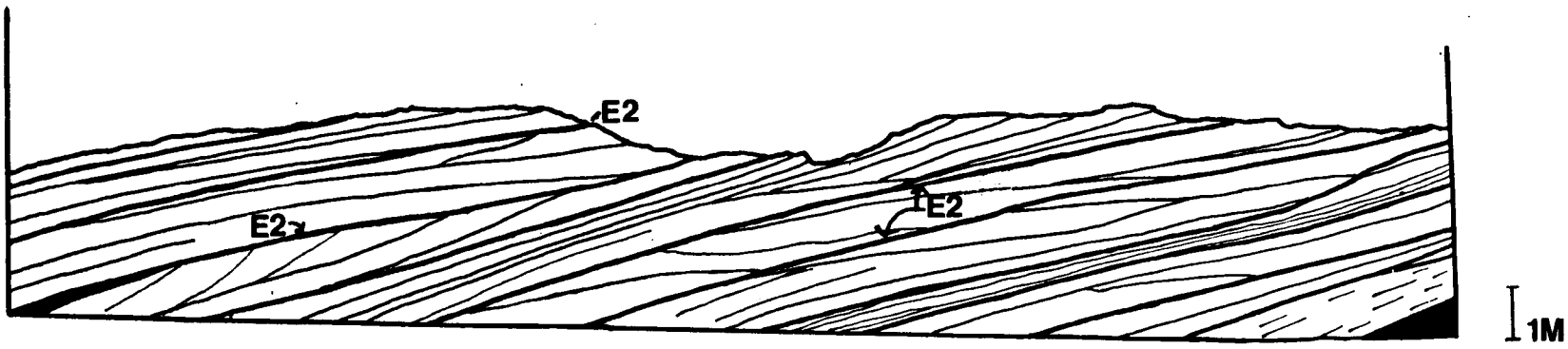


Figure 53. Outcrop Sketch of Facies A/PVR. The gently dipping (after restoration) second-order bounding surfaces (E2) are interpreted to represent forset planes of large sand waves. This bedding geometry is somewhat similar to Allen's (1980a) Class V model.

on the sand wave's surface produced local velocity fluctuations, resulting in a wide array of dune celerities. Differential migration rates produced the reactivation surfaces (third-order bounding surfaces) which truncate trough cross-stratification. DeMowbray and Visser (1984) explained that reactivation surfaces which have a low dip and extend irregularly across the whole set are usually formed by a dune overtaking and eroding an underlying dune. Reactivation surfaces resulting from bidirectional flows were not observed at Powell Mountain. During fairweather periods, ebb currents were weak and at the most, were only capable of generating small current ripples. Also during this time, thin, discontinuous clay drapes accumulated during slackwater and neap periods (Allen, 1982). These muds were commonly reworked by storms producing the numerous mud intraclasts found along bedding planes in Facies A/PVR.

Other features observed in Facies A/PVR which attest to both a low and high current (tidal/storm) offshore-marine environment include:

(1) thinning and fining-upward sequences of cross-sets (Driese, 1987);

(2) winnowed granule lags concentrated at the top of several cross-set and troughs (Levell, 1980; Cotter 1983a);

(3) a trace fossil suite dominated by a Cruziana assemblage (low energy) with a minor interbedded Skolithos assemblage (high energy) Walker (1984), and

(4) a dominantly unimodal paleocurrent pattern to the northwest, suggesting ebb-dominated flow. These features are consistent with those observed by Fischer (1987) and Driese (1987) for the Clinch Sandstone at Clinch Mountain, east of Powell Mountain.

Large-scale, planar-tabular cross-stratification; tidal bundle sequences (like those described by Visser (1980) and Driese (1987) and deeply incised channel surfaces with lag horizons (Allen and Howard, 1984) are three important tidal-deposit indicators which were not observed at Powell Mountain. The absence of these features does not preclude a tidal/storm origin, but rather places the depositional site of Facies A/PVR farther from the paleoshoreline. The absence of planar-tabular cross-stratification may be attributed to unsteady oscillatory currents produced during a storm, which were subsequently superimposed on a tidal maximum ebb current. These complex and irregular offshore-directed currents would have been accelerated due to flow constriction over the crests of the sand waves. As a result, the dominant feature found between second-order bounding surfaces would be trough cross-stratification. Minor amounts of planar-tabular cross-stratification may indeed exist at Powell Mountain but were not recognized due to the intense diagenetic alteration (silicification) and weathering which has taken place.

Well-organized tidal-bundle sequences may not have developed in an area far from the paleoshoreline. Boersma and Terwindt (1981) documented that the degree of tidal dominance affects the formation

and preservation of tidal bundles. During neap tides, large-scale bedforms, such as the megaripples superimposed on sand waves, may become inactive and either are replaced by smaller-scale ripples or mantled by clay. Facies A/PVR may have experienced only very weak spring ebb-tidal currents between storm events and an even further reduction of current strength during neap tides. Therefore, the incomplete neap-spring-neap cycles at the distal A/PVR paleosite left no record of tidally bundled strata in these Poor Valley Ridge rocks.

A distal offshore position for Facies A/PVR can be justified by the absence of channel features within these rocks. However, a consideration of the nature and geometry of a sand wave complex may also help explain the absence of channels. Sand waves of the scale responsible for the deposition of Facies A/PVR are inferred to have been very long and continuous bedforms oriented transverse to the flow direction. Both ebb-tide and storm currents flowed across the stoss slope continuing up and over the lee slope; flow separation may or may not have taken place. Consistent with observations in modern large sand waves, the breaching of their crests by strong tidal/storm current pulses is quite rare. Therefore, seaward-directed return currents would tend to flow up and over the gently sloping stoss flanks rather than incising channels perpendicular to the bedform's crest. Any preservable channels existing within the sand wave complex probably occurred as small local features or larger ones located between termini of individual sand waves. The above sand wave/channel relationships are contrasted with the study of Fischer

(1987) who observed channels in the sand ridge (bank) facies of the Poor Valley Ridge at Clinch Mountain. Channels commonly exist between the current parallel sand ridges (Houbolt, 1968; Caston, 1972; Swift and Field, 1981) which Fischer inferred as the depositional mechanism for his Poor Valley Ridge rocks. Another possibility explaining the absence of channel forms in the rocks at Powell Mountain is preservational bias (omission) due to the limited outcrop extent.

Several additional factors indicate that the Poor Valley Ridge rocks at Powell Mountain represent deposition in shelf regions more distal from the paleoshoreline than laterally equivalent rocks (to the east) previously studied. These factors are:

(1) the dominance of a Cruziana trace fossil assemblage over a subordinate Skolithos assemblage;

(2) the finer-grained size for the quartzarenite in this study as opposed to coarser grain-sizes recorded in previous studies (see Appendix II);

(3) the generally thin-bedded geometry of the sandstone units within Facies A/PVR;

(4) the abundance of interbedded mudstone or shale horizons between sandstone units and

(5) numerous storm-generated mud chips or intraclasts between bedding planes as opposed to continuous clay drapes or tidal bundle sequences found to the east.

Facies B/PVR

The fine- to coarse-grained, massive and densely bioturbated clay-rich sandstone of Facies B/PVR is interpreted to have been formed during periods of reduced current movement and sediment input. The high degree of bioturbation destroyed most primary sedimentary structures, thereby making the exact interpretation of this facies extremely difficult. It is not unreasonable to assume, however, that Facies B/PVR represents a stillstand period in sand wave activity which led to the colonization of the sediments by infaunal suspension feeders like Skolithos and Monocraterion.

Stride (1982) explained that during periods of sand wave inactivity, an explosive population of infaunal suspension feeders may become established in the sediment. The predominance of suspension-feeder traces in Facies B/PVR contrasts with the Cruziana trace fossil assemblage dominating in Facies A/PVR. In the latter, the burrowed clay foreset planes, replete with Arthrophycus and Planolites, represent deposition during times of reduced sedimentation rates. Reduced sedimentation occurred mainly by suspension fallout of clay between the infrequent high-energy storms. During these periods, organisms may have mined the nutrient-rich mud-draped foresets of the stabilized sand wave downward following each horizon to the base of the cross-set (Driese, 1987).

Although generally quiet conditions prevailed during the deposition of Facies B/PVR, it did experience minor fairweather current activity. The presence of an abundant Skolithos fossil

assemblage indicates that mild currents were present in order to keep small food particles in suspension (Seilacher, 1978). Thin granule-lag zones and concentrations of the inarticulate brachiopod Lingula also attest to the winnowing effects of currents.

It is proposed that the thickly-bedded units of B/PVR accumulated during gradual, but continuous sedimentation rates, rather than during a single major storm event. Individual tubes of Skolithos extend downward for only a few centimeters, however, entire sequences several meters thick are completely bioturbated. Therefore, bed thickness exceeds the penetration length of Skolithos observed by Chamberlain (1978). The low but constant sedimentation rates inferred for this facies, would have allowed organisms to completely rework the sediment, with successive generations shifting upwards as the deposit slowly accumulated (Seilacher, 1978).

Facies B/PVR falls within the zone of suspension feeders (Skolithos) of Seilacher (1967). These coarse-grained sequences represent sublittoral sand deposited in water more shallow than that for Facies A/PVR. Original sedimentary structures are obliterated by intense bioturbation, making the determination of the specific mode of deposition difficult, however, lag accumulations of Lingula and the coarse-grained nature of these rocks support a more proximal environment of deposition than that for A/PVR. The proposed paleoenvironment did not favor extremely high-energy conditions (swash zone) as inferred by the abundant clay matrix between grains (see Appendix II).

Facies C/PVR

The shale of Facies C/PVR is stratigraphically intercalated with the sand wave lithology of Facies A/PVR. These thin shale horizons, which pinch-out laterally in both directions, are interpreted to represent suspension fallout deposits collecting in the troughs between large sand waves. These shale units are to be differentiated from the 1 cm thick mudstone partings found between major sandstone beds of Facies A/PVR. Both features originated as suspension accumulations during times of high mud concentration in the water column and during periods of reduced current activity. However, the two shale types differ genetically in terms of the exact location in the sand wave complex where each deposit accumulated. Shale of Facies A/PVR is interpreted to have been discontinuously deposited on the steep lee slope of the sand wave and subsequently buried by sand as the bedform slowly advanced (Stride, 1982). Any mud deposited on the gentle stoss slope was more than likely eroded, thus ending up as the mud intraclasts commonly observed between bedding planes. Shale horizons of Facies C/PVR, on the other hand, are much thicker (up to 0.8 m) and contain suspension-fallout, horizontal laminations of silt, in addition to small-scale current-ripple laminations. Many workers studying modern large-scale sand waves attest to their extremely large wavelengths (several thousand meters) which enclose troughs dominated by finer-grained deposits (Stride et al., 1982). They also agree that although these muds are thin and pinch-out laterally, they are indeed more persistent than the mud accumulating upon foreset planes near the

sand wave's crest. Therefore, based on the lithology, geometry, sedimentary structures and stratigraphic position of Facies C/PVR, it is not unreasonable to assume that these shale zones represent deposits forming in the troughs between large-scale sand waves.

Low tidal current velocity or wave activity (during slack-water periods) are not entirely responsible for the deposition of the shale of Facies C/PVR and the mudstone drapes and intraclasts within Facies A/PVR. McCave (1970; 1971b) found that deposition of mud is inhibited by high wave activity, although, with suitable sediment concentrations, mud may be deposited in shallow water along a high energy exposed coast. When suspended sediment concentrations become high (100 mg/l or more), mud deposits will form irrespective of strong tidal currents (surface velocity of 1.5 knots) and high wave activity at the bed (McCave, 1971b). Mud concentrations were possibly high during Poor Valley Ridge sedimentation judging from the abundance of mud intraclasts, drapes and laminae between sandstone bedding planes.

Facies D/PVR

Facies D/PVR is composed of a coarsening/thickening-upward sequence of interbedded, fine-grained sandstone and shale. Silt content of the shale increases upwards as well as bed thickness and the scale of sedimentary structures. Detrital feldspar content and the amount of iron-mineralization decreases upward.

Facies D/PVR is interpreted as a transition zone facies between the underlying distal storm influenced shelf deposits of the Hagan

Shale (sub-facies B2/HS) and the overlying sand wave deposits of Facies A/PVR, B/PVR and C/PVR. The interbedded nature, sharp/erosional bases, massive bedding and micro-hummocky cross-laminations of Facies D/PVR suggest deposition on a storm-dominated shelf near the transition zone of Aigner and Reineck (1982).

Sedimentation took place as episodic bedload transport, followed by only minor reworking by burrowing organisms. Rippled upper bedding surfaces testify to waning energy conditions and mild currents reworking the sediments after storm conditions. Depositional conditions of Facies D/PVR were more proximal to the shoreline than those of sub-facies B2/HS (Hagan Shale), and represent transition-zone deposits based on the following observations:

(1) unit bed thickness in Facies D/PVR is greater and increases upward in the section, possibly suggesting development of a minor regressive or progradational (shoaling-upward) phase in the overall Lower Silurian transgression,

(2) the presence of micro-hummocky cross-laminations, which indicate a more important role of oscillatory currents superimposed upon offshore-oriented unidirectional storm than in sub-facies B2/HS, and

(3) the increased amount of iron-mineralization in these units as opposed to most units in B1/HS or B2/HS, possibly suggesting depositional conditions similar to those postulated for

Facies D/HS (closer to the shoreline than surrounding B2/HS lithology).

It is interesting to note the stratigraphic context in which Facies D/PVR is located. If indeed these rocks represent a transition sequence between the offshore, storm-dominated facies of the Hagan's B2/HS and the storm/tide influenced, quartzose sandstone of the Poor Valley Ridge sand wave complex, then this transitional phase, must have taken place relatively quickly if preservation bias (omission) is not accounted for. Rather than having to incorporate a major eustatic regression into an overall Lower Silurian transgressive model (which would contradict a sea-level rise early on in Poor Valley Ridge time proposed by Fischer, 1987) it seems more plausable to attribute this change to local progradation of Poor Valley Ridge sands over underlying Hagan mud. This progradational mechanism may have been assisted by a minor lowering of sea level. The proposed hypothesis is in accordance with the earlier conclusions of Schoner (1984) and Fischer (1987). In addition, a rejuvenation of the Taconic Highlands source terrain to the east may explain the anomalously high percentage of feldspar grains in the sandstone units of D/PVR. During early Poor Valley Ridge time, as the sediment supply into the area continued to increase, nearshore sand waves started to prograde oceanward. The coarsening/thickening-upward lithology of Facies D/PVR may therefore represent the distal tongues of the overlying sand wave complex (Facies A/PVR, B/PVR and C/PVR).

Johnson et al. (1981) and Stride (1982) both described zones of smaller sand waves and flat-bedded deposits which occur in the distal (oceanward) extents of sand wave compelexes (Fig. 48, p. 119; Fig. 51, p. 127). Johnson (1981) explained that there exists a relatively abrupt transition observed for zones of large sand waves, small sand waves and offshore mud layers in the North Sea. It is further postulated that the zone of large sand waves (Facies A/PVR, B/PVR and C/PVR) was not immediately laterally conterminous (shoreward) to Facies D/PVR during early Poor Valley Ridge time. In modern environments, large sand waves require an adequate sand supply (Stride, 1982), a supply probably not available during earliest D/PVR time. The absence of a shoreward zone of large sand waves during the initial deposition of D/PVR explains the position of the conformably overlying Facies B/PVR (interpreted as littoral to sublittoral proximal deposits). As conditions during deposition of D/PVR continued, increasingly larger amounts of terrigenous material was introduced into the basin of deposition, although the small sand waves' vulnerability to storms prevented them from developing to maturity.

Storm currents and the winnowing action of waning fairweather currents (higher in Facies D/PVR) commonly flattened the small sand waves (Terwindt, 1971 and Stride, 1982). In the stratigraphic record, the resulting sharp based, hummocky and ripple-topped storm layers are the preserved lithology of the aforementioned processes (Dott and Bourgeois, 1982).

As a final note, the feldspar content, which decreases upward in Facies D/PVR, never reaches a zero value for the Poor Valley Ridge Sandstone. Even in the most well-sorted, arenaceous and texturally mature units within the overlying facies, the feldspar content never decreased below 0.25 percent. These petrographic observations are in disagreement with the data of Fischer (1987) for the Poor Valley Ridge at Clinch Mountain who observed no feldspar in his samples. These findings, however, further substantiate a more distal depositional setting for the Clinch rocks at Powell Mountain than the Clinch studied by Schoner (1984) and Fischer (1987). Odom (1978), while studying ancient sandstone sequences, discovered that the total amount of feldspar in quartz-rich sandstones is commonly related to grain-size of the sand and energy of the depositional setting. He also observed that some sandstone units grade laterally from medium- and coarse-grained quartzose sandstone to very fine-grained, slightly feldspathic sandstone. Such is the case for the Clinch Sandstone between the Clinch and Powell Mountain strike belts. In addition, because there was no abrupt change in both the texture and detrital mineralogy between the two members of the Clinch Sandstone at Powell Mountain (but rather a transitional change, namely Facies D/PVR), the single provenance hypothesis of Fischer (1987) is favored by this author.

The Rose Hill Formation

General

The contact of the (Late) Silurian Rose Hill Formation and the underlying Clinch Sandstone is conformable and easily recognizable at Powell Mountain, Virginia. The red, maroon and purple siltstone and sandstone intercalated with green mudstone are a striking contrast to the light-colored, homogenous quartzarenite of the underlying Poor Valley Ridge Member of the Clinch Sandstone (Fig. 54). The major emphasis of this study is on both members of the Clinch Sandstone, however, because the stratigraphically contiguous Rose Hill Formation is exposed at Powell Mountain and the rocks contain interesting sedimentological features, a brief summary of this Formation is given below. In addition, the entire depositional model for the Clinch Sandstone can better be understood by combining it with observations made of the Rose Hill Formation.

The geological character of the Rose Hill will be presented first. Included are general descriptions of the lithology, sedimentary structures, biogenic structures, bedding relationships and petrography. Secondly, a brief summary will be given concerning the depositional conditions during Rose Hill time by comparing the following lithologic observations with conclusions drawn from other workers (Folk, 1960; Hunter, 1970; Diecchio, 1973; Lampiris, 1975).

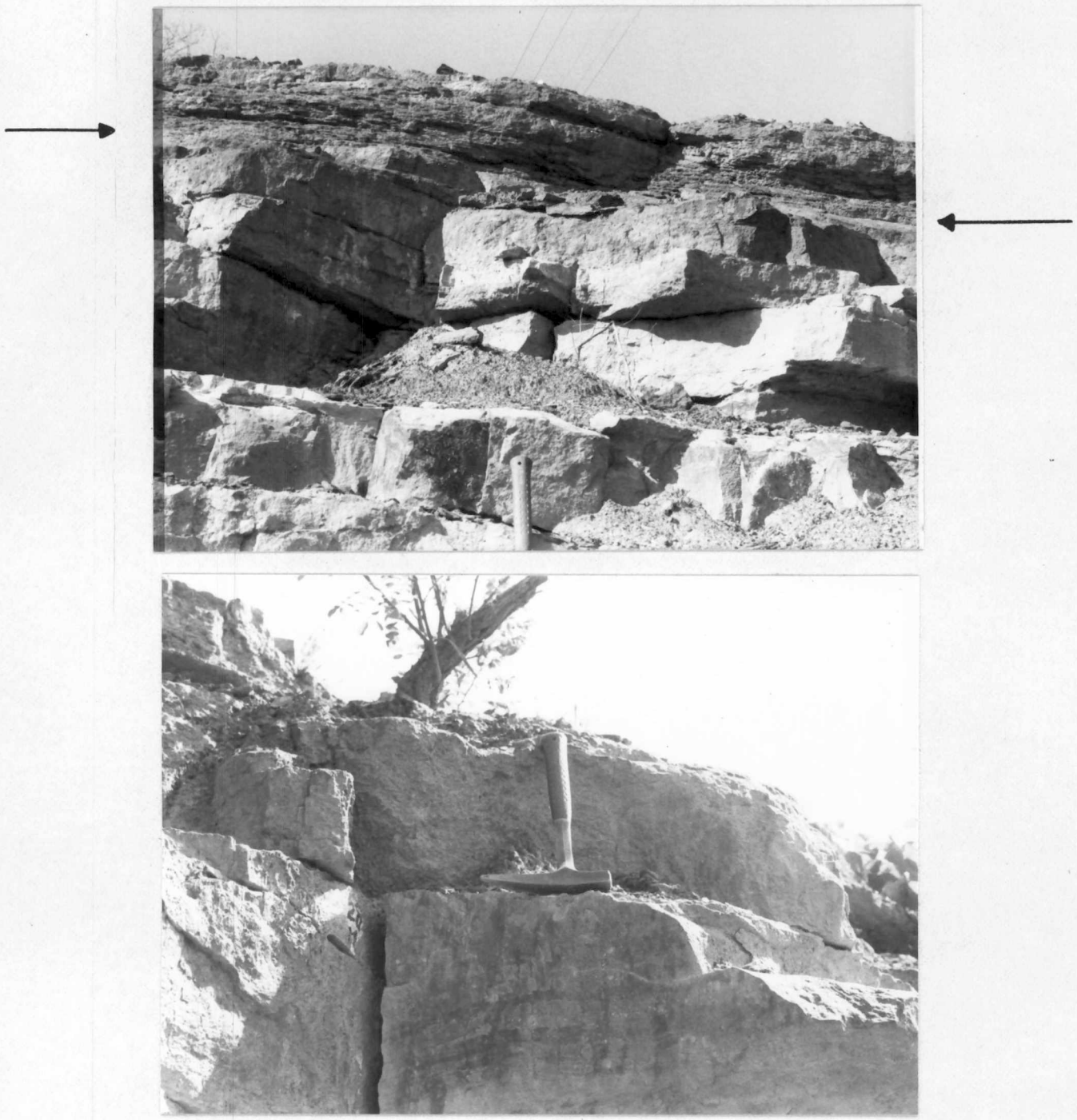


Figure 54. Conformable Contact Between the Poor Valley Ridge Member of the Clinch Sandstone and Overlying Maroon Mudstone and Shale of the Rose Hill Formation. Upper photo: the contact is gradational over approximately 0.5 m with maroon mud and silt extending downward in burrows and horizontal laminations of the Poor Valley Ridge Sandstone. (Hammer for scale.) Lower photo: close-up of the contact.

Lithologic Description

Lithology. The lithology of the Rose Hill Formation at Powell Mountain is extremely varied. Beginning at the contact with the Poor Valley Ridge sandstone, the siltstone of the Rose Hill is medium to dark maroon, somewhat friable and heavily cemented by hematite. A meter or so upward into the Formation, siltstone content remains unchanged, however, thin (0.1 m) units of fine-grained hematite-cemented sandstone become interbedded with the surrounding lithology. These units are only slightly greater in grain size and of the same color as the surrounding hematite-cemented siltstone and, therefore, extremely hard to differentiate.

Light to medium gray, thinly bedded units of fine-grained quartzarenite appear at approximately 4.5 m above the base of the Rose Hill Formation. These units are interbedded with the maroon siltstone and light green-gray mudstone of the "lower" Rose Hill. Higher up in the section, the volumetric content of the maroon siltstone becomes reduced giving way to an increase in light-gray mudstone. The light to medium gray quartzarenite is thinly bedded and exhibits heavy diagenetic alteration, weathering to various shades of yellow, red, brown and black. Higher up in the section (approximately 9 m above the base of the Rose Hill Formation) the quartzarenite becomes medium-bedded and shows only very weak signs of diagenetic alteration (weathers to a light yellow). This "sheet-like" quartzarenite is the highest lithotype on Powell Mountain before loss of outcrop by erosion. The sand grains are very fine-grained, well-sorted,

texturally mature and cemented by silica giving these rocks a strong resemblance to the Keefer Sandstone. According to Folk (1960) a marked change takes place in the "upper" Rose Hill in west-central Virginia in which the olive shale and red sandstone/siltstone may be part of an expanded Keefer section (Fig. 55). The sandstone which caps the Silurian section at Powell Mountain, southwestern Virginia may indeed be an extension of the Keefer Sandstone, however, evidence for this hypothesis is inconclusive.

Sedimentary Structures

As was the case for the lithology, the sedimentary structures found in the Rose Hill Formation show a wide variety of types. Near the Poor Valley Ridge/Rose Hill contact, the small- to medium-scale trough cross-stratification of the former gives way to even-parallel, closely spaced, horizontal laminations. Within the bulk of the Rose Hill, these laminations are only weakly present or altogether absent due to the amalgamating effects of burrowing organisms. At approximately 0.8 m above the base of the Rose Hill, the thinly bedded, hematitic siltstone and very fine-grained sandstone take on a host of interesting sedimentary structures including wave ripple marks, interference ripples and mudcracks. The wave and interference ripples are well preserved and occur on the tops of entire bedding surfaces (Fig. 56). Ripples commonly exhibit crestline bifurcations with the crest heights measuring 2 cm and wavelengths measuring 5 cm.

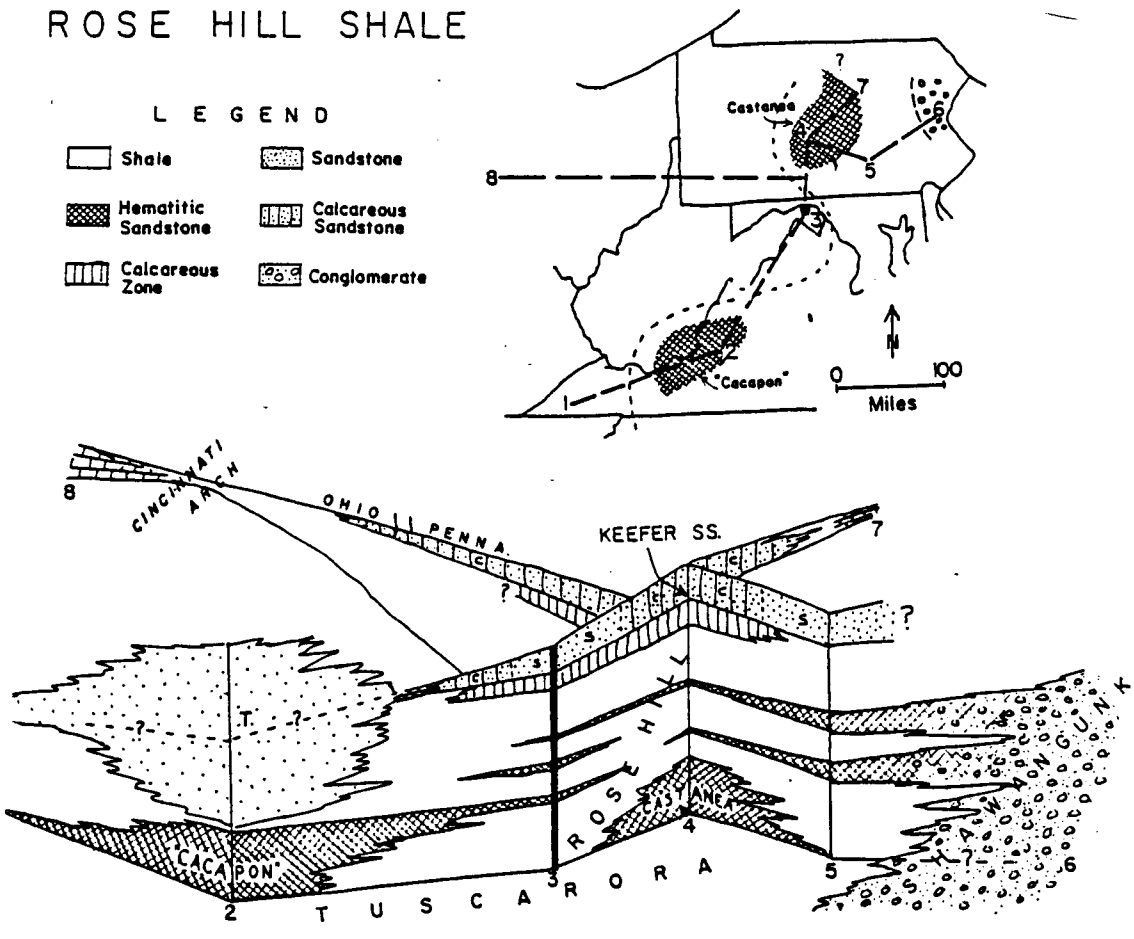


Figure 55. Regional Variation in the Rose Hill Shale. Number one on the map and fence diagram is the approximate location of the Silurian studied in this report. (Taken from Folk, 1960).

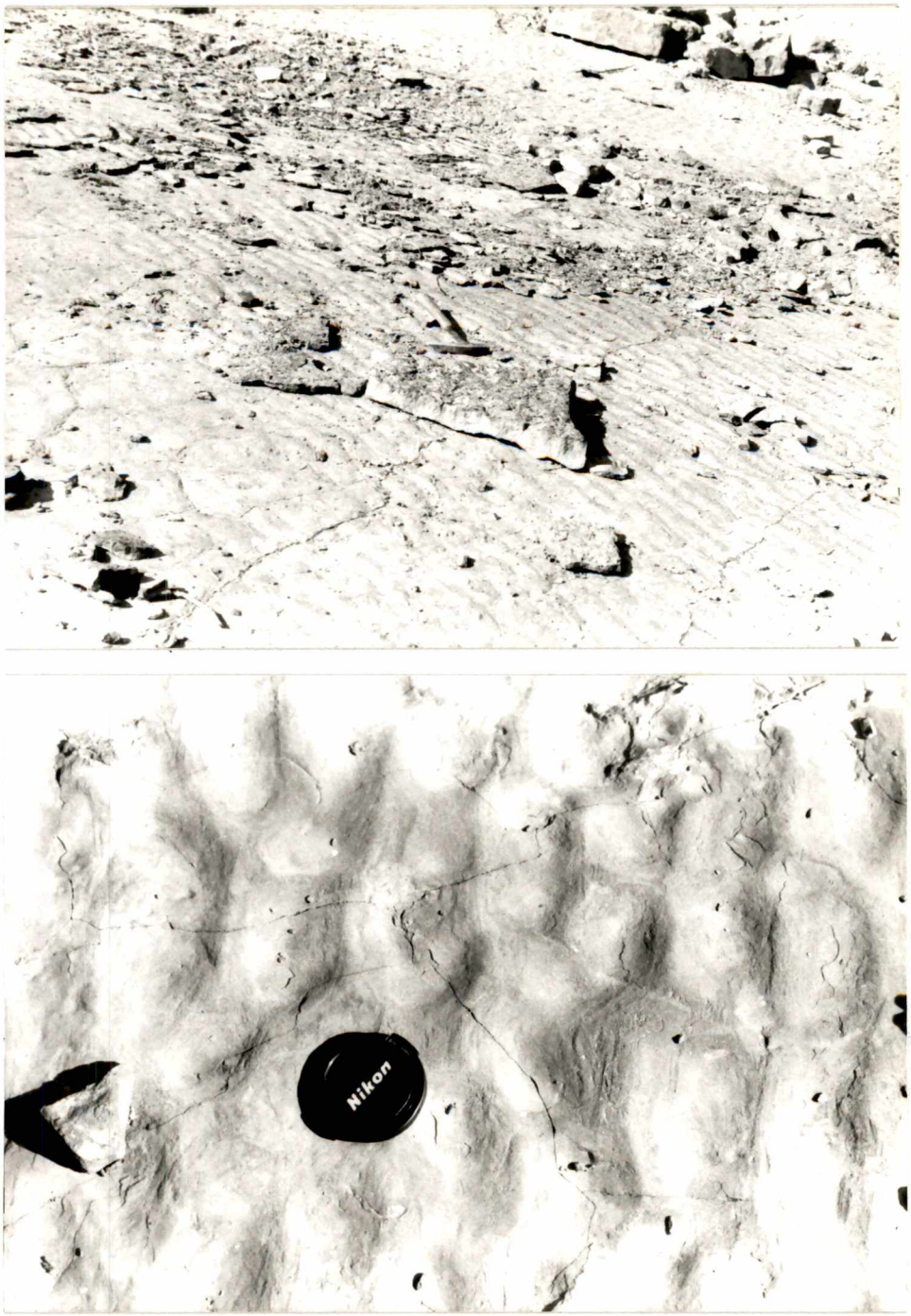


Figure 56. Wave and Interference Rippled Upper Bedding Surfaces, Rose Hill Formation. Upper photo: wave ripples with mud cracks. Lower photo: close-up of interference ripples. (Hammer and lens cap for scale.)

Mudcrack polygons are irregular and show at least two episodes of drying (Fig. 57).

The thin bedded quartzarenite sandstone higher up in the section contains small-scale trough cross-stratification, rare internal horizontal laminations and lunate current-rippled upper bedding surfaces. The surrounding maroon siltstone contains several siltstone intraclasts and wavy-parallel horizontal laminations. Intraclasts average 0.5 cm in diameter, are irregular, rounded, light gray to white and show internal laminations within maroon siltstone. These intraclasts are heavily concentrated at the bases of maroon siltstone units and are generally overlain by horizontal laminations.

The "Keefer-like" quartzarenite capping the Silurian strata at Powell Mountain contains sedimentary structures similar to the Poor Valley Ridge Member of the Clinch Sandstone with the exception of the presence of abundant horizontal laminations and low-angle laminations. The horizontal laminations generally trend throughout the entire thickness of the unit. Light-gray, irregular mud intraclasts and form-discordant wave ripples are found capping several bedding surfaces of these "sheet" sandstones. The intercalations of mudstone are usually less than 1 cm thick.

Biogenic Structures

Skolithos and Monocraterion are the major trace fossils throughout the Rose Hill Formation. Skolithos is especially common in the maroon siltstone/sandstone units and is found at the contact with

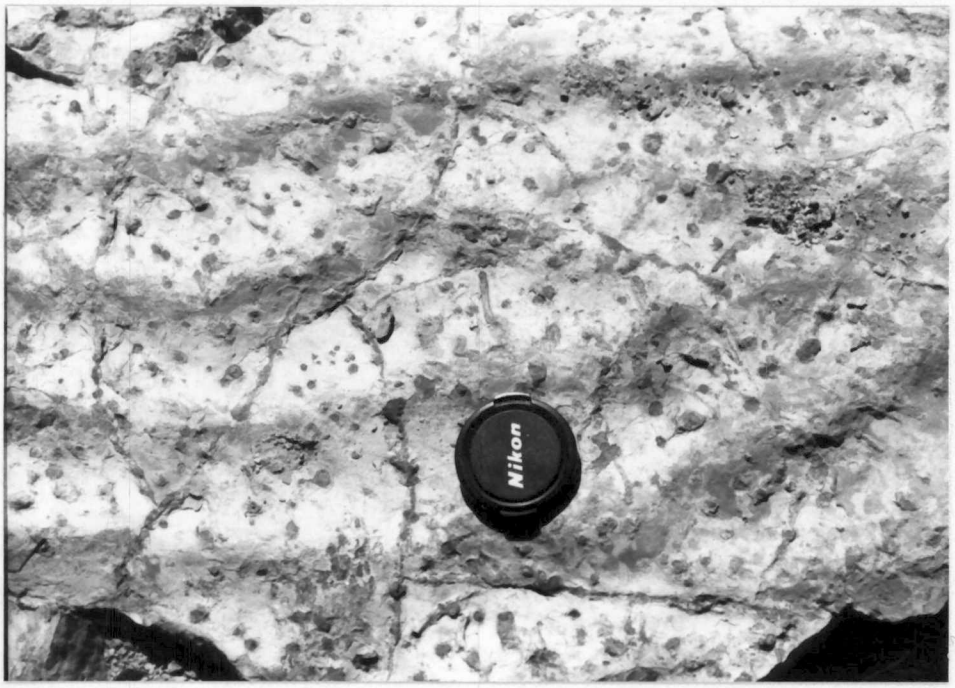


Figure 57. Mudcracks in the "lower" Rose Hill Formation. The thinly bedded hematitic siltstone/very fine-grained sandstone contains internal horizontal laminations, wave and interference rippled upper surfaces with mudcrack polygons and iron-stained tubes of Skolithos. (Lens cap for scale.)

the underlying Poor Valley Ridge Member of the Clinch Sandstone. Burrows average 0.8 cm wide by 7 cm in length. Burrows are infilled with heavily iron-stained siltstone or light green-gray mudstone (Fig. 58).

Monocraterion occurs at higher stratigraphic levels and is preferrentially associated with the "Keefer-like" quartzarenite. These burrows average 0.7 cm at their widest end and extend downward for about 3.5 cm. Monocraterion is found along the upper surfaces of sandstones beds.

Rare occurrences of Arthropycus and Planolites are found at some localities in the Rose Hill. These two horizontal burrows are found along lower bedding surfaces of the maroon siltstone and especially along the "Keefer-like" quartzarenite. Despite these occurrences, horizontal burrows were generally lacking in the Rose Hill Formation.

Algal laminations are exclusively found in the Rose Hill Formation and occur approximately 3.3 m above its base. Laminations are extremely fine (0.5 mm or less in diameter), are slightly undulatory to wavy and show anti-gravitational structures. These laminations trend throughout the entire thickness of thin-bedded, fine-grained and iron-stained sandstone and can only be observed after slabbing the rock.

Bedding Relationships

Units are thinly bedded in the lower Rose Hill with the average bed thickness not exceeding 8 cm. Contacts are sharp/planar with

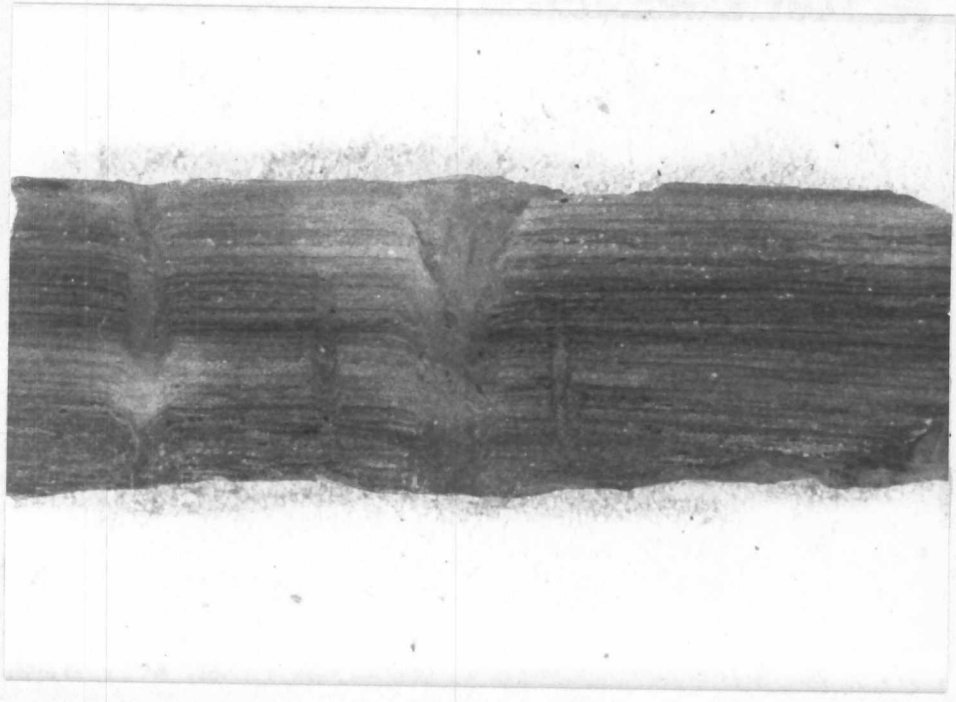


Figure 58. Cut-Slab of a Rose Hill Siltstone. Polished surface exhibits burrows disrupting horizontal laminations. This sample was collected from the "lower" Rose Hill Formation. Marks on scale equal 1 cm.

units showing a constant lateral thickness. At approximately 2 meters above the base of the Rose Hill, the thin maroon siltstone and fine-grained sandstone gives way to the more massive and thick-bedded maroon siltstone. Beds still maintain constant lateral thickness, however, they now average 0.5 m thick. Contacts are sharp/planar or transitional/planar.

Quartzarenite beds of the upper Rose Hill are thin (generally 8 cm) and pinch-out in the lateral direction over several meters. Contacts are sharp and planar. Quartzarenite beds of the "Keefer-like" lithology are extremely "sheet-like," showing a very constant lateral thickness over the entire outcrop face. In addition, the beds average 0.4 m thick with sharp/planar bedding surfaces.

Petrography

Thin sections representing the Rose Hill petrographic suite include P19-A, P20-A, P21-D, P21-UB, P22-E1, P22-UA and P24-E1; the last three samples were collected from the "Keefer-like" quartzarenite near the top of the section (Appendix II).

The thin-bedded, maroon siltstone and fine-grained sandstone found near the base of the Rose Hill are represented by thin sections P19-A and P20-A (Fig. 59). Both are classified as extremely fine-grained, iron-stained quartzarenites, however, the fabric of sample P20-A shows bioturbation, which reduces the sorting value and destroys most sedimentary structures. The primary cementing agents in both samples are hematite and silica. Coatings of hematite occur on

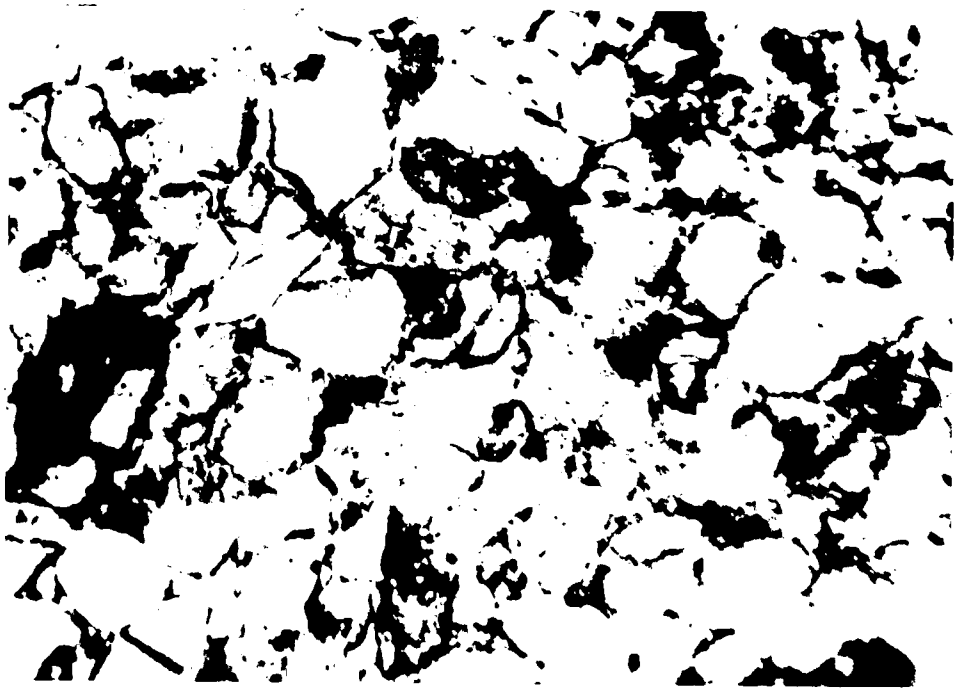


Figure 59. Photomicrograph of Thin-Section P19-A. This sample was collected from the maroon siltstone and very fine-grained quartzarenite near the base of the Rose Hill Formation. Field of view from left to right is approximately 2 mm.

the detrital quartz grains and are encased by quartz overgrowths indicating that the iron-mineralization process took place before silicification. Quartz is the dominant framework mineral with trace amounts of feldspar, muscovite, hornblende, and zircon occurring in both samples. Thin- sections P21-D, P21-UB and P22-E1 were collected from the massive and thick-bedded maroon siltstone and some sandstone beds of the middle Rose Hill. These samples are similar to the previous two from the lower Rose Hill, although they do contain a higher percentage of clay matrix and some sedimentary rock fragments.

Thin-sections P22-UA and P24-UA were sampled from the "Keefer-like" lithology of the upper Rose Hill and are very different petrographically than any of the previous samples. Both are classified as fine-grained, well-sorted, mature quartzarenite with silica and hematite cement (Fig. 60). Despite the hematite cement, these rocks take on only a buff or light yellow-brown color upon weathering. Trace amounts of hornblende, feldspar, chert fragments, tourmaline and zircon were also identified petrographically.

Depositional Environment

Most earlier workers investigating the Rose Hill Formation agreed that deposition of its various members took place both nearshore and offshore of a coastal plain with extensive tidal flats dissected by large turbid rivers. Deposition took place farther offshore in a relatively calm, moderately deep-water open-marine environment experiencing low bottom sedimentation conditions (Folk, 1960).

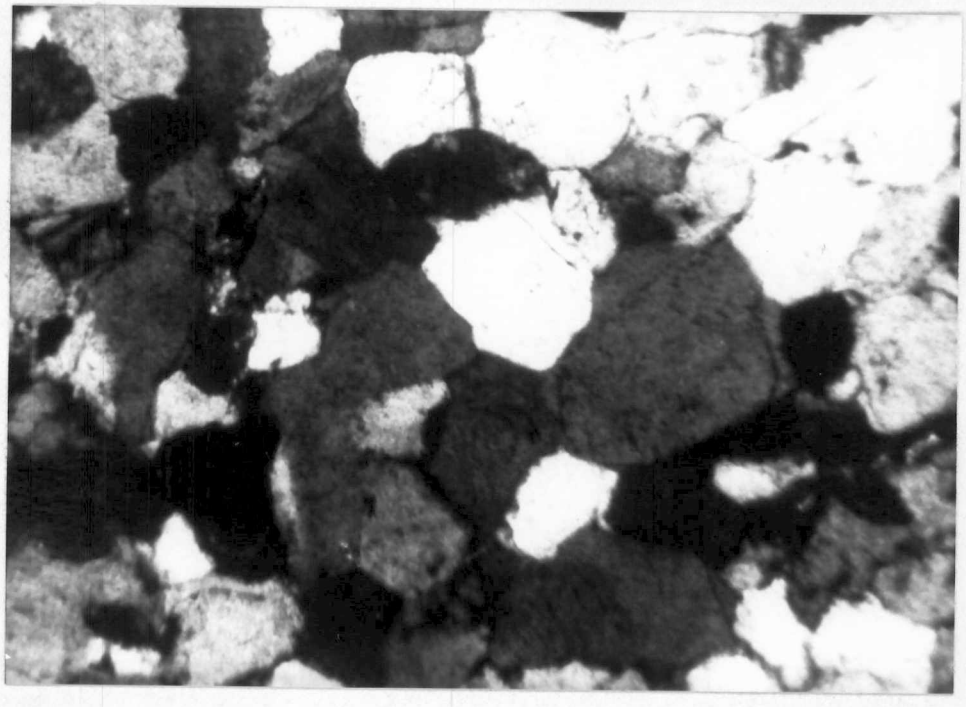


Figure 60. Photomicrograph of Thin-Section P22-UA. This sample was collected from the "Keefer-like" lithology of the upper Rose Hill Formation. Field of view from left to right is approximately 2 mm.

Between the offshore mud and shoreface tidal flats existed an extensive series of offshore bars, which served to further restrict circulation within the intertidal environment (Lampiris, 1975).

Hematite-cemented, maroon siltstone and sandstone constitute the bulk of the Rose Hill section at Powell Mountain. This lithology, slightly above the Poor Valley Ridge/Rose Hill contact, is more thinly bedded and shows signs of subaerial exposure, in contrast to the maroon siltstone/sandstone higher up in the sequence. However, both lithotypes can be combined genetically as originating as tidal flat deposits laid down in shallow-water above and below low tide-line. This lithology closely resembles Hunter's (1970) Hematite-Cemented Sandstone Facies of the Rose Hill, which he interpreted to have been formed on a tidal flat. The abundant wave and interference ripples, mudcracks, algal laminations, the prevailing Skolithos trace fossil assemblage and overall color of the rocks leaves little doubt for such an interpretation. Currents must have been strong enough to winnow away most of the fine clay matrix between sand grains, thereby giving these rocks a somewhat mature texture. Occasionally, these currents had enough erosive power to rip up fragments of the offshore gray and light green-gray clay deposits and incorporated them as mud intraclasts found along the bases of some units. This process may have taken place during storms. It is uncertain whether these sandstone strata owe their hematite content to post-depositional oxidation of iron-bearing minerals or to the preservation of iron oxide derived from the eastward source area. Hunter (1970) stated

that much of the hematite is probably a diagenetic recrystallization product of iron oxide and iron-rich silicate that was present as thin oolitic coatings on the sand grains during the time of deposition. Later crystallization or recrystallization after burial may have put much of the iron into the solution.

The gray and light green-gray, slightly fissile to slightly blocky shale of the Rose Hill is interpreted to have been deposited in a relatively calm, moderately deep-water, open-marine environment. This environment is stratigraphically not well-represented at Powell Mountain and data from the thin shale horizons are meager. Folk (1960) made similar interpretations of the olive clay-shale which dominated 90% of his Rose Hill sections. Folk asserted that deposition must have taken place by exceedingly calm currents, because the featureless shale contains greater than 95% clay, with less than 5% randomly orientated silt grains. In addition, the lack of biogenic reworking and preserved body fossils supports the idea that the sea bottom was largely devoid of organisms (Folk, 1960).

The "Keefer-like" quartzarenite observed at the top of the Powell Mountain sections differs in its bedding thickness, geometry, color and textural maturity from rocks lower in the Rose Hill Formation. The environment of deposition must have been one of high energy to produce the good sorting and elimination of rock fragments. These characteristics, taken in consideration with the sheet-like geometry, Skolithos trace fossil assemblage, and an abundance of low-angle and horizontal laminations lead one to assign a high-energy

beach environment of origin. Hunter (1969) studied the Keefer Sandstone in Pennsylvania and found strong evidence for a beach environment of deposition. Folk (1960) and Lampiris (1975) working in Virginia concluded a similar environment for the Keefer. It is uncertain whether the quartzarenite observed at Powell Mountain is true "Keefer," however, lithological and paleoenvironmental similarities exist with documented studies.

CHAPTER IV

PALEOCURRENTS

Unidirectional and bidirectional paleocurrent data were collected from a wide range of sedimentary structures from both members of the Clinch Sandstone at Powell Mountain, southwestern Virginia. Additional measurements were taken from the wave rippled upper bedding surfaces in the lowermost Rose Hill Formation, approximately 0.9 m above the contact with the underlying Poor Valley Ridge Member of the Clinch Sandstone. Examples of recorded unidirectional paleocurrent indicators include cross-strata, flute casts and asymmetrical ripple cross-laminations. Bidirectional indicators that were measured include trends of wave ripple crests, aligned bioclasts and gutter casts. These measurements were collected and processed for interpretations on the paleoslope orientation, direction of flow, paleogeography and individual sand wave orientations.

Of the total 93 paleocurrent measurements recorded at Powell Mountain, 42 were taken of trough cross-stratification, 24 from wave ripple crests, 23 from gutter casts and 4 from flute casts. The few asymmetrical ripple cross-laminations were grouped into the trough cross-strata category. Trough cross-stratification occurred mainly in the Poor Valley Ridge Member where numerous bedding planes and excellent exposure yielded well-preserved three-dimensional foreset planes. Wave ripple crests were found predominantly in the Hagan Shale, both as protuberances on upper bedding surfaces and as isolated

or starved ripple forms. Exposure of three-dimensional rippled surfaces was enhanced by the friability of the surrounding shale. Gutter casts were also most common in the Hagan Shale, occurring as rounded scours along sandstone/siltstone basal surfaces or as isolated features surrounded by shale. Flute casts were found in the Hagan Shale.

Measurements of the aforementioned features, along with the structural dip and strike of the rocks, were taken in the field using a Brunton Compass. Each measurement was subsequently corrected for structural deformation by use of the Schmidt Equal Area Stereonet. The correction method employed was adopted from Tucker (1982). The resulting corrected azimuths were grouped into classes 15° in width and plotted on a rose diagram scaled for number of readings. Azimuths were analyzed with a computer program (by Maher and Dott, 1979) in order to determine the vector mean (θ), the magnitude of the resultant vector (r), the angular deviation (s) and the F-statistic (F). The rose diagrams and statistical results are plotted on Figure 62 (page 169).

Unidirectional Data

Unidirectional paleocurrent indicators were abundant, especially in the Poor Valley Ridge Sandstone where the 42 measurements of trough cross-stratification yielded on overall vector mean of 332° (Fig. 61). The number of data points (42) well exceeds the minimum necessary for statistically valid paleocurrent results (Tucker, 1982).

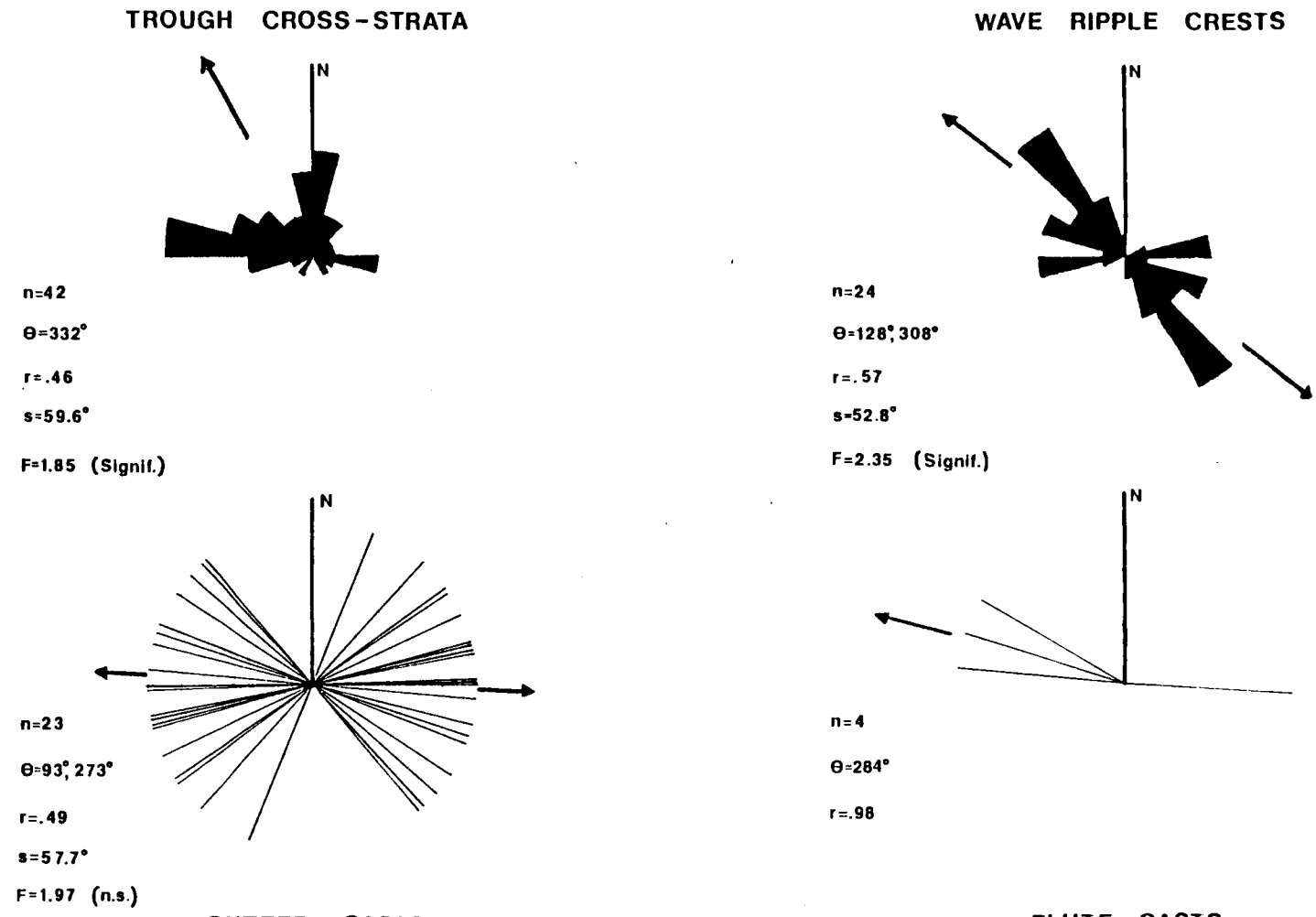


Figure 61. Rose Diagram of Paleocurrent Data. Measurements were taken from the Hagan Shale (wave ripple crests, gutter casts and flute casts) and Poor Valley Ridge Members (trough cross-strata) of the Clinch Sandstone. O=azimuth of mean vector; r=magnitude of mean vector; s=angular deviation; F=F-statistic for circular distribution; n=number of observations. (Heavy arrow indicates vector mean).

Comparison of the obtained vector mean (N28°W) with those of previous studies shows excellent correlation, especially with the data of Hayes (1974) for the Tuscarora Formation in southwestern Virginia (Fig. 62). The magnitude of the vector mean (r) is 0.46, whereas the angular deviation (s) is 59.6°. The F-statistic is 1.85. This value was compared to tables by Pearson and Hartley (1954, in Draper and Smith, 1966) and was found to be of a sufficient value for a 99% confidence interval, therefore indicating that the data are significantly oriented.

Bidirectional Data

Bidirectional paleocurrent indicators were represented by wave ripple crests and gutter casts, which were found primarily in the Hagan Shale. The wave ripple crests show overall vector means of 128°/308° whereas the gutter casts have a strong concentration of azimuths in the east-west orientation with vector means of 93°/273°. For wave ripple crests, the magnitude of the vector mean (r) is 0.57, the angular deviation (s) is 52.8° and the F-statistic is 2.35, a significant value. The gutter casts have a vector mean (r) of 0.49, an angular deviation (s) of 57.7°, and a F-statistic of 1.97, a non-significant value.

Interpretation of Data

As stated earlier, the overall vector mean for cross stratification in the Clinch Sandstone is N28°W, which indicates a source direction to the southeast. An extensive source area was proposed for

Author	Paleocurrent Vector Mean	Formation	Study Location
Yeakel (1962)	N38°W	Tuscarora	Central Appalachians
Martini (1971)	N34°W	Medina	New York and Ontario
Epstein and Epstein (1972)	N42°W/N29°W	Shawangunk	Eastern Pennsylvania
Hayes (1974)	N29°W	Tuscarora	Southwestern Virginia
Whisonant (1977)	N48°W	Tuscarora	Western Virginia
Schoner (1985)	N30°W	Clinch	Northeastern Tennessee
Fischer (1987)	N2°W	Clinch	Northeastern Tennessee
Marks (this study)	N28°W	Clinch	Southwestern Virginia

Figure 62. Summary of Paleocurrent Studies of the Clinch Sandstone and its Stratigraphic Equivalents. (Modified from Fischer, 1987).

the linear deposits of Lower Silurian sediment stretching from New York to Georgia (Dennison, 1970; Whisonant, 1977). Yeakel (1962) determined the source of these sediments to be an uplift to the southeast, which produced the Taconic Highlands. The dunes migrating obliquely atop sand wave backs may have produced the unusual north and west orientation of data in the trough cross-strata category (Fig. 61). The small number of readings oriented in the east, southeast sector probably represent infrequent times when flood current in the tidal regime were strong enough to produce cross-stratification. Flute casts represent scour during northwesterly flowing storm currents, possibly of storm-surge-ebb nature.

The bidirectional data are represented by wave ripple crests trending NW-SE (128°, 308°) which indicate the sense of current flow to be NE-SW. When analyzed with respect to the proposed paleoshoreline (trending NE-SW) it seems evident that the currents which produced these ripples were orientated parallel to the shoreline. Such longshore currents are usually found in more distal zones where alongshore winds and storm systems produced shore-parallel wave trains in deeper water (Aigner, 1985). In response to the Coriolis effect, any offshore directed storm currents would be deflected to the left (to the Southwest) in zones at some distance from the paleoshoreline. Because most of the ripple data were collected from sub-facies B2/HS, the distal paleoenvironment proposed for these rocks is further supported by paleocurrent reconstructions.

Gutter casts and rare flute casts found at the bases of some sandstones strata in the Hagan Shale indicate that current flow was approximately east-west (with some variation in the former). This flow was approximately perpendicular to the paleoshoreline, indicating that strong, very erosive, bottom-hugging return flows occasionally extended into the distal areas. Such erosive flows may have been generated by storm-surge-ebb (relaxation) flows which later evolved into relaxation flows farther out on the shelf (possibly in the area of Rockwood deposition). Scour and gutter casts are found in the B1/HS and B2/HS sub-facies, thereby indicating the presence of these currents in the proximal as well as the distal portions of the Hagan Shelf.

CHAPTER V

SUMMARY AND CONCLUSIONS

The Clinch Sandstone (Lower Silurian) at Powell Mountain, southwestern Virginia consists of the Hagan Shale Member and overlying Poor Valley Ridge Sandstone Member, two texturally different lithologies are interpreted to have been deposited within somewhat distal to nearshore reaches of a shallow-marine shelf setting.

Four distinct facies were delineated in the Hagan Shale. Facies A/HS, the basal unit of the Hagan Shale, directly overlies and is conformable with the subaerially exposed tidal-flat deposits of the Upper Ordovician Juniata Formation. Facies A/HS consist of a thick, basal, calcareous quartzarenite with overlying, thin bedded sandstone, siltstone and shale. Textural grading, and to a lesser extent, bioturbation are present in these rocks. Facies B/HS was divided into two sub-facies based on very subtle differences in lithology, sedimentary structures, bedding geometry and mineralogical character. The lowermost of the two, sub-facies B1/HS, is comprised of thinly interbedded, calcareous quartzarenite and shale. Sedimentary structures within the sandstone, in the order of decreasing abundance, include horizontal laminations, wave ripple marks and cross-laminations, form-discordant wave ripples and rare current ripples. Most bedding surfaces are sharp and planar, exhibiting a uniform lateral thickness. Sub-facies B2/HS consists of very thinly interbedded, very fine-grained, calcareous quartzarenite,

wackestone/packstone units and intervening shale. Sedimentary structures, in the order of decreasing abundance, include horizontal laminations, current ripples and cross-laminations, form-discordant wave ripples and graded beds. Bedding surfaces are generally sharp but undulatory, with gutter casts and lenticular bedding more common than in sub-facies B2/HS. Beds pinch-out laterally. Facies C/HS is a medium to dark gray, fissile to slightly blocky shale. There is a general paucity of sedimentary structures with the exception of rare, extremely thin horizontal laminations and thin wisps of flat-lensed silt beds. Burrows of Planolites and Skolithos were uncommon, as were concentrations of body fossils (mainly brachiopods). Four individual beds comprise Facies D/HS, whose anomalous characteristics and heavy iron-mineralization warranted a separate facies classification for these beds. Facies D/HS consists of a ferruginous bryozoan packstone, a fossiliferous quartzarenite and a ferruginous sandstone conglomerate. Integrated features of these units not found anywhere in the Hagan Shale include heavy iron-mineralization, high concentrations and wide variations of preserved body fossils, thick and complex bedding geometries and small-scale trough cross-stratification. In general, the terrigenous material and bioclasts are more coarse-grained than in the previous three facies.

The aforementioned facies within the Hagan Shale represent deposition in laterally contiguous subenvironments on a shallow-marine shelf. Deposition took place within the transition zone and on the middle shelf, both above and below fairweather wave base. Facies A/HS

is interpreted to represent the shallowest, most nearshore deposits of the Late Ordovician, Early Silurian marine transgression. This transgressive sheet deposit contains a basal lag zone (containing brachiopod shells and phosphate grains) and some evidence of bioturbation by Skolithos. Tidal currents and both fairweather-wave and storm-wave flows reworked the initial deposit, forming the overlying thin-bedded units in Facies A/HS. As the Silurian transgression continued, progressively deeper-water environments became superimposed upon the former depositional site, and as a result, the effects of storms were better preserved in the sedimentary record. Facies B/HS represents deposition in a marine, sublittoral, storm-shelf setting with sub-facies B1/HS representing a paleoenvironment more proximal to the shoreline than that of sub-facies B2/HS. The sandstone and wackestone/packstone units of B/HS contain several features indicative of formation from initially strong currents, which progressively waned throughout a major storm event. The intercalated shales represent the placid "background sedimentation" of fine silt and mud between episodic storm events. Facies C/HS represents similar but more prolonged periods of quiet-water sedimentation than the intercalated shale of B/HS. The increased thickness of this shale resulted from either a paleoenvironment of greater distance from the shoreline (generated by a peaked transgression) or during times when episodic storm events were at a minimum. Throughout Hagan time, minor and short-lived regressions within the overall transgressive pattern caused

megarippled and rippled sand shoals (Facies D/HS) to migrate over pre-existing environments. Tidal currents as well as storm generated currents affected the proposed transition zone to nearshore environment for Facies D/HS. In addition, conditions were favorable for the transportation and concentration of iron.

The transitional contact between the Hagan Shale and overlying Poor Valley Ridge Sandstone marks a change in lithology, sedimentary structures, bioturbation, bedding geometry and mineralogy, all of which suggest a change to higher-energy, storm, and to a lesser extent, tidally influenced environments. Sandstone units of the Poor Valley Ridge Member are coarser-grained, more quartz-rich and show a higher textural maturity than those of the Hagan Shale Member, features indicative of preferential sorting in high-energy paleoenvironments.

Four facies define the Poor Valley Ridge Sandstone. Facies A/PVR consists of medium-bedded, compound cross-stratified, fine-grained quartzarenite sandstone containing intercalations of shale <2 cm. Ubiquitous trough cross-stratification is enclosed within large-scale second-order bounding surfaces. Current ripples, mudstone intraclasts, claystone drapes and reactivation surfaces were found throughout the facies. Third-order bounding surfaces pinch-out in both directions, whereas second-order bounding surfaces are subparallel and dip in the same general direction. The Cruziana trace fossil assemblage dominates. Facies B/PVR is comprised of a heavily bioturbated, fine- to coarse-grained, clay-rich quartzarenite.

Lag concentrations of phosphatic Lingulid brachiopods, nodules and coarse-grained quartz clasts are found throughout this facies. The Skolithos trace fossil assemblage dominates. Facies C/PVR consist of fissile to slightly blocky shale. Thin streamers of siltstone, sparse Arthrophycus and several concretions of pyrite were found throughout this facies. Facies D/PVR is the lowermost facies of the Poor Valley Ridge Sandstone and constitutes the transitional contact with the underlying Hagan Shale. Sandstone composition ranges from subarkosic to quartzarenitic with current ripples, horizontal laminations and micro-hummocky cross-laminations occuring lower in the facies. Higher in the facies, sandstone beds become more quartz-rich, texturally mature and massive. Skolithos, Planolites and rare Rusophycus are found within beds and along the sharp/planar or sharp/undulatory bedding surfaces. Unit thickness increases upward in this facies.

The facies of the Poor Valley Ridge Sandstone are interpreted to have been deposited in various subenvironments within a marine-shelf sand-wave complex (Fig. 63). Strong, northwest-oriented storm flows (possible storm-surge-ebb currents) in combination with weaker, normal tidal flows modified the large-scale sand waves and adjacent environments. Facies A/PVR represents the "bulk-deposits" of individual sand waves superimposed upon one another. The large-scale, second-order bounding surfaces represent foreset planes of the giant sand waves. The intricate internal trough cross-stratification represents deposition by sinuous-crested dunes migrating across the

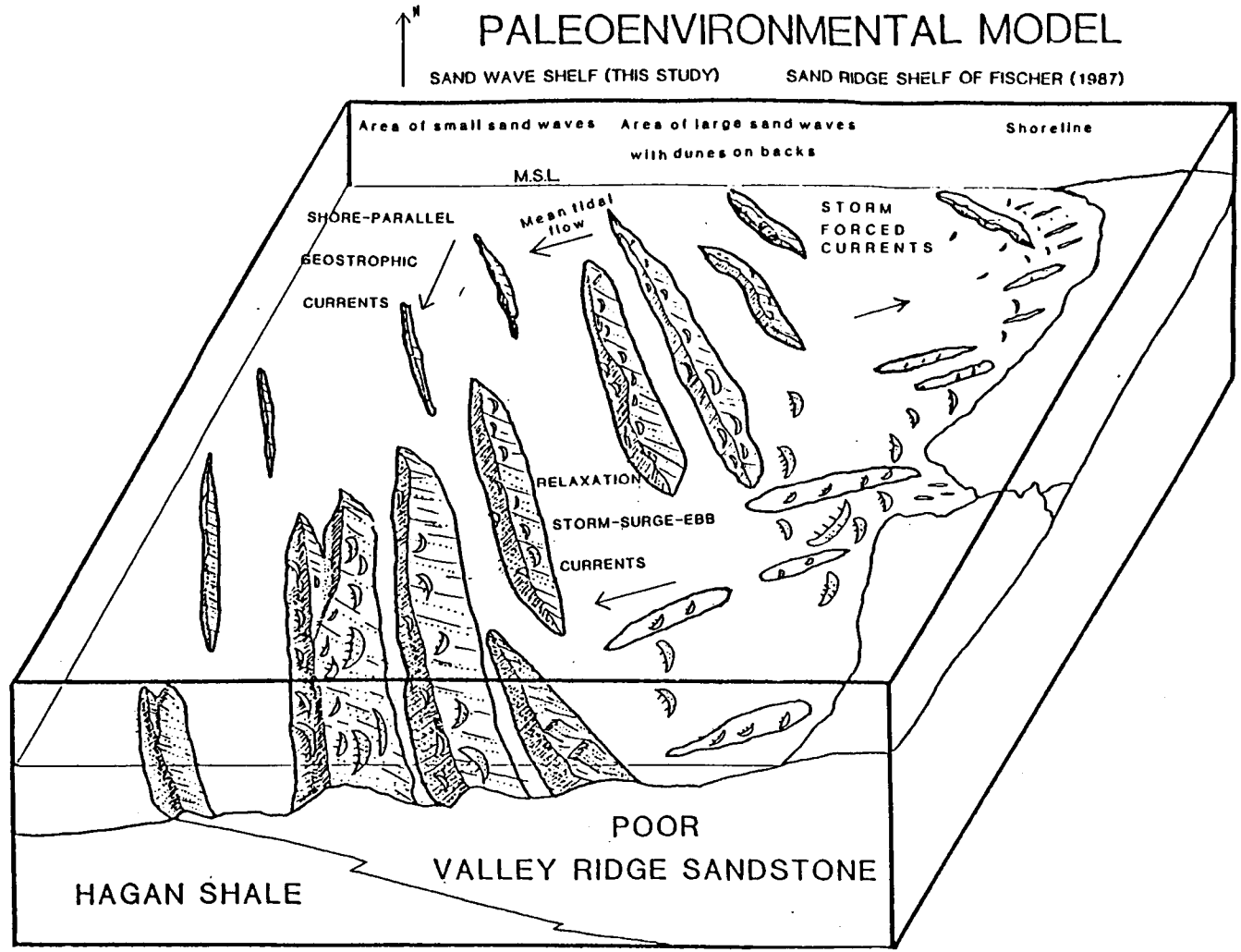


Figure 63. Summary Model of a Sand Wave Shelf Setting. These depositional conditions are proposed for the Poor Valley Ridge Member. Note the sand ridge setting to the east proposed by Fisher (1987). No specific lateral scale implied.

backs of sand waves, especially during high-energy storm events. The thickly-bedded, heavily bioturbated quartzarenite of Facies B/PVR accumulated during times of reduced sand wave activity. Mild fairweather current activity was substantial enough to remove much of the fine sand, however, a dense Skolithos trace fossil assemblage homogenized the sediment destroying most primary sedimentary structures. In addition, this burrowing activity produced a textural inversion by mixing mud and fine silt with the coarser-grained quartz. The shale of Facies C/PVR represents suspension fallout deposits collecting in the troughs between the large-scale sand waves of Facies A/PVR. Periods of reduced current activity and high concentrations of mud in the water column proved favorable for the accumulation of C/PVR sediments. The coarsening/thickening-upward sequence of interbedded fine-grained sandstone and shale of Facies D/PVR is interpreted as a transitional deposit between the sand wave lithology of the Poor Valley Ridge sandstone and underlying storm-shelf sequence of the Hagan Shale. Indeed, Facies D/PVR represents the early stages of the Poor Valley Ridge clastic progradational wedge (distal zone of small sand waves) which covered underlying Hagan sediments. As the sand supply continued to increase from the eastern Taconic Highland source, progradation continued and eventually offset the effects of the ongoing Early Silurian transgression. A new, shallower and higher-energy environment of the overlying sand wave complex was formed. Facies B/PVR, therefore, may represent the period when the effects of clastic progradation and the background marine

transgression were in equilibrium, thus creating a stalled or low sedimentation phase. As progradation reached its end later in Poor Valley Ridge time, a possible minor marine regression led to the deposition of the iron-rich, fine-grained, subaerially exposed sediment of the Rose Hill Formation.

Johnson et. al (1985) and Johnson (1987) plotted sea-level changes for the North American and Yangtze Platforms during Early Silurian time. These authors used community replacement patterns in brachiopod benthic assemblage zones to recognize sea-level fluctuations in the rock record. Bathymetric maps were constructed after stratigraphic correlation. These authors found that after the initial transgression at the onset of the Silurian, four smaller cycles of sea-level fluctuation occurred on the North American Platform. Peaks were found in the A_4-B_1 positions, C_1 position, C_4 position, and C_6 position. Driese (1987 - in review) used trace fossil distribution, brachiopod zonations and a careful analysis of proximality parameters to construct relative sea-level curves for the Rockwood Formation in east Tennessee. These curves correlated very well with the curves of McKerrow (1979) and Johnson (1987).

Figure 64 illustrates the relative sea-level changes for the Clinch at Powell Mountain. Fossils were generally fragmented or sparse in the Hagan Shale and rare in the Poor Valley Ridge Sandstone. In addition, proximality trends (as employed by Easthouse, 1987) were

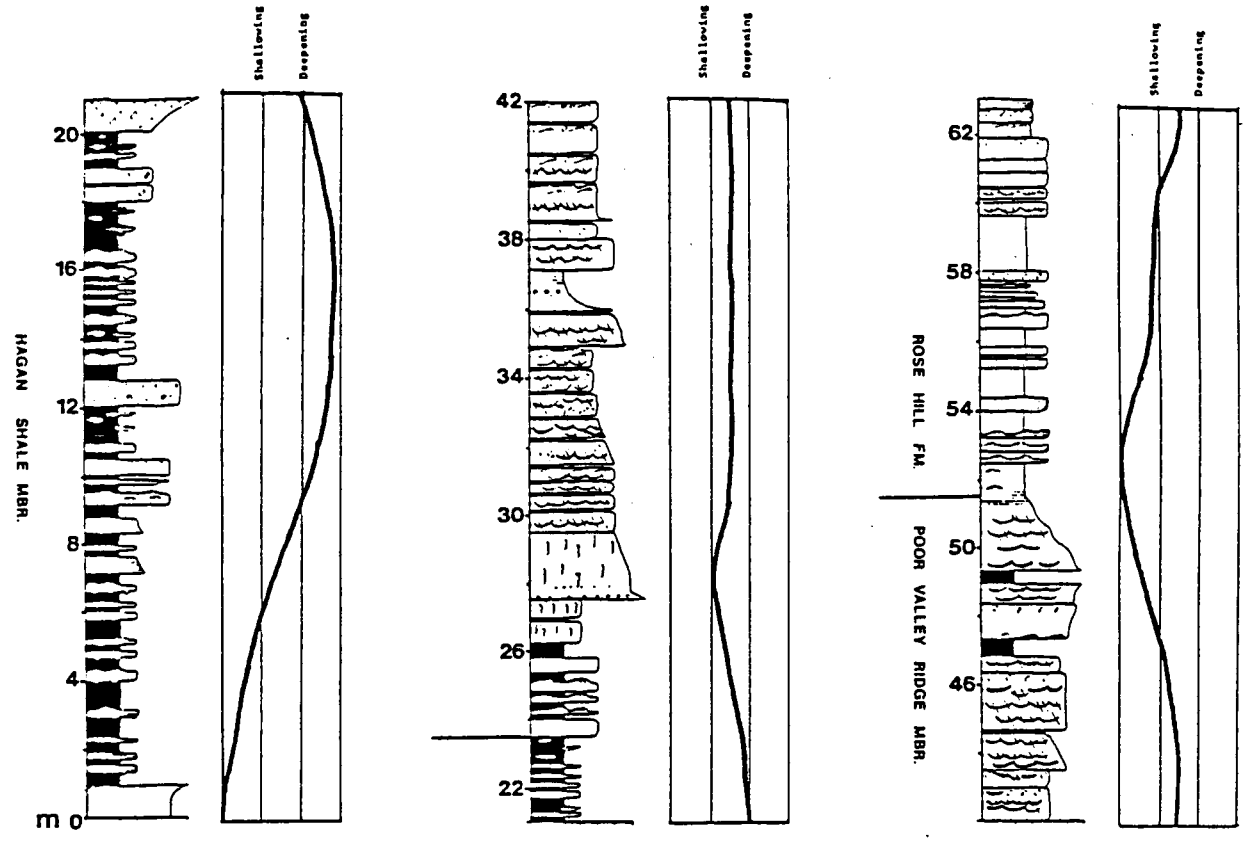


Figure 64. Relative Sea-Level Changes Inferred for the Clinch Sandstone.

not used due to the limited extent and lack of indicators in the Hagan Shale. Therefore, the conclusions of Figure 64 are based solely on general and pragmatic observations of lithologic character, and to a lesser extent, biogenic structures or preserved body fossils. Whether sea-level fluctuations proposed herein were produced by tectonic events, changes in the rate of terrigenous influx, or eustatic changes in sea-level cannot be uniquely determined, however, general observations can be drawn.

The basal calcareous sandstone of the Hagan Shale (Facies A/HS) can be correlated to the initial transgression during earliest Silurian time (early Rhuddanian). This transgressive lag deposit was laid down directly upon the subaerial exposed tidal flat deposits of the Upper Juniata Formation. As relative sea-level increased throughout the Hagan, shelf muds and storm sands became preserved in the rock record. Sometime in the late Hagan (possibly at the occurrence of the shoaling sequences of Facies D/HS) relative sea-level progressively started to shallow. The heavily bioturbated, coarse-grained sandstone of Facies B/PVR represents a minor shallowing period based on the occurrence of Lingulid brachiopods and may be comparable to the low sea-level stand during late Fronian (C_3 position) of Johnson et. al (1985). Relative sea-level remained somewhat uniform throughout the remainder of Poor Valley Ridge deposition but culminated in a terminal regression near the beginning of Rose Hill deposition (also observed by Cotter, 1983 for the top of the Tuscarora Formation in Pennsylvania). Shallowing and subsequent

emergence is indicated by the red coloration, algal laminations, abundant Skolithos burrows and mudcracks within the Rose Hill sandstone. The initiation of Rose Hill sedimentation took place in the C_4 position, later in Landovery time (Berry and Boucot, 1970; Johnson et al. 1985).

BIBLIOGRAPHY

BIBLIOGRAPHY

Aigner, T., and Reineck, H. E., 1982, Proximality trends in modern storm sands from the Helgoland bight (North Sea) and their implications for basin analysis: Senckenbergiana Maritima, v. 14, p. 183-215.

Aigner, T., 1985, Storm Depositional Systems: Berlin and Springer-Verlag Berlin Heidelberg, 174 p.

Allen, J. R. L., 1963, The classification of cross-stratified units with notes on their origin: Sedimentology, v. 2, p. 556-591.

Allen, J. R. L., 1968, Current Ripples: North-Holland, Amsterdam, 139 p.

Allen, J. R. L., 1980a, Sandwaves: a model of origin and internal structure: Sed. Geology, v. 26, p. 281-328.

Allen, J. R. L., 1980b, Sand-wave immobility and internal master bedding of sand-wave deposits: Geol. Magazine, v. 23, p. 437-446.

Allen, J. R. L., 1982, Mud drapes in sand-wave deposits: a physical model with application to the Folkestone Beds (early Cretaceous, southern England): Philsoph. Trans. Royal Soc. London, v. 306, p. 291-345.

Allen, P. and Homewood, P., 1984, Evolution and mechanics of a Miocene tidal sandwave: Sedimentology, v. 31, p. 38-81.

Amsden, T. W., 1955, Lithofacies map of Lower Silurian deposits in central and eastern United States and Canada: Am. Assoc. Petroleum Geologists Bull., v. 39, p. 60-74.

Anderton, R., 1976, Tidal shelf sedimentation: an example from the Scottish Dalradian: Sedimentology, v. 23, p. 429-458.

Baars, D. L., and Seager, W. R., 1970, Stratigraphic control of petroleum in White Rim Sandstone (Permian) in and near Canyonlands National Park, Utah: Am. Assoc. Petroleum Geologists Bull., v. 54, p. 709-718.

Banarjee, I., 1980, A subtidal bar model for the Eze-Aku sandstones, Nigeria: Sed. Geology, v. 25, p. 291-309.

Belderson, R. H. and Stride, A. H., 1969, Tidal currents and sand wave profiles in the north-eastern Irish Sea: Nature, (London), v. 222, p. 74-75.

Belderson, R. H., Johnson, M. A. and Stride, A. H., 1978, Bed-load partings and convergences at the entrance to the White Sea, USSR, and between Cape Cod and Georges Bank, USA: Marine Geology, v. 28, p. 65-75.

Berry, W. B. N. and Boucot, A. J., 1970, Correlation of the North American Silurian rocks: Geol. Soc. Amer. Spec. Paper 102, 289 p.

Blakey, R. C., 1984, Marine sand-wave complex in the Permian of central Arizona: Jour. Sed. Petrology, v. 54, p. 29-51.

Blatt, H., Middleton, G. V., and Murray, R. C., 1972, Origin of sedimentary rocks: Prentice-Hall, New Jersey, 634 p.

Blodgett, R. H., 1985, Paleovertisols as indicators of climate: Amer. Assoc. Petroleum Geologists Bull., v. 69, p. 239.

Boersma, J. R., 1969, Internal structure of some tidal mega-ripples on a shoal in the Westerschelde Estuary, the Netherlands, report of a preliminary investigation: Geol. en Mijnb., v. 48, p. 409-414.

Boersma, J. R., and Terwindt, J. H. J., 1981, Neap-spring tide sequences of intertidal shoal deposits in a mesotidal estuary: Sedimentology, v. 28, p. 151-170.

Bouma, A. H., 1962, Sedimentology of some flysch deposits: Amsterdam, Elsevier, 168 p.

Brenchley, P. J., Newall, G. and Stanistreet, I. G., 1979, A storm surge origin for sandstone beds in an epicontinental platform sequence, Ordovician, Norway: Sed. Geology, v. 22, p. 185-217.

Brenchley, P. J., and Newall, G., 1982, Storm influenced inner-shelf sand lobes in the Caradoc (Ordovician) of Shropshire, England: Jour. Sed. Petrology, v. 52, p. 1257-1269.

Brenchley, P. J., 1985, Storm influenced sandstone beds: Mod. Geology, v. 9, p. 369-396.

Brenner, R. L., 1980, Construction of process-response models for ancient epicontinental seaway depositional systems using partial analogs: Am. Assoc. Petroleum Geologists Bull., v. 64, p. 1223-1244.

Butts, Charles, 1927, Oil and gas possibilities at Early Grove, Scott County, Virginia: Virginia Geol. Survey Bull., v. 27, p. 133-165.

Butts, Charles, 1933, Geologic map of the Appalachian Valley in Virginia with explanatory text: Virginia Geol. Survey Bull., v. 52, 568 p.

Butts, Charles, 1940, Geology of the Appalachian Valley in Virginia: Virginia Geol. Survey Bull., v. 52, 271 p.

Butts, C., and Gildersleeve, B., 1948, Geology and mineral resources of the Paleozoic area in northwest Georgia: Georgia Geol. Survey Bull., v. 54, 176 p.

Byers, C. W., 1974, Shale fissility: relation to bioturbation: Sedimentology, v. 21, p. 479-484.

Caston, V. N. D., 1965, Localized sediment transport and submarine erosion in Tremadot Bay, northern Wales: Marine Geology, v. 3, p. 401-410.

Caston, V. N. D., 1972, Linear sandbanks in the southern North Sea: Sedimentology, v. 18, p. 63-78.

Chamberlain, K. C., 1978, Recognition of trace fossils in cores: in Basan, P.B., (ed.), Trace Fossil Concepts: S.E.P.M. Short Course, No. 5, p. 133-184.

Chowns, T. M., 1972, Molasse sedimentation in the Silurian rocks of northwest Georgia, in Chowns, T. M., (compiler), Sedimentary Environments in the Paleozoic Rocks of Northwest Georgia: Georgia, Geol. Soc., Guidebook no. 11, p. 13-23.

Cluff, R. M., 1980, Paleoenvironment of the New Albany Shale Group (Devonian-Mississippian) of Illinois: Jour. Sed. Petrology, v. 50, p. 767-780.

Cooper, B. N., 1939, Geology of the Draper Mountain area, Virginia: Virginia Geol. Survey, Bull., v. 55, 98 p.

Cooper, B. N., 1944, Geology and mineralogy of the Burkes Garden quadrangle, Virginia: Virginia Geol. Survey, Bull., v. 60, 299 p.

Cotter, E., 1983a, Shelf, paralic and fluvial environments and eustatic sea-level fluctuations in the origin of the Tuscarora Formation (Lower Silurian) of Central Pennsylvania: Jour. Sed. Petrology v. 53, p. 25-49.

Cotter, E., 1983b, Silurian depositional history in Silurian Depositional History and Alleghenian Deformation in the Pennsylvania Valley and Ridge (Guidebook): Harrisburg, PA, 48th Annual Field Conf. of Penn. Geologists, p. 3-28.

Darton, N. H., 1896, Piedmont folio: U.S. Geol. Survey Atlas, no. 28, p. 2.

Defant, A., 1961, Physical Oceanography, Vol. 2, Pergamon Press, Oxford, 729 p.

DeMowbray, T. and Visser, M. J., 1984, Reactivation surfaces in subtidal channel deposits, Oosterschelde, southwest Netherlands: Jour. Sed. Petrology, v. 54, p. 811-824.

Dennison, J. M. and Boucot, A. J., 1974, Reference section for Silurian Clinch Sandstone and most nearly complete Devonian section in eastern Tennessee: Southeastern Geol., v. 16, no. 2, p. 79-101.

Diecchio, R. J., 1973, Lower and Mid-Silurian ichnofacies and their paleoenvironmental significance, central Appalachian Basin of the Virginias: Duke University, unpub. M.S. Thesis, 100 p.

Dott, R. H., Jr. and Bourgeois, 1982, Hummocky stratification: significance of its variable bedding sequences: Geol. Soc. Amer. Bull., v. 93, p. 663-680.

Drapeau, G., 1970, Sand waves on Browns Bank observed from the shelf diver: Maritime Sediments, v. 6, p. 90-101.

Draper, N. R., and Smith, H., Jr., 1966, Applied regression analysis: New York, John Wiley & Sons, 407 p.

Driese, S. G., 1985, Marine shelf storm deposits, Rockwood Formation (Silurian), east Tennessee: Geol. Soc. Amer., Abst. with Progs., v. 17, p. 89.

Driese, S. G., 1986a, Fairweather and storm shelf sequences, Rockwood Formation (Silurian), east Tennessee: Appal. Basin Indust. Assoc. Program, v. 10, p. 133-175.

Driese, S. G., 1986b, Fairweather and storm shelf sequences, Rockwood Formation (Silurian), east Tennessee: Geol. Soc. Amer., Abst. with Progs., v. 18, p. 218-219.

Driese, S. G., Fischer, M. W., Easthouse, K. A., and Schoner, A. E. 1986c, Tidal and storm wave deposition in Lower Silurian shelf sequences, east Tennessee (Abst.): Am. Assoc. Petroleum Geologic Bull., v. 70, p. 585-584.

Driese, S. G., Fischer, M. W., and Easthouse, K. A., 1986d, Silurian siliciclastic and carbonate storm-shelf sequences, east Tennessee: Soc. Econ. Paleon. Mineral. Annual Midyear Meeting, Abstracts v. III, p. 31.

Driese, S. G., and Easthouse, K. A., in review, Paleobathymetry of a silurian shelf system: Application of proximality trends and ichnofacies distributions, (submitted to Palaios).

Driese, S. G., Fischer, M. W., Easthouse, K. A., and Marks, G. T., in press, Model for genesis of shelf sandstone sequences, southern Appalachians: Paleoenvironmental reconstruction of an Early Silurian shelf system, in Swift, D. J. P., Oertel, G. F., and Tillman, R. W. (eds.), Shelf Sand and Sandstone Bodies: Geometry, Facies and Distribution: S. E. P. M. Special Publication No.

Easthouse, K. A., 1987, The paleoenvironmental analysis of the Lower Silurian Rockwood Formation at Green Gap, White Oak Mountain, southeastern Tennessee: Univ. of Tennessee, unpub. M.S. Thesis, 218 p.

Epstein, J. B., and Epstein, A. G., 1972, The Shawangunk Formation (Upper Ordovician (?) to Middle Silurian) in eastern Pennsylvania: U.S. Geological Survey Prof. Paper 744, 45 p.

Folk, R. L., Andrews, P. B., and Lewis, D. W., 1970, Detrital sedimentary rock classification and nomenclature for use in New Zealand: New Zealand Jour. Geology and Geophysics, v. 13, p. 937-968.

Fischer, M. W., 1987, Sedimentology of the Clinch Sandstone (Lower Silurian) along Clinch Mountain, northeastern Tennessee: Univ. of Tennessee, unpub. M.S. Thesis, 156 p.

Folk, R. L., 1960, Petrography and origin of the Tuscarora, Rose Hill, and Keefer Formations, Lower and Middle Silurian of eastern West Virginia: Jour. Sed. Petrology, v. 30, p. 1-58.

Goldring, R. and Bridges, P., 1973, Sublittoral sheet sandstones: Jour. Sed. Petrology, v. 43, p. 736-747.

Gray, M. B., 1984, Slickensided soil fractures - Indicators of strain and deformation processes in the Bloomsburg Formation, central Pennsylvania: Geol. Soc. Amer. Abstracts with Programs, v. 16, p. 19.

Hamblin, A. P. and Walker, R. G., 1979, Storm-dominated shallow marine deposits: the Fernie-Kootenay (Jurassic) transition, southern Rocky Mountains: Canadian Journal of Earth Sciences, v. 16, p. 1673-1690.

Harms, J. C., 1969, Hydraulic significance of some sand ripples: Geol. Soc. Amer. Bull., v. 80, p. 363-396.

Harris, L. D. and Miller, R. L., 1963, Geology of the Stickleyville quadrangle, Virginia: U.S. Geol. Survey Quad. Map GQ-238.

Harris, L. D. and Miller, R. L., 1958, Geology of the Duffield quadrangle, Virginia: U.S. Geol. Survey Quad. Map GQ-111.

Hayes, A. W., 1974, Origin of the Tuscarora Formation (Lower Silurian), southwestern Virginia: Virginia Polytech. Inst. and State Univ., unpub. Ph.D. Dissertation, 162 p.

Hayes, C. W., 1891, The overthrust faults of the southern Appalachians: Geol. Soc. Amer. Bull., v. 2, p. 141-154.

Hayes, M. O., 1967, Hurricanes as geological agents, south Texas coast: Am. Assoc. Petroleum Geologists Bull., v. 51, p. 937-942.

Hobday, D. K., and Reading, H. G., 1972, Fairweather versus storm processes in shallow marine sand bar sequences in the Late Precambrian of Finnmark, North Norway: Jour. Sed. Petrology, v. 42, p. 318-324.

Hobday, D. K., and Tankard, A. J., 1978, Transgressive-barrier and shallow-shelf interpretation of the Lower Paleozoic Penninsula Formation, South Africa: Geol. Soc. Amer. Bull., v. 89, p. 1733-1744.

Houbolt, J. J. H. C., 1968, Recent sediments in the southern bight of the North Sea: Geol. en Mijnb., v. 47, p. 245-273.

Hunter, R. E., 1969, Eolian microridges on modern beaches and a possible ancient example: Jour. Sed. Petrology, v. 39, p. 1573-1578.

Hunter, R. E., 1970, Facies of iron sedimentation in the Clinton Group, in Ficher, G. W., Pettijohn, F. J., Reed, J. C., Jr., and Weaver, K. N., (eds.), Studies of Appalachian Geology, Central and Southern: Wiley-Interscience, New York, p. 101-121.

Hunter, R. E., 1977, Basic types of stratification in small eolian dunes: Sedimentology, v. 24, p. 361-387.

Hunter, R. E., and Clifton, H. E., 1982, Cyclic deposits and hummocky cross-stratification of probable storm origin in Upper Cretaceous rocks of Cape Sebastian area, southwestern Oregon: Jour. Sed. Petrology, v. 52, p. 127-144.

Johnson, H. D., 1975,Tide-and wave-dominated inshore and shoreline sequences from the late Precambrian, Finnmark, North Norway: Sedimentology, v. 22, p. 45-74.

Johnson, H. D., 1977, Shallow marine sand bar sequences: an example from the Late Precambrian of North Norway: Sedimentology, v. 24, p. 245-270.

Johnson, M. A., Stride, A. H., Belderson, R. H. and Kenyon, N. H., 1981, Predicted sand wave formation and decay on a large offshore tidal current sand sheet, in Holocene Marine Sedimentation in the North Sea Basin, Nio, S. D., Shuttenhelm, R. T. E. and T. J. C. E. van Weering, Special Publication, No. 5, Int. Assoc. Sedimentologists, Oxford, Blackwell Scientific Publishing, p. 247-256.

Johnson, M. E., 1987, Extent and bathymetry of North American platform seas in the Early Silurian: Paleoceanography, v. 2, p. 185-211.

Johnson, M. E., Rong, J.-Y., and Yang, X.-C., 1985, Intercontinental correlation by sea-level events in the Early Silurian of North America and China (Yangtze Platform): Geol. Soc. Amer. Bull., v. 96, p. 1384-1397.

Jordan, G. F., 1962, Large submarine sand waves: Science, v. 136, p. 839-848.

Kelling, G., and Mullin, P. R., 1975, Graded limestone and limestone-quartzite couplets: possible storm-deposits from the Moroccan Carboniferous: Sed. Geology, v. 13, p. 161-190.

Kenyon, N. H. and Stride, A. H., 1968, The crest length and sinuosity of some marine sand waves: Jour. Sed. Petrology, v. 38, p. 255-259.

Komar, P. D., 1974, Oscillatory ripple marks and the evaluation of ancient wave conditions and environments: Jour. Sed. Petrology, v. 44, p. 169-180.

Kreisa, R. D., 1981, Storm-generated sedimentary structures in subtidal marine facies with examples from the Middle and Upper Ordovician of southwestern Virginia: Jour. Sed. Petrology, v. 51, p. 823-848.

Kumar, N., and Sanders, J. E., 1976, Characteristics of shoreface storm deposits: modern and ancient examples: Jour. Sed. Petrology, v. 46, p. 145-162.

Lampiris, N., 1975, Stratigraphy of the clastic Silurian rocks of central western Virginia and adjacent West Virginia: Virginia Polytech. Inst. and State Univ., unpub. Ph.D. Dissertation, 85 p.

Langeraar, W., 1966, Sand waves in the North Sea: Hydrogr. Newsletter, v. 1, p. 243-246.

Langhorne, D. N., 1973, A sand wave field in the Outer Thames Estuary: Marine Geology, v. 14, p. 129-143.

Leckie, D. A. and Walker, R. G., 1982, Storm- and tide-dominated shorelines in Cretaceous Moosebar-Lower Gates interval--outcrop equivalents of Deep Basin Gas Trap in western Canada: Amer. Assoc. Petroleum Geologists Bull., v. 66, p. 138-157.

Levell, B. K., 1980, Evidence for currents associated with waves in Late Precambrian shelf deposits from Finnmark, North Norway: Sedimentology, v. 26, p. 153-166.

Levington, J. S., 1982, Marine Ecology: Prentice Hall, Englewood Cliffs, New Jersey, 526 p.

Madsen, O. S., 1976, Wave climate on the continental margin: elements of its mathematical description, in Stanley, D. J., and Swift, D. J. P., eds., Marine Sediment Transport and Environmental Management: New York, John Wiley and Sons, p. 65-87.

Maher, L. J., and Dott, R. H., Jr., 1979, Program for analysis of directional orientation data (for generalized basic): Univ. of Wisconsin, unpub. computer program.

Martini, I. P., 1971, Regional analysis of sedimentology of Medina Formation (Silurian), Ontario and New York: Am. Assoc. Petroleum Geologists Bull., v. 55, p. 1249-1261.

McCave, I. N., 1970, Deposition of fine-grained suspended sediment from tidal currents: Jour. of Geophysical Research, v. 75, 4151-4159.

McCave, I. N., 1971a, Sand waves in the North Sea off the coast of Holland: Marine Geology, v. 10, p. 199-225.

McCave, I. N., 1971b, Wave effectiveness at the sea bed and its relationship to bed-forms and deposition of mud: Jour. Sed. Petrology, v. 41, p. 89-96.

McKerrow, W. S., 1979, Ordovician and Silurian changes in sea-level: Geol. Soc. London Quat. Journ., v. 136, p. 137-145.

Middleton, G. V., and Southard, J. B., (eds.) 1984, Mechanics of sediment movement: Society of Economic Paleontologists and Mineralogists, Special Publication, no. 3, 401 p.

Milici, R. C., and Wedow, H., 1977, Upper Ordovician and Silurian stratigraphy in Sequatchie Valley and parts of the adjacent Valley and Ridge: U.S. Geological Survey Prof. Paper 996, 38 p.

Miller, R. L., 1954, Geology and oil resources of the Rose Hill district - the fenster area of the Cumberland overthrust block - Lee County, Virginia: Virginia Geol. Survey Bull., v. 71, 383 p.

Miller, R. L., 1976, Silurian nomenclature and correlations in southwest Virginia and northeast Tennessee: U.S. Geological Survey Bull. 1405-H, 23 p.

Miller, R. L., and Brosge, W. P., 1954, Geology and oil resources of the Jonesville district, Lee County, Virginia: U.S. Geological Survey Bull. 990, 240 p.

Mount, J. F., 1982, Storm-surge-ebb origin of hummocky cross-stratified units of the Andrews Mountain Member, Campito Formation (Lower Cambrian), White-Inyo Mountains, eastern California: Jour. Sed. Petrology, v. 52, p. 941-958.

Murray, S. P., 1970, Bottom currents near the coast during Hurricane Camille: Jour. Geophysical Research, v. 75, p. 4579-4582.

Nicholson, F. H., 1978, Sedimentology of the Clinch Sandstone, northeastern Tennessee and southwestern Virginia: Univ. of Kentucky, unpub. M.S. Thesis, 65 p.

Nio, S. D., 1976, Marine transgressions as a factor in the formation of sand wave complexes: Geol. en Minjb., v. 55, p. 18-40.

Nio, S. D., and Nelson, H., 1982, The North Sea and northeastern Bering Sea: a comparative study of the occurrence and geometry of sand bodies of two shallow epicontinental shelves: Geol. en Mijnb, v. 61, p. 105-114.

Nelson, C. H., 1982, Modern shallow-water graded sand layers from storm surges, Bering shelf: a mimic of Bouma sequences and turbidite systems: Jour. Sed. Petrology, v. 52, p. 537-545.

Odom, I.E., 1978, Mineralogy of Late Cambrian and Early Ordovician sandstones, Upper Mississippi Valley: in Odom, I. E., (ed.), Lithostratigraphy, petrology and sedimentology of Late Cambrian-Early Ordovician rocks near Madison, Wisconsin: Geol. and Natur. Hist. Surv., Univ. of Wisconsin, Madison, Wisconsin, p. 46-51.

Pearson, E. S., and Hartley, H. O., 1954, Biometrika tables for statistics, v. 1: New York, Cambridge University Press.

Pryor, W. A., and Amaral, E. J., 1971, Large-scale cross-stratification in the St. Peter Sandstone: Geol. Soc. Amer., Bull., v. 82, p. 239-244.

Raisz, E., 1957, Landforms of the United States, map; published by the author, Cambridge, Mass.

Reineck, H. E., and Singh, I. B., 1980, Depositional Sedimentary Environments, Berlin, Springer-Verlag, 549 p.

Rodgers, J., 1953, Geologic map of East Tennessee with explanatory text: Tennessee Div. Geol. Bull., v. 58, 168 p.

Safford, J. M., 1869, Geology of Tennessee: S. C. Mercer State Printers, Nashville, Tenn., p. 151-323.

Safford, J. M., and Killebrew, J. B., 1900, The elements of the geology of Tennessee: Nashville, Tenn., Foster and Webb, 264 p.

Sandin, Walter, 1960, A facies study of the Red Mountain Formation of Northwest Georgia: Ga. Min. Newsletter, v. 13, p. 106-107.

Schoner, A. E., 1985a, The sedimentology and sedimentary petrology of the Lower Silurian Clinch Sandstone at Beans Gap, Grainger County, Tennessee: Univ. of Tennessee, unpub. M.S. Thesis, 227 p.

Schoner, A. E., 1985b, The Clinch Sandstone (Lower Silurian) along Highway 25E at Beans Gap: in Walker, K. R., ed., The geologic history of the Thorn Hill Paleozoic section (Cambrian-Mississippian), eastern Tennessee: Studies in Geol. No. 10, Dept. of Geol. Sci., Univ. of Tennessee, p. 100-110.

Seilacher, A., 1967, Bathymetry of trace fossils: Marine Geology, v. 5, p. 413-428.

Seilacher, A., 1978, Use of trace fossils for recognizing depositional environments: in Basan, P. B., (ed.), Trace fossil concepts: Soc. Econ. Paleon. Mineral. Short Course Notes No. 5, p. 185-201.

Sheldon, R. P., 1970, Sedimentation of iron-rich rocks of Llandovery age (Lower Silurian) in the Southern Appalachian Basin, in Berry, W. B. N., and Boucot, A. J., (eds.), Correlation of the North American Silurian rocks: Geol. Soc. Amer. Spec. Paper 102, p. 107-112.

Stamp, L. D., 1922, An outline of the Tertiary geology of Burma: Geol. Mag., v. 59, p. 481-501.

Stewart, H. B. and Jordan, G. F., 1964, Underwater sand ridges on Georges Shoal, in R. L. Miller, (ed.), Papers in Marine Geology, R. L. Miller, ed., New York: Macmillan, p. 102-114.

Stride, A. H., 1970, Shape and size trends for sand waves in a depositional zone of the North Sea: Geological Magazine, v. 107, p. 469-477.

Stride, A. H. and Tucker, M. J., 1960, Internal waves and waves of sand: Nature (London), v. 188, p. 933.

Stride, A. H., 1982, Offshore Tidal Sands: Chapman and Hall, London, Ltd., 222 p.

Swartz, C. K., Prouty W. F., Ulrich, E. O., and Bassier, R. S., 1923, Stratigraphic and paleontologic relations of the Silurian strata of Maryland: Maryland Geol. Survey, Silurian, v. 8, p. 25-51.

Swartz, C. K., and Swartz, F. M., 1930, Age of the Shawagunk Conglomerate of eastern New York: Am. Jour. Sci., v. 20, p. 467-474.

Swift, D. J. P., 1968, Coastal erosion and transgressive stratigraphy: Jour. Geology, v. 76, p. 444-456.

Swift, D. J. P., Sanford, R. B., Dill, C. E., and Avignone, N. F., 1971, Textural differentiation on the shoreface during erosional retreat of an unconsolidated coast, Cape Henery to Cape Hatteras, western North Atlantic Shelf: Sedimentology, v. 16, p. 221-250.

Swift, D. J. P., 1975, Barrier-island genesis: evidence from the central Atlantic shelf, eastern U.S.A.: Sed. Geology, v. 14, p. 1-43.

Swift, D. J. P., 1975, Tidal sand ridges and shoal-retreat massifs: Marine Geology, v. 18, p. 105-134.

Swift, D. J. P. and Field, M. E., 1981, Evolution of a classic sand field: Maryland sector, North American inner shelf: Sedimentology, v. 28, p. 461-482.

Swift, D. J. P., Figueiredo, A.G., Freeland, G. L. and Oertel, G. F., 1983, Hummocky cross stratification and megaripples: a geological double standard?: Jour. Sed. Petrology, v. 53, p. 1295-1317.

Swift, D. J. P., and Niedoroda, A. H., 1985, Fluid and sediment dynamics on continental shelves, in Tillman, R. W., Swift, D. J. P. and Walker, R. G., (eds.), Shelf Sands and Sandstone Reservoirs: S.E.P.M. Short Course Notes No. 13, p. 47-136.

Swift, D. J. P., Stanley, D. J., and Curray, J. R., 1971, Relict sediments on continental shelves: a reconsideration: Jour. Geology, v. 79, p. 322-346.

Terwindt, J. H. J., 1971, Sand waves in the South Bight of the North Sea: Marine Geology, v. 10, p. 51-67.

Thompson, A. M., 1970, Tidal-flat deposition and early dolomitization in Upper Ordovician rocks of southern Appalachian Valley and Ridge: Jour. Sed. Petrology, v. 40, p. 1271-1286.

Thompson, J. R., 1984, Depositional environments of the Sequatchie and Rockwood Formations: Univ. of Tennessee, unpub. M.S. Thesis, 199 p.

Tucker, M. E., 1982, The Field Description of Sedimentary Rocks: Wiley, New York, 112 p.

Van Veen, J., 1935, Sand waves in the North Sea: Hydrogr. Rev., v. 12, p. 95-112.

Visser, M. J., 1980, Neap-spring cycles reflected in Holocene subtidal large-scale bedform deposits: a preliminary note: Geology, v. 8, p. 543-546.

Walker, K. R., and Diehl, W. W., 1986, The effect of synsedimentary substrate modification on the composition of paleocommunities: paleoecologic succession revisited: Palaios, v. 1, p. 65-74.

Walker, R. G., 1984, Shelf and shallow marine sands, in Walker, R. G., (ed.), Facies Models, 2nd edition: Geoscience Canada Reprint Series 1, p. 141-170.

Walker, R. G., 1985, Geological evidence for storm transportation and deposition on ancient shelves, in Tillman, R. W., Swift, D. J. P. and Walker, R. G. (eds.), Shelf Sands and Sandstone Reservoirs: S.E.P.M. Short Course Notes No. 13, p. 243-303.

Wedow, H. Jr., 1960, Sequatchie and Rockwood Formations in Southeast Tennessee and part of Northwest Georgia [abs.]: Geol. Soc. Amer. Bull., v. 71, no. 12, p. 2028.

Whisonant, R. C., 1977, Lower Silurian Tuscarora (Clinch) dispersal patterns in western Virginia: Geol. Soc. Amer. Bull., v. 88, p. 215-220.

Whittaker, J. H. M., 1973, "Gutter Casts," a new name for scour- and-fill structures: with examples from the Llandoverian of Ringerike and Malmoya, Southern Norway: Norsk. Geog. Tidsskr., v. 53, p. 403-417.

Yeakel, L. S., 1962, Tuscarora, Juniata and Bald Eagle paleocurrents and paleogeography in the Central Appalachians: Geol. Soc. Amer. Bull., v. 73, p. 1515-1540.

APPENDICES

APPENDIX I

DETAILED MEASURED SECTION

Unit Thickness (m)	Cumulative Thickness (m)	Description
Juniata Formation		
0.00	0.00	Contact with overlying Clinch Sandstone, Hagan Shale Member. Transitional over 5 cm.
0.25	0.25	Interbedded shale, mudstone and sandstone. Shale is maroon, brittle and fissile. Mudstone is green and weathers blocky. Sandstone is maroon-gray and is fine-grained. It forms a lenticular bedding of flat lenses and small scours (50 mm by 20 mm).
0.70	0.95	Interbedded shale and siltstone. Shale is predominantly maroon, however some green coloration is present. Siltstone is maroon, very thinly bedded (30 mm average), shows faint horizontal laminations and has sharp, planar bedding contacts. One siltstone bed shows small (25 mm by 10 mm) scours at its base.
0.45	1.40	Silty mudstone, dominantly maroon with some green mottling. Weathers blocky to slightly fissile and extremely brittle. Paleovertisol features include occasional ped-like clasts and slickensided pedogenic fractures.
0.14	1.54	Siltstone, maroon and structureless. Shows sharp, planar bedding contacts with surrounding mudstone. Consistent lateral thickness.

Unit Thickness (m)	Cumulative Thickness (m)	Description
0.48	2.02	Interbedded shale, mudstone and occasional siltstone. Shale dominates this interval, is maroon and slightly fissile to fissile. Mudstone is green, fissile to blocky and bioturbated. Mudstone occurs in horizons 20 mm or less in thickness and contains vertical burrows and escape structures. Skolithos is 15 mm in diameter by several cm in length. Problematic "vee-shaped" escape structures measure 7 mm at the tops and are 25 mm in length. Green mudstone intervals have transitional contacts. Siltstone is maroon, structureless and has sharp, planar bedding contacts. All beds show consistent lateral thickness.
2.08	4.10	Interbedded shale, mudstone and siltstone. Shale is maroon and fissile. Mudstone is green, fissile to blocky and slightly bioturbated. Mudstone contacts with surrounding shale are transitional, bedding is laterally discontinuous and averages 30 mm thick. Siltstone is maroon to maroon-gray and shows low-profile current-rippled tops and slightly scoured bases. Bedding contacts are sharp.
Hagan Shale Member of the Clinch Sandstone		
0.00	0.00	Contact with underlying Juniata Formation.
0.30	0.30	Calcareous sandstone. Medium gray but weathers to a slight red-brown-gray. Very fine-grained but the top of the bed is inversely graded over 2 cm with

Unit Thickness (m)	Cumulative Thickness (m)	Description
		very coarse sand capping it. Faint horizontal laminations internally. Upper bed boundary sharp, lower boundary transitional with Juniata.
0.21	0.51	Interbedded shale and sandstone. Shale is medium to dark gray and fissile. Rare Skolithos (12 mm in diameter) extend vertically 2 cm. Sandstone is light gray, medium- to coarse-grained and internally structureless. Average bed thickness is 1.5 cm with diffuse and wavy-parallel bed boundaries. Fragmented trilobite debris found within some beds.
2.19	2.70	Interbedded shale and sandstone. Shale is medium to dark gray, fissile to slightly blocky with sparse Skolithos (4 mm to 8 mm in diameter). Sandstone is light to medium gray and very fine-grained. Internal structures include even-parallel and discontinuous-wavy-nonparallel horizontal laminations. Some tops of beds show symmetrical wave-ripple crests with weak chevron internal structures. Bed thickness is generally 2cm to 5cm with sharp upper and lower contacts. Some Planolites (5mm in diameter) along bases. Sandstone beds within this interval show a consistent lateral thickness and becomes slightly calcareous around 2 m. One thin sandstone at 1.6 m contains fragmented echinoderm and trilobite debris forming horizontal laminations.
1.29	3.99	Interbedded shale and siltstone. Shale dominates this interval

Unit Thickness (m)	Cumulative Thickness (m)	Description
		(90%), is medium to dark gray, and fissile near the base. Higher up, the shale turns fissile to blocky, very friable and has a "conchoidal-like" weathering pattern on outcrop. Siltstone is medium to dark gray and weathers slightly red. Even-parallel horizontal laminations and wave ripple cross-laminations internally with occasional flute and tool marks found on the undersurface of beds. Symmetrical wave ripple crests capping beds have height to length ratios of 5 mm/25 mm. Rare scours (40 mm by 25mm) at the bases of some siltstone beds. Average siltstone thickness is 1 cm with sharp, wavy bedding surfaces.
0.61	4.60	Interbedded shale and sandstone. Shale is medium to dark maroon-gray, fissile to slightly blocky and somewhat uniform. Sandstone is light to medium gray, very fine-grained with wave ripple cross-laminations internally and wave ripple crests capping beds. Average sandstone thickness is 2.3 cm with slightly transitional and wavy-parallel bedding surfaces.
1.17	5.77	Interbedded shale and sandstone. Shale is medium to dark maroon-gray, fissile to slightly blocky and somewhat uniform. Sandstone is light to medium gray, very fine-grained with form-discordant wave ripples overlying even-parallel horizontal laminations within the same bed. Bed thickness averages 3.2 cm, with upper bedding surfaces

Unit Thickness (m)	Cumulative Thickness (m)	Description
		sharp/wavy and lower bedding surfaces sharp/planar.
0.42	6.19	Fossilferous shale. Medium to dark maroon-gray, blocky and uniform. Contains crinoid columnals (2 mm and 8 mm in diameter), brachiopods and bivalves. Some very fine sand-filled gutter casts at the base are slightly asymmetrical (5 cm by 10 cm).
1.23	7.42	Interbedded shale and sandstone. Shale is medium to dark maroon-gray, fissile to slightly blocky and contains few Planolites (8 mm in diameter). Sandstone is calcareous, light to medium gray and generally very fine-grained (sometimes silt-sized). Even-parallel to wavy-parallel horizontal laminations with normal grading or current-ripple cross-laminations overlying horizontal laminations within the same bed. Also some wave ripple cross-laminations overlying horizontal laminations. Sparse Skolithos (9 mm in diameter) and problematic vertical escape structures running through entire thickness of some sandstones. Bed thickness averages 1 cm near the base, however, increases to 7.5 cm upward. There are two such thickening-upward patterns in this interval. Upper bedding surfaces sharp/wavy or sharp/planar, lower bedding surfaces sharp/planar. Micro-hummocky cross-laminations occur at 7.25 m.
0.11	7.53	Sandstone, light to medium gray, generally fine-grained and

Unit Thickness (m)	Cumulative Thickness (m)	Description
		even-parallel horizontally laminated. Base of unit shows normal grading with large (up to 1.2 cm) fossil debris including high-spiralled gastropods, articulate brachiopods and ramose bryozoans. "V-shaped" vertical burrows (25 mm at top, extending downwards for 4 cm) and sharp/planar bedding surfaces. Unit pinches out to the west.
1.28	8.81	Interbedded shale and sandstone. Shale is medium to dark maroon-gray and fissile to very fissile. Sandstone is light to dark gray, extremely fine-grained and slightly calcareous. Even-parallel horizontal laminations or horizontal laminations overlain by form-discordant wave ripples found in some beds. Sandstone thickens upwards (0.5 cm at base increasing to 5 cm). Two such thickening-upward patterns in this interval. Upper bedding surfaces sharp/planar or sharp/wavy, lower bedding surfaces sharp/planar. A medium-grained, skeletal-rich sandstone at 8.6 m shows normal grading from large skeletal debris (0.5 mm) to mud. Beds vary in thickness laterally.
0.14	8.95	Interbedded shale and sandstone. Shale is medium to dark maroon-gray and fissile. Sandstone is medium to dark gray, medium- to coarse-grained and skeletal-rich. Fossils include trilobites, crinoids, echinoderm plates, and brachiopods. Long axes of allochems are orientated parallel to bedding. Beds show

Unit Thickness (m)	Cumulative Thickness (m)	Description
		normal grading from skeletal debris (several mm) to mud. Upper and lower bedding surfaces sharp and somewhat planar. Beds vary in thickness laterally.
0.92	9.87	Interbedded shale and sandstone. Shale is medium maroon-gray and slightly fissile to blocky. Sandstone is light to medium gray, extremely fine-grained and slightly to extremely dolomitic. Even-parallel horizontal laminations or structureless beds predominate. Beds average 4 cm thick with a consistent lateral thickness. Rounded phosphate nodules (2 mm in diameter) occur at 9.5 m. A quartz-rich dolomitic biosparite at 9.6 m contains fragmented trilobites, articulate brachiopods, echinoderm plates and ramose bryozoans. Thickness is 1.5 cm with sharp/planar bedding surfaces.
2.05	11.92	Interbedded shale and sandstone. Shale is dark gray and fissile with rare Lingula (brachiopods). Sandstone is light to medium gray, extremely fine-grained showing single or connected lenticular bedding with thick lenses. Thicker beds show even-nonparallel horizontal laminations or some form-discordant wave ripples. Gutter casts at 10.45 m and 11.8 m average 17 cm wide by 5 cm deep, some with internal structures. Some gutters have coarse-fragmented skeletal debris at base. Sandstone beds pinch out to the east.

Unit Thickness (m)	Cumulative Thickness (m)	Description
0.08	12.00	A quartz-rich, ferruginous, bryozoan packstone, light brown to medium gray with maroon mottling. Discontinuous and continuous, wavy-parallel horizontal laminations produced by maroon-mud intraclasts. Fragmented fossils show long axes parallel to bedding and include trilobites, crinoids, echinoderm plates, high-spiralled gastropods, ramose bryozoans and rare bivalves. Fossils are iron-stained. Sharp and somewhat planar bedding surfaces, uniform lateral thickness.
1.12	13.12	Interbedded shale and sandstone. Shale is medium to dark gray and fissile to slightly blocky. Sandstone is medium gray, fine-grained and structureless, however, form-discordant wave ripples were found at 12.1 m and 12.25 m. Sandstone is lenticular-bedded with single or connected flat lenses. Bed thickness averages 2.5 cm with sharp upper and lower bedding surfaces. A dolomitic biosparite at 12.21 m is similar, but more fine-grained than the underlying biosparite at 11.92 m.
2.08	15.20	Interbedded shale and sandstone. Shale is medium to dark gray, fissile to slightly blocky and contains horizontal burrows of Planolites (5 mm in diameter) which are slightly flattened and continuous for 10 cm. Sandstone is dark maroon-gray, very fine-grained and contains even-parallel horizontal laminations and form-discordant wave ripple cross-lamination.

Unit Thickness (m)	Cumulative Thickness (m)	Description
		Some minor sand-filled scours at the bases of beds and form-discordant wave ripples at the tops (height to length ratio is 4 cm/22 cm). Normal grading of fine sand at 14.43 m, small flute marks at 14.81 m and sand-filled, cross-laminated gutter casts at 14.63 m. Large sandstone lense (5 m by 12 cm) at 14.57 m shows wave-ripple cross-laminations. Average sandstone bed thickness 1.5 cm, with sharp/planar or sharp/wavy bedding surfaces. Beds pinch out laterally.
1.90	17.10	Interbedded shale and sandstone. Shale is medium to dark gray, fissile to slightly blocky and contains Planolites (1.5 cm in diameter). Small problematic vertical burrows (3 mm in diameter, 20 mm in length) at 16.72 m. Shale becomes more abundant higher up in this sub-interval. Sandstone is medium maroon-gray, very fine-grained, with even-parallel horizontal laminations capped by form-discordant wave ripples, and low-relief current ripples. Some sandstone beds contain Planolites (1.2 cm to 1.7 cm in diameter) at their bases. Average bed thickness 1.75 cm but decreases upwards to thin flat-lenses. Sharp/planar to sharp/wavy bedding surfaces, which pinch out laterally.
1.10	18.20	Shale is dark gray to black, finely fissile to slightly blocky and contains Planolites (6.5 mm in diameter) at 8.10 m to 8.20 m.

Unit Thickness (m)	Cumulative Thickness (m)	Description
		Rare Lingula brachiopods throughout.
0.21	18.41	Sandstone is medium gray, tinted light red-brown, fine- to medium-grained and fossiliferous. Form-discordant wave ripples at top. Fossils include ramose bryozoans, echinoderms, crinoids, cephalopods, and gastropods. Lense-shaped geometry (9 m in length, 0.2 m in width), with sharp/planar lower and sharp/wavy upper bedding surfaces.
0.92	19.33	Interbedded shale and sandstone. Shale is medium gray, fissile to slightly blocky and contains small Skolithos (6 mm in diameter), Planolites and a few problematic vertical burrows. Sandstone is dark maroon-gray, extremely fine-grained (to silt) with form-discordant wave ripples, basal scours, small gutter casts (15 cm by 3 cm) and flat-lens lenticular bedding. Some discontiuous wavy bedding. Bedding surfaces sharp/wavy.
0.87	20.20	Shale is medium to dark-gray with brown, green and maroon mottling. Fissile to slightly blocky lithology contains sand-filled burrows of Planolites (8 mm in diameter) and possible Skolithos (2 mm in diameter). Rare wispy and flat-lens fine-grained sandstone.
0.19	20.39	Conglomeratic sandstone is medium to dark gray with red, brown, green and black mottling. Grain size varies from medium sand to gravel at the top (inversely graded). Mud intraclasts are

Unit Thickness (m)	Cumulative Thickness (m)	Description
		imbricated and show oxidation rims. Current ripples (height/length ratio is 1cm/12cm) at upper bedding surface. Lens geometry is approximately 20 m in length by 1.1 m width. Sharp/planar lower and sharp/wavy upper bedding surfaces. This unit shows heavy diagenetic alteration and iron-mineralization.
1.03	21.42	Interbedded shale and sandstone. Shale is medium to dark gray, fissile to slightly blocky and contains minor problematic vertical burrows (5 mm in diameter). Sandstone is medium gray, fine- to coarse-grained with current-rippled upper surfaces. Medium to coarse sand-filled gutters, thick lensoid and wavy bedding predominate. Average bed thickness 2 cm, with sharp/wavy upper and lower bedding surfaces. Most beds pinch out laterally over several m.
1.83	23.25	Predominantly shale with few interbedded siltstone and fine-grained sandstone beds. Shale is medium to dark maroon-gray, fissile to slightly blocky and contains sand-filled burrows of Skolithos (2 mm in diameter) and Planolites (12 mm in diameter). Shale gradually increases in silt content from 22.6 m until predominantly siltstone at the contact with the overlying Poor Valley Ridge Member. Sandstone is light to medium brown-gray, fine-grained and occurs as flat-lenses or wavy bedding. Average bed thickness is 9 cm. Beds pinch out laterally.

Unit Thickness (m)	Cumulative Thickness (m)	Description
		Near the PVR contact, sandstone beds take on a yellow gray-brown coloration, become thin and bioturbated. Average bed thickness is 4 cm. Contact with PVR is transitional.
Poor Valley Ridge Member of the Clinch Sandstone		
0.00	0.00	Contact with underlying Hagan Shale Member.
0.13	0.13	Sandstone is dark gray, weathers red brown or maroon-brown, extremely fine-grained with hummocky cross-laminations, current ripples and current-ripple cross-laminations. Skolithos (3 mm in diameter). Transitional/planar lower and sharp/wavy upper bedding surfaces. Bed maintains a uniform lateral thickness.
1.04	1.17	Interbedded shale and sandstone. Shale is dark brown-gray and extremely fissile. Sandstone is dark maroon-gray weathering to yellow brown, very fine-grained with current ripple cross-laminations, current ripples and some scoured bases. Some gastropod trails (8 mm in diameter) at 0.75 m. Average bed thickness is 1.5 cm with slightly wavy-parallel bedding. Sharp/planar lower and sharp/wavy upper bedding surfaces. Uniform lateral thicknesses of beds.
1.01	2.18	Interbedded silty shale and sandstone. Silty shale is dark brown-gray and extremely fissile. Sandstone medium gray, very

Unit Thickness (m)	Cumulative Thickness (m)	Description
		fine-grained and structureless with bed thickness ranging from 0.75 cm to 20 cm. Skolithos and Rusophycus increase in abundance upward. Sharp/planar bedding surfaces and uniform lateral thicknesses.
1.63	3.81	Sandstone is medium to dark gray, weathers yellow-brown, fine-grained and intensely bioturbated by Skolithos (6 mm in diameter), and a problematic horizontal burrow. General mottled and friable nature. Several coarse-grained lag zones (3.2 m and 3.5 m) contain rounded pebbles of quartz, phosphate nodules and Lingula brachiopods. Slight coarsening-upward trend over entire interval. Sharp/planar bedding surfaces. Bed maintains a uniform lateral thickness.
1.99	5.80	Sandstone is medium gray, weathers green yellow-brown, coarse-grained and structureless. The basal 0.5 m shows normal grading from gravel to coarse sand. Isolated Lingula brachiopods, phosphate nodules and abundant Skolithos (3 mm in diameter). Sharp/planar lower and transitional/planar upper bedding surfaces. Bed maintains a uniform lateral thickness.
0.98	6.78	Sandstone is medium to dark gray, weathers red yellow-brown, very fine-grained and moderately bioturbated by Skolithos (4 mm in diameter). Faint, small-scale trough cross-stratification rare. Generally thin- to medium-bedded with some intercalated mudstone

nit Thickness (m)	Cumulative Thickness (m)	Description
		(up to 0.5 cm thick) between beds. Bed maintains a uniform lateral thickness. Most bedding surfaces are sharp/planar.
4.15	10.93	Sandstone is light to medium gray, weathers light yellow-brown, fine- to very fine-grained with medium-scale trough cross-stratification and current ripples capping some beds. Some troughs contain granule lag streamers. Rounded mud intraclasts (up to 4 cm), coarse-grained quartz and Cruziana trails (1.5 cm wide) occur in the upper few cm of many beds. Sandstone is medium-bedded with some intercalated mudstone (up to 0.5 cm thick) between beds. Slight fining-upward trend over entire interval with sharp/planar bedding surfaces. Wedge-like beds pinch out laterally in both directions.
0.49	11.42	Interbedded shale and sandstone. Shale is medium to dark gray-brown, weathers red brown, fissile to slightly blocky with thin, even-parallel horizontal laminations and current ripple cross-lamination. Rare Skolithos (4 mm in diameter, 20 mm in length). Sandstone is light to medium gray with dark gray mottling, medium-grained with current ripples, even-parallel laminations and heavily bioturbated zones of Arthrophycus (12 mm in diameter) found on lower bedding surfaces. Sandstone bed thickness ranges from 2 cm to 6 cm, sharp/planar lower and sharp/wavy upper bedding surfaces.

Unit Thickness (m)	Cumulative Thickness (m)	Description
		Wedge-like beds pinch out laterally in both directions.
0.60	12.02	Sandstone is light to medium brown-gray, coarse- to very fine-grained and normally graded over the entire interval (grades into overlying shale). Medium-scale trough cross-stratification, and at the tops of beds, Arthrophycus (14 mm in diameter) and Cruziana (11 mm in diameter). Some even-parallel horizontal laminations in very fine-grained sandstone near the overlying shale. Transitional upper contact. Wedge-like beds pinch out laterally in both directions.
0.76	12.78	Shale is light gray-brown with black mottling and occasional black pyrite concretions. Few Arthrophycus (12 mm in diameter) scattered throughout bed. Also flat-lensoid, fine-grained, lenticular bedding at 12.75 m.
2.27	15.05	Sandstone is light to medium gray, weathers light brown, fine- to medium-grained with medium-scale trough cross-stratification, and on upper bedding surfaces, current ripples and rounded mud intraclasts. Arthrophycus (12 mm in diameter) and Rhizocorallium (at 14.7 m) internally and along bedding surfaces. Cruziana along upper surfaces. Occasional intercalations of dark red-gray mudstone between beds, some clay drapes internally. Wedge-like beds pinch out laterally in both directions. Also granule-lag streamers within some trough

Unit Thickness (m)	Cumulative Thickness (m)	Description
		cross-stratification and granule or coarse-grained layers capping many sandstone units (inversely graded). Sharp/planar bedding surfaces. Wedge-like beds pinch out laterally in both directions.
0.95	6.00	Sandstone is light to medium-gray, weathers light yellow-brown, generally fine-grained with medium-scale trough cross-stratification, and on upper bedding surfaces, current ripples, rounded light-gray mud intraclasts and some Arthrophycus (1 cm in diameter). Rare Diplocraterion, and filling some troughs, granule lag streamers or mud intraclasts. Base of unit is normally graded from coarse to fine sandstone (over 20 cm) and the top, inversely graded (fine- to coarse sand) over 10 cm. Rare pyrite nodules occur throughout entire unit, which is medium bedded with sharp/planar surfaces. Wedge-like beds pinch out laterally in both directions.
3.18	19.18	Sandstone is light to medium gray, weathers light yellow-brown, fine- to medium-grained with medium to large scale trough cross-stratification, reactivation surfaces, and limited wave ripple cross-laminations. General paucity of mud intraclasts and clay drapes. Arthrophycus (8 mm in diameter) and Diplocraterion (12 mm in diameter). Scattered coarse-grained quartz commonly associated with bioturbation. Thin (1 cm) mudstone layers between some sand units. Sequence is medium-bedded with sharp/planar

Unit Thickness (m)	Cumulative Thickness (m)	Description
		bedding surfaces. Semi wedge-like beds pinch out laterally in both directions.
1.14	21.12	Sandstone light to medium gray, weathers light red-yellow-brown, medium- to fine-grained with medium-scale trough cross-stratification and rounded mud intraclasts throughout. Sandstone intercalated with thin mudstones and clay drapes, Arthrophycus and possible Planolites associated with mud horizons. Normal grading throughout entire unit from medium sand (base) to fine sand (top of unit). Average thickness of sandstone beds 40 cm with sharp/planar bedding surfaces. Semi wedge-like beds pinch out laterally in both directions.
1.87	22.99	Sandstone is light to medium gray, weathers to light red-yellow-brown, medium-grained with medium scale trough cross-stratification and minor Arthrophycus between sandstone beds. Paucity of mud intraclasts and clay drapes. Some reverse grading from medium to coarse sand at the tops of some beds. Average sandstone thickness is 45 cm with sharp/planar bedding surfaces. Semi wedge-like beds pinch out laterally in both directions.
1.07	24.06	Interbedded shale and sandstone. Shale is dark gray and slightly fissile. Arthrophycus (17 mm in diameter) and possible Planolites throughout shale and along sandstone/shale contacts. Shale 1 cm to 5 cm thick, pinches out

Unit Thickness (m)	Cumulative Thickness (m)	Description
		laterally. Sandstone light to medium gray, weathers light red-yellow-brown with medium-scale trough cross-stratification and current ripples capping beds. Medium-bedded (20 cm), with sharp/planar contacts. Beds show a semi-consistent lateral thickness.
1.68	25.74	Sandstone is light yellow-gray, weathers light red-yellow-brown, fine- to medium-grained with some medium-scale trough cross-stratification, wave-ripple cross-lamination and current ripples on top of beds. Minor Arthrophycus and rounded mud intraclasts. Sandstone is medium-bedded (30 cm thick), with two coarsening-upward sequences with coarse-grained sand capping some beds. Sharp/planar bedding surfaces. Beds show semi-consistent lateral thickness.
0.52	26.26	Shale is medium gray, weathers light brown-gray, fissile and featureless. Upper and lower contacts with sandstone are sharp/planar.
1.59	27.85	Sandstone is light to medium gray, weathers light orange-brown with medium-grained sand grading upward to fine sand. Medium-scale trough cross-stratification, Arthrophycus (15 mm in diameter) along bedding surfaces and a problematic vertical burrows (8 mm in diameter) within beds. Thin (up to 2 cm) intercalations of mudstone found between the medium-bedded sandstone. Some even-parallel horizontal stratification. Maroon

Unit Thickness (m)	Cumulative Thickness (m)	Description
		siltstone lithology of the overlying Rose Hill Formation found within trough cross-stratification near the contact.
Rose Hill Formation		
0.00	0.00	Contact with underlying Poor Valley Ridge Sandstone. Maroon siltstone of Rose Hill Formation extends downward into trough cross-stratification and burrows of Skolithos (7 mm in diameter). Fine-grained quartzose sandstone passes upward to maroon silt, a transitional change over 40 cm. No evidence for an unconformity.
2.50	2.50	Siltstone is dark maroon, weathers light gold-yellow-brown with even parallel horizontal laminations, wave ripple cross-laminations and several wave-rippled tops of beds (height/length ratio is 20 mm/55 mm). Also, interference ripples, ripples with planed-off crests, Skolithos (7 mm in diameter), Planolites (9 mm in diameter) and mudcracks showing several episodes of drying. Siltstone is thin bedded (average thickness 8 cm) with some intercalations of mudstone measuring 8 mm thick. Bed contacts are sharp/planar or transitional/planar. Light green-gray silt nodules at 2.2 m showing diffuse boarders, 11 mm in diameter and are concentrated in horizons parallel to bedding.
1.71	4.21	Interbedded mudstone, siltstone and sandstone. Mudstone is light green-gray, fissile to blocky with

Unit Thickness (m)	Cumulative Thickness (m)	Description
		an average thickness of 10 cm, which changes laterally. Siltstone is dark maroon, weathers light orange-brown and contains even-parallel, wavy-parallel and wavy-nonparallel horizontal laminations. Skolithos (8 mm in diameter or less) infilled with light green sandstone, Planolites (11 mm in diameter) common. Many siltstone units are graded with rip-up mud intraclasts at bases. Internal fabric bioturbated, some algal laminations and possible desiccation features. Sandstone is light maroon-gray, weathers gold yellow-brown, fine-grained and contains wave ripples, wave ripple cross-lamination, wavy-parallel algal laminations, current ripples and small-scale, low-angle trough cross-stratification. Siltstone and sandstone generally have sharp/planar bedding surfaces. Bed thickness changes laterally.
0.29	4.50	Sandstone is light yellow-gray showing maroon mottling, fine-grained with small-scale, low-angle trough cross-stratification, current-ripple lamination and current ripples. Horizontal algal laminations and problematic vertical burrows (2 mm in diameter) also present. Disc-shaped, light-gray mud intraclasts at 4.25 m. Unit is medium-bedded with sharp/planar contacts. Bedding shows constant lateral thickness.
1.31	5.81	Covered Interval.

Unit Thickness (m)	Cumulative Thickness (m)	Description
0.62	6.43	Interbedded siltstone and sandstone. Siltstone is light gray, weathers yellow brown in beds 2-3 cm thick. Sandstone light to medium gray, fine-grained and weathers yellow-brown with black mottling. Even-parallel horizontal laminations and few mud intraclasts. Bed thickness 10-12 cm with sharp contacts. Evidence for soft-sediment deformation.
0.64	7.07	Interbedded mudstone and sandstone. Mudstone is light green-gray with thin streamers of silt. Sandstone is light to medium gray, weathers yellow-brown, very fine- to fine-grained with wave- and current ripple cross-laminations. Both ripple types also found at tops of beds. Sandstone thickness ranges from 1 cm to 14 cm. Two sandstone units show normal grading throughout their entire thickness. Uppermost sandstone grades into overlying massive, maroon siltstone. All other bedding surfaces sharp/planar.
2.05	9.12	Siltstone is light maroon with white and light green mottling, massive at base turning more fine-grained and fissile upward. Discontinuous and diffuse bedding. Skolithos (7 mm in diameter) filled with light green silt. Excessive bioturbation gives rock a mottled appearance. Siltstone changes to a light green color higher up in the sequence.
3.08	12.20	Interbedded siltstone and sandstone. Siltstone is light yellow-brown, generally 3 cm

Unit Thickness (m)	Cumulative Thickness (m)	Description
		thick. Sandstone is medium gray to light brown-gray, weathers red orange-brown and medium-grained. Medium-scale trough cross-stratification and wave ripples. Bed thickness ranges from 10 cm to 40 cm, with sharp/planar bedding surfaces. Minor problematic vertical burrows (9 mm in diameter), Monocraterion (7 mm in diameter) and Diplocraterion (11 mm in diameter). Bed thickness increases upward and has a wedge-like geometry.
1.60	13.80	Sandstone is light gray, weathers yellow-gray and very fine-grained. Faint medium-scale trough cross-stratification, lunate current ripples and form-discordant wave ripples. Planolites, Monocraterion and light gray, rounded mud intraclasts. Average bed thickness 20cm with sharp/planar contacts and a sheet-like geometry.
0.61	14.41	Sandstone is light gray, weathers light red to yellow-brown and very fine-grained. Wave ripples and rounded mud intraclasts. Average bed thickness 35 cm with sharp/planar contacts and a sheet-like geometry.
2.99	17.40	Sandstone is light gray, weathers light red-yellow-brown and very fine-grained. Even-parallel horizontal laminations and Skolithos (2 mm in diameter). Average bed thickness is 30 cm, with sharp/planar contacts and a sheet-like geometry.

APPENDIX II

PETROGRAPHIC ANALYSIS

Sample No: P13-A

Formation: Poor Valley Ridge Member of the Clinch Sandstone.

Stratigraphic Position: 19.0 m above base of PVR

Rock Name: Quartzarenite

Grain Size:
- Maximum: 0.80 mm (rare)
- Minimum: 0.088 mm
- Mode: 0.275 mm

Sorting: Well sorted, θ=0.33

Roundness: Subrounded

Sphericity: Medium

Composition:
- Quartz (97%)
  - Monocrystalline (94%)
  - Polycrystalline (2%)
- Orthoclase (0.5%)
- Microcline (trace)
- Chert (trace)
- Muscovite (trace)
- Tourmaline (trace)
- Zircon (trace)
- Opaques (trace)
- Matrix (0.5%)
  - Phyllosilicates, fine grained opaques and quartz.
- Cement (1.5%)
  - Silica (1%)
  - Phyllosilicates (0.5%)

Recalculated percent for Folk et al. (1970).
- Q = 99%
- F = 1%
- R = 0%

Other Features:
Fine-grained, slightly stylolitized, cross-laminated quartzarenite. Recrystallization of quartz grains forms a tight, interlocking mosaic. Phyllosilicates and silt are concentrated along thin, irregular, discontinuous stylolites. Cross-laminations formed by concentrations of coarse-grained quartz.

Sample No: P14-A

Formation: Poor Valley Ridge Member of the Clinch Sandstone

Stratigraphic Position: 19.3 m above base of PVR.

Rock Name: Quartzarenite

Grain Size:
- Maximum: 0.5 mm
- Minimum: 0.088 mm
- Mode: 0.25 mm

Sorting: Well sorted, θ=0.45

Roundness: Subangular to subrounded

Sphericity: Medium

Composition:
- Quartz (95%)
  - Monocrystalline (91%)
  - Polycrystalline (4%)
- Sedimentary Rock Fragments (1.5%)
- Orthoclase (0.5%)
- Chert (trace)
- Tourmaline (trace)
- Zircon (trace)
- Opaques (trace)
- Matrix (0.5%)
  - Phyllosilicates
- Cement (1.5%)
  - Silica and hematite cement.

Recalculated percent for Folk et al. (1970).
- Q = 98%
- F = 0.5%
- R = 1.5%

Other Features:
Fine-grained, well-sorted, cross-laminated quartzarenite. Recrystallization of quartz grains forms a tight, interlocking mosaic. Sedimentary rock fragments consist of mud intraclasts which show a preferred orientation (long dimensions parallel to bedding). Cross-laminations contain high concentrations of phyllosilicates and mud intraclasts. This sample was point-counted for 350 points.

Sample No: P10-6

Formation: Poor Valley Ridge Member of the Clinch Sandstone

Stratigraphic Position: 14.2 m above base of PVR.

Rock Name: Quartzarenite

Grain Size:
- Maximum: 0.710 mm (rare)
- Minimum: 0.062 mm
- Mode: 0.177 mm

Sorting: Well-sorted for each mode, θ=0.35.

Roundness: Subangular (fine mode) and subrounded (coarse mode).

Sphericity: Low (fine mode) and medium (coarse mode).

Composition:
- Quartz (95%)
  - Monocrystalline (90%)
  - Polycrystalline (5%)
- Orthoclase (0.5%)
- Microcline (trace)
- Muscovite (0.5%)
- Chert (trace)
- Tourmaline (trace)
- Zircon (trace)
- Matrix (2%)
  - Phyllosilicates and rare glauconite.
- Cement (1%)
  - Silica and hematite.

Recalculated percent for Folk et al. (1970).
- Q = 99%
- F = 1%
- R = 0%

Other Features:
Biomodal, well-sorted quartzarenite. Recrystallization of quartz grains forms a tight, interlocking mosaic. Phyllosilicates and feldspars restricted primarily to the fine-grained layers. Cross-laminations are formed by the coarse-size fraction. Feldspars show only weak alteration to clay minerals.

Sample No: P17-A

Formation: Poor Valley Ridge Member of the Clinch Sandstone

Stratigraphic Position: 23.25 m above base of PVR

Rock Name: Quartzarenite

Grain Size:
- Maximum: 0.6 mm (rare)
- Minimum: 0.088 mm
- Mode: 0.25 mm

Sorting: Well-sorted, θ=0.40

Roundness: Subrounded to rounded

Sphericity: Low to medium

Composition:
- Quartz (97%)
  - Monocrystalline (87%)
  - Polycrystalline (10%)
- Muscovite (0.5%)
- Chert (0.5%)
- Zircon (0.5%)
- Tourmaline (trace)
- Opaques (trace)
- Orthoclase (trace)
- Matrix (0.5%)
  - Phyllosilicates
- Cement (0.5%)
  - Silica

Recalculated percent for Folk et al. (1970).
- Q = 99.5%
- F = 0.5%
- R = 0%

Other Features:
Fine-grained, well-sorted quartzarenite. Recrystallization of quartz grains forms a tight, interlocking mosaic. Quartz overgrowths hard to recognize. This sample was point-counted for 350 points.

Sample No: UH5-8

Formation: Hagan Shale Member of the Clinch Sandstone

Stratigraphic Position: 8.6 m above base of Hagan

Rock Name: Quartz-rich dolomite, Biosparite

Grain Size: N/A
- Maximum: N/A
- Minimum: N/A
- Mode: N/A

Sorting: Fossils poorly sorted, θ=1.50

Roundness: Fossils fragmented

Sphericity: N/A

Composition:
- Fossil Allochems (9%)
  - Echinoderm Fragments (7%)
  - Brachiopods (1%)
  - Trilobites (1%)
  - Fenestrae (trace)
- Other Framework Grains (43%)
  - Quartz (35%)
    - Monocrystalline (35%)
    - Polycrystalline (0%)
  - Opaques (4%)
  - Orthoclase (1%)
  - Microcline (1%)
  - Plagioclase (trace)
  - Chlorite (trace)
  - Hornbnlende (trace)
  - Muscovite (trace)
- Matrix (1%)
  - Fine-grained opaques
- Cement (47%)
  - Dolomite (40%)
  - Calcite (7%)
  - Hematite (trace)

Recalculated percent for Folk et al. (1970).
- Q = N/A
- F = N/A
- R = N/A

Other Features:
A poorly sorted, finely laminated, quartz-rich, dolomitic biosparite. Faint horizontal laminations consisting of skeletal debris. Only largest skeletal allochems show a preferred orientation, long axis parallel to bedding. Dolomite replaces previous micrite.

Sample No: P2-1

Formation: Poor Valley Ridge Member of the Clinch Sandstone

Stratigraphic Position: 0.4 m above base of PVR

Rock Name: Subarkose

Grain Size:
- Maximum: 0.15 mm
- Minimum: 0.065 mm
- Mode: 0.10 mm

Sorting: Well-sorted, θ=0.50

Roundness: Subangular

Sphericity: Very low

Composition:
- Quartz (79%)
  - Monocrystalline (58%)
  - Polycrystalline (21%)
- Albite (3%)
- Microcline (2%)
- Orthoclase (1.5%)
- Opaques (0.5%)
- Hornblende (trace)
- Chlorite (trace)
- Muscovite (trace)
- Chert (trace)
- Zircon (trace)
- Matrix (6%)
  - Phyllosilicates
- Cement (7%)
  - Calcite (6%)
  - Iron-stained phyllosilicates (0.5%)
  - Silica (0.5%)

Recalculated percent for Folk et al. (1970)
- Q = 92.5%
- F = 7.5%
- R = 0%

Other Features:
Very fine-grained, well-sorted, cross-laminated subarkose. Recrystallization of quartz grains forms a tight, interlocking mosaic. Fine laminations consist of phyllosilicates and hematite cement. Grains within laminae are finer-grained. Feldspars altering to clays and calcite. This sample was point-counted for 350 points.

Sample No: UH11-1

Formation: Hagan Shale Member of the Clinch Sandstone

Stratigraphic Position: 21.3 m above base of Hagan

Rock Name: Quartzarenite

Grain Size:
- Maximum: 0.500 mm (rare)
- Minimum: 0.135 mm
- Mode: 0.350 mm

Sorting: Well-sorted, θ=0.35

Roundness: Subangular

Sphericity: Medium

Composition:
- Quartz (92.5%)
  - Monocrystalline (85%)
  - Polycrystalline (7.5)
- Orthoclase (1.5%)
- Sedimentary Rock Fragments (1%)
- Brachiopods (0.5%)
- Echinoderm Fragments (trace)
- Chert (trace)
- Zircon (trace)
- Matrix (1%)
  - Hematite and phyllosilicates
- Cement (3%)
  - Dolomite (1%)
  - Silica (1%)
  - Hematite (0.5%)
  - Phyllocilicates (0.5%)

Recalculated percent for Folk et al. (1970).
- Q = 97.5%
- F = 1.5%
- R = 1%

Other Features:
A moderately sorted, iron-stained, fine-grained, quartzarenite. Recrystallized quartz forms a tight, interlocking mosaic. This sample was point-counted for 350 points.

Sample No: UH5-10

Formation: Hagan Shale Member of the Clinch Sandstone

Stratigraphic Position: 9.6 m above base of Hagan

Rock Name: Quartz-rich Biosparite

Grain Size:
- Maximum: N/A
- Minimum: N/A
- Mode: N/A

Sorting: Poorly sorted, θ=1.25

Roundness: Fossils Fragmented

Sphericity: N/A

Composition:
- Fossil Allochems (24%)
  - Echinoderm Fragments (17%)
  - Bryozoans (6.5%)
  - Brachiopods (trace)
  - Trilobites (trace)
- Other Framework Grains (11%)
  - Quartz (10%)
    - Monocrystalline (10%)
    - Polycrystalline (0%)
  - Glauconite (trace)
  - Orthoclase (trace)
  - Chlorite (trace)
- Matrix (1%)
  - Phyllosilicates
- Cement (64%)
  - Dolomite (55%)
  - Calcite (8%)
  - Hematite (1%)

Recalculated percent for Folk et al. (1970)
- Q = N/A
- F = N/A
- R = N/A

Other Features:
Horizontally laminated, quartz-rich biosparite with slight stylolitization. Fossil allochems fragmented and show a preferred orientation, long axis parallel to bedding.

Sample No: P19-A

Formation: Rose Hill

Stratigraphic Position: 1.19 m above base of Rose Hill

Rock Name: Quartzarenite

Grain Size:
- Maximum: 0.475 mm (rare)
- Minimum: 0.050 mm
- Mode: 0.062 mm and 0.125 mm

Sorting: Well-sorted for each mode, θ=0.35

Roundness: Subangular

Sphericity: Low

Composition:
- Quartz (93.5)
  - Monocrystalline (93.5%)
  - Polycrystalline (0%)
- Orthoclase (trace)
- Microcline (trace)
- Plagioclase (trace)
- Hornblende (trace)
- Opaques (trace)
- Zircon (trace)
- Muscovite (trace)
- Matrix (trace)
  - Minor phyllosilicates
- Cement (6%)
  - Quartz overgrowths and hematite occuring as fine crystals and amorphous pools between grains.

Recalculated percent for Folk et al. (1970).
- Q = 99.5%
- F = 0.5%
- R = 0%

Other Features:
Horizontally laminated, maroon, very fine-grained quartzarenite showing a bimodal texture. Small size-fraction concentrated in thin, heavily iron-cemented horizontal laminae. Recrystallized quartz grains form a tight, interlocking mosaic. Slight preferred orientation to grains, long axis parallel to bedding. This sample was point-counted for 350 points.

Sample No: P24-E1

Formation: Rose Hill

Stratigraphic Position: 9.14 m above base of Rose Hill

Rock Name: Quartzarenite

Grain Size:
- Maximum: 0.45 mm
- Minimum: 0.075 mm
- Mode: 0.175 mm

Sorting: Moderately sorted, θ=0.50

Roundness: Subangular (Rounded large floating grains of quartz).

Sphericity: Low (Medium to high on large floating grains of quartz).

Composition:
- Quartz (90%)
  - Monocrystalline (89%)
  - Polycrystalline (1%)
- Hornblende (trace)
- Zircon (trace)
- Opaques(trace)
- Tourmaline (trace)
- Orthoclase (trace)
- Matrix (1%)
  - Kaolinite and other phyllosilicates between grains.
- Cement (8%)
  - Hematite as amorphous pools between grains.
  - Some clay cement.

Recalculated percent for Folk et al. (1970).
- Q = 99.5%
- F = 0.5%
- R = 0%

Other Features:
An iron-stained, fine-grained, well sorted quartzarenite. Recrystallization of quartz grains forms a tight interlocking mosaic. Grains coated with a thin layer of hematite cement, with some phyllosilicates between grains. Orthoclase altered to sericite. This sample was point-counted for 350 points.

Sample No: P22-UA

Formation: Rose Hill

Stratigraphic Position: 4.49 m above base of Rose Hill.

Rock Name: Quartzarenite

Grain Size:
- Maximum: 0.177 mm (rare)
- Minimum: 0.062 mm
- Mode: 0.100 mm

Sorting: Very well-sorted, θ=0.25

Roundness: Subangular to subrounded

Sphericity: Low

Composition:
- Quartz (95%)
  - Monocrystalline (93%)
  - Polycrystalline (2%)
- Biotite (trace)
- Chert (trace)
- Zircon (trace)
- Matrix (3.5%)
  - Hematite and phyllosilicates
- Cement (0.5%)
  - Hematite, clay and limited silica cement.

Recalculated percent for Folk et al. (1970).
- Q = 100%
- F = 0%
- R = 0%

Other Features:
Well sorted, uniform, very fine-grained quartzarenite. Extremely fine horizontal laminations are formed by concentrations of hematite cement and other opaques. Recrystallization of quartz grains forms a tight interlocking mosaic. Some iron coatings on quartz. This sample was point-counted for 350 points.

Sample No: P21-D

Formation: Rose Hill

Stratigraphic Position: 3.59 m above base of Rose Hill

Rock Name: Quartzarenite

Grain Size:
- Maximum: 0.475 mm
- Minimum: 0.050 mm
- Mode: 0.065 mm

Sorting: Moderately sorted, θ=0.45

Roundness: Subangular (Large floating quartz grains subrounded).

Sphericity: Low (Large floating quartz grains show medium sphericity).

Composition:
- Quartz (77%)
  - Monocrystalline (77%)
  - Polycrystalline (0%)
- Mud fragments (7.5%)
- Microcline (trace)
- Orthoclase (trace)
- Plagioclase (trace)
- Hornblende (trace)
- Muscovite (trace)
- Opaques (trace)
- Zircon (trace)
- Matrix (4%)
  - Phyllosilicates between grains but mostly in seams or in bioturbated areas.
- Cement (10%)
  - Hematite cement as fine crystals or amorphous masses between grains (6%).
  - Silica (4%) overgrowths on quartz grains and amorphous silica.

Recalculated percent for Folk et al. (1970).
- Q = 99.5%
- F = 0.5%
- R = 0%

Other Features:
Poorly sorted, bioturbated, maroon, very fine-grained sublitharenite. Mottled fabric shows disrupted horizontal laminations, loose packing and selective iron cementation of bioturbated zones.

Sample No: P21-UB

Formation: Rose Hill

Stratigraphic Position: 3.24 m above base of Rose Hill

Rock Name: Siltstone

Grain Size:
- Maximum: 0.275 mm
- Minimum: 0.040 mm
- Mode: 0.050 mm

Sorting: Well-sorted, θ=0.35 (some large quartz found).

Roundness: Subangular (Large floating quartz grains subrounded).

Sphericity: Low (Large floating quartz grains show medium sphericity).

Composition:
- Quartz (93%)
  - Monocrystalline (93%)
  - Polycrystalline (0%)
- Opaques (1%)
- Orthoclase (0.5%)
- Chert (trace)
- Plagioclase (trace)
- Muscovite (trace)
- Biotite (trace)
- Zircon (trace)
- Matrix (1%)
  - Small opaques and phyllosilicates between grains.
- Cement (4%)
  - Hematite and quartz overgrowths.

Recalculated percent for Folk et al. (1970).
- Q = 99.5%
- F = 0.5%
- R = 0%

Other Features:
Finely laminated, maroon, extremely fine-grained quartzarenite or siltstone. Generally homogenous. Thin horizontal laminations consist of hematite cement. Recrystallization of quartz forms a tight interlocking mosaic. Slight preferred orientation, long axes of quartz parallel to bedding. Orthoclase altered to sericite. This sample was point-counted for 350 points.

Sample No: P22-E1

Formation: Rose Hill

Stratigraphic Position: 6.09 m above base of Rose Hill

Rock Name: Quartzarenite

Grain Size:
- Maximum: 0.125 mm
- Minimum: 0.062 mm
- Mode: 0.080 mm

Sorting: Very well-sorted, θ=0.25

Roundness: Angular to subangular

Sphericity: Low to medium

Composition:
- Quartz (96%)
  - Monocrystalline (64%)
  - Polycrystalline (32%)
- Orthoclase (0.5%)
- Opaques (0.5%)
- Chert (0.5%)
- Zircon (0.25%)
- Muscovite (trace)
- Tourmaline (trace)
- Matrix (1.5%)
  - Hematite and Phyllosilicates.
- Cement (0.5%)
  - Silica cement between grains.

Recalculated percent for Folk et al. (1970).
- Q = 99.5%
- F = 0.5%
- R = 0%

Other Features:
Well-sorted, uniform, very fine-grained quartzarenite. Homogenous and structureless. Recrystallization of quartz grains forms a tight, interlocking mosaic. This sample was point-counted for 350 points.

Sample No: P20-A

Formation: Rose Hill

Stratigraphic Position: 2.59 m above base of Rose Hill

Rock Name: Quartzarenite

Grain Size:
- Maximum: 0.5 mm
- Minimum: 0.075 mm
- Mode: 0.125 mm

Sorting: Moderately sorted, θ=0.65

Roundness: Subangular to subrounded

Sphericity: Low to medium

Composition:
- Quartz (94%)
  - Monocrystalline (92%)
  - Polycrystalline (0%)
- Orthoclase (0.5%)
- Zircon (trace)
- Carbonate Rock Fragments (trace)
- Microcline (trace)
- Plagioclase (trace)
- Opaques (trace)
- Hornblende (trace)
- Matrix (1%)
  - Phyllosilicates
- Cement (4%)
  - Quartz overgrowths, also hematite cement as fine crystals or amorphous cavity fillings.

Recalculated percent for Folk et al. (1970).
- Q = 99%
- F = 1%
- R = trace

Other Features:
An iron-stained, very fine-grained quartzarenite. Rare, large (0.5 mm) floating quartz grains. Recrystallization of quartz grains forms a tight interlocking mosaic. Dust traces within quartz overgrowths show grains rounded and spherical before recrystallization. Slight preferred orientation of grains with long axes parallel to bedding.

Sample No: P1-1

Formation: Poor Valley Ridge Member of the Clinch Sandstone

Stratigraphic Position: 0.1 m above base of PVR

Rock Name: Subarkose

Grain Size:
- Maximum: 0.10 mm
- Minimum: 0.030 mm
- Mode: 0.065 mm

Sorting: Very well sorted, θ=0.30

Roundness: Subangular to angular

Sphericity: Low

Composition:
- Quartz (85%)
  - Monocrystalline (65%)
  - Polycrystalline (20%)
- Albite (2%)
- Microcline (2%)
- Orthoclase (2%)
- Opaques (0.5%)
- Hornblende (trace)
- Muscovite (trace)
- Chlorite (trace)
- Chert (trace)
- Matrix (4%)
  - Phyllosilicates
- Cement (4%)
  - Calcite (3%)
  - Silica (0.5%)
  - Hematite (0.5%)

Recalculated percent for Folk et al. (1970).
- Q = 93%
- F = 7%
- R = 0%

Other Features:
Very fine-grained, well-sorted, horizontally laminated subarkose. Recrystallized quartz grains forms a tight, interlocking mosaic. Horizontal laminations consist of opaques, phyllosilicates and hematite cement. Feldspars show alterations to phyllosilicates and calcite. This sample was point-counted for 350 points.

Sample No: UH8-2

Formation: Hagan Shale Member of the Clinch Sandstone

Stratigraphic Position: 18.35 m above base of Hagan

Rock Name: Fossiliferous Quartzarenite

Grain Size:
- Maximum: 0.100 mm
- Minimum: 0.050 mm
- Mode: 0.062 mm

Sorting: Poorly sorted, θ=1.50

Roundness: Subangular to angular

Sphericity: Low

Composition:
- Quartz (70%)
  - Monocrystalline (66%)
  - Polycrystalline (4%)
- Trepostome Bryozoans (10%)
- Cryptostome Bryozoans (1%)
- Orthoclase (2%)
- Plagioclase (1.5%)
- Microcline (0.5)
- Opaques (1%)
- Crinoids (0.5%)
- Chert (0.5%)
- Echinoderm Fragments (0.5%)
- Biotite (trace)
- Chlorite (trace)
- Muscovite (trace)
- Zircon (trace)
- Matrix (1%)
  - Phyllosilicates
- Cement (10%)
  - Calcite (9%)
  - Dolomite (0.5%)
  - Hematite (0.5%)
  - Silica (trace)

Recalculated percent for Folk et al. (1970).
- Q = 95%
- F = 5%
- R = 0%

Other Features:
A poorly sorted, very fine-grained, fossiliferous quartzarenite. Recrystallization of quartz grains forms a tight, interlocking mosaic. Fossils show a preferred orientation, long axes parallel to bedding. Fossils are iron-stained with pore spaces filled with micrite and silt. This sample was point-counted for 350 points.

Sample No: UH10-1 and UH10-2

Formation: Hagan Shale Member of the Clinch Sandstone

Stratigraphic Position: 20.25 m and 20.4 m above base of Hagan

Rock Name: Sandstone Conglomerate

Grain Size:
- Maximum: 5 mm
- Minimum: 0.125 mm
- Mode: 0.375 mm

Sorting: Very poor, θ=2.0

Roundness: Subangular among finer grains, subrounded among larger grains.

Sphericity: Low among finer grains, high among coarser grains.

Composition:
- Quartz (76%)
  - Monocrystalline (75%)
  - Polycrystalline (1%)
- Sedimentary Rock Fragments (20%)
- Trilobite Fragments (2%)
- Orthoclase (0.5%)
- Microcline (trace)
- Plagioclase (trace)
- Hornblende (trace)
- Opaques (trace)
- Zircon (trace)
- Chert (trace)
- Matrix (trace)
  - Fine-grained opaques and phyllosilicates.
- Cement (1%)
  - Hematite, silica and dolomite.

Recalculated percent for Folk et al. (1970).
- Q = 76.5%
- F = 23.0%
- R = 0.5%

Other Features:
A very poorly sorted, iron-rich, matrix-supported sandstone conglomerate, sedimentary rock fragments consist of: (1) structureless micritic mudstone, (2) clay-rich siltstone clasts with minor opaques, (3) structureless terrigenous mudstone, (4) fine-grained sandstone showing angular grains embedded in an opaque cement, and (5) horizontally laminated mudstone. Most clasts show oxidation rims and slight imbrication.

ample No: UH6-6

Formation: Hagan Shale Member of the Clinch Sandstone

Stratigraphic Position: 12.3 m above base of Hagan

Rock Name: Quartz-rich Biosparite

Grain Size:
- Maximum: N/A
- Minimum: N/A
- Mode: N/A

Sorting: Poorly sorted, θ=1.50

Roundness: Fossils fragmented

Sphericity: N/A

Composition:
- Fossil Allochems (12%)
  - Trepostome Bryozoans (7%)
  - Echinoderms (5%)
- Other Framework Grains (36%)
  - Quartz (25%)
    - Monocrystalline (25%)
    - Polycrystalline (0%)
  - Pyrite (10%)
  - Orthoclase (0.5%)
  - Microcline (trace)
  - Plagioclase (trace)
  - Zircon (trace)
  - Chlorite (trace)
- Matrix (1%)
  - Opaques and phyllosilicates
- Cement (51%)
  - Dolomite (48%)
  - Calcite (2%)
  - Silica (0.5%)
  - Hematite (0.5%)

Recalculated percent for Folk et al. (1970).
- Q = N/A
- F = N/A
- R = N/A

Other Features:
A wavy-laminated, quartz-rich biosparite. Tightly packed fabric from recrystallization of quartz grains and dolomitization. Laminations consist of hematite cement. Abundant pyrite mineralization.

Sample No: UH6-5

Formation: Hagan Shale Member of the Clinch Sandstone

Stratigraphic Position: 11.9 m above base of Hagan

Rock Name: Dolomitic Biosparite

Grain Size:
- Maximum: N/A
- Minimum: N/A
- Mode: N/A

Sorting: N/A

Roundness: Fossils Fragmented

Sphericity: N/A

Composition:
- Fossil Allochems (42%)
  - Trepostome Bryozoans (28%)
  - Cryptostome Bryozoans (2%)
  - Echinoderm Fragments (6%)
  - Gastropods (4%)
  - Fenestrae (1%)
  - Others (1%)
  - Mollusca (trace)
- Other Framework Grains (6%)
  - Quartz (5%)
  - Opaques (0.5%)
  - Sedimentary Rock Fragments (trace)
  - Plagioclase (trace)
- Matrix (15.5%)
  - Micrite (15%)
  - Phyllosilicates (0.5%)
- Cement (36.5%)
  - Dolomite (30%)
  - Calcite (6%)
  - Silica (trace)
  - Hematite (trace)

Recalculated percent for Folk et al. (1970).
- Q = N/A
- F = N/A
- R = N/A

Other Features:

A poorly sorted, bioturbated, quartz-rich, dolomitic biosparite. No sedimentary structures. Heterogeneous, jumbled fabric. Fossil allochems iron-stained. Quartz angular, fine-grained and concentrated within cavities of fossils. Micrite occurs within bioturbated zones. Extremely thin, irregular stylolites showing concentrations of hematite.

Sample No: UH6-13

Formation: Hagan Shale Member of the Clinch Sandstone

Stratigraphic Position: 15.3 m above base of Hagan

Rock Name: Calcareous Siltstone

Grain Size:
- Maximum: 0.088 mm
- Minimum: 0.045 mm
- Mode: 0.060 mm

Sorting: Very well sorted, θ=0.25

Roundness: Subangular to angular

Sphericity: Low

Composition:
- Quartz (84%)
  - Monocrystalline (76%)
  - Polycrystalline (8%)
- Orthoclase (0.5%)
- Microcline (0.5%)
- Plagioclase (trace)
- Opaques (3%)
- Chlorite (0.5%)
- Biotite (trace)
- Zircon (trace)
- Glauconite (trace)
- Chert (trace)
- Trilobite Fragments (trace)
- Echinoderm Fragments (trace)
- Matrix (1%)
  - Phyllosilicates
- Cement (10%)
  - Calcite (9.5%)
  - Dolomite (trace)
  - Silica (trace)

Recalculated percent for Folk et al. (1970).
- Q = 98.5%
- F = 1.5%
- R = 0%

Other Features:
Very fine-grained, well-sorted, horizontally laminated calcareous siltstone. Recrystallized quartz grains form a tight, interlocking mosaic. Fine horizontal laminations are composed of fine-grained opaques or fragmented skeletal debris. Heavy iron-mineralization in some areas of slide. Feldspar is relatively unaltered. Very slight preferred orientation of quartz and trilobite fragments with long axes of grains parallel to bedding. This sample was point-counted for 350 points.

Sample No: UH5-5

Formation: Hagan Shale Member of the Clinch Sandstone

Stratigraphic Position: 6.4 m above base of Hagan

Rock Name: Highly calcareous quartzarenite

Grain Size:
- Maximum: 0.125 mm (rare)
- Minimum: 0.050 mm
- Mode: 0.050 mm and 0.088 mm

Sorting: Each mode is well-sorted, θ=0.35

Roundness: Both modes subangular

Sphericity: Both modes low

Composition:
- Quartz (62%)
  - Monocrystalline (55%)
  - Polycrystalline (7%)
- Echinoderm Fragments (3%)
- Orthoclase (1%)
- Microcline (0.5%)
- Plagioclase (0.5%)
- Opaques (1%)
- Chert (0.5%)
- Chlorite (trace)
- Muscovite (trace)
- Tourmaline (trace)
- Zircon (trace)
- Matrix (1%)
  - Fine-grained opaques, phyllosilicates and quartz.
- Cement (30%)
  - Calcite (28%)
  - Dolomite (1%)
  - Silica (1%)

Recalculated percent for Folk et al. (1970).
- Q = 97%
- F = 3%
- R = 0%

Other Features:
Fine-grained, poorly sorted, horizontally laminated, calcareous quartzarenite. Bimodal, recrystallized quartz grains form a tight interlocking mosaic. Horizontal laminations due to selective calcite cementation (echinoderm plates) and size differences of the quartz. This sample was point-counted for 350 points.

Sample No: UH2-3

Formation: Hagan Shale Member of the Clinch Sandstone

Stratigraphic Position: 2.4 m above base of Hagan

Rock Name: Quartzarenite

Grain Size:
- Maximum: 0.095 mm
- Minimum: 0.062 mm
- Mode: 0.075 mm

Sorting: Very well-sorted, θ=0.25

Roundness: Subangular

Sphericity: Low

Composition:
- Quartz (79%)
  - Monocrystalline (70%)
  - Polycrystalline (9%)
  - Orthoclase (1.5%)
- Plagioclase (1%)
- Microcline (0.5%)
- Opaques (1%)
- Chert (0.5%)
- Chlorite (trace)
- Biotite (trace)
- Muscovite (trace)
- Zircon (trace)
- Matrix (1%)
  - Fine-grained opaques, quartz and phyllosilicates.
- Cement (15%)
  - Calcite (12%)
  - Silica (3%)

Recalculated percent for Folk et al. (1970).
- Q = 96.5%
- F = 3.5%
- R = 0%

Other Features:
Very fine-grained, well-sorted, horizontally laminated calcareous quartzarenite. Recrystallized quartz grains form a tight interlocking mosaic. Faint horizontal laminations composed of selectively precipitated calcite cement. Feldspar relatively unaltered. This sample was point-counted for 350 points.

Sample No: UH2-5

Formation: Hagan Shale Member of Clinch Sandstone

Stratigraphic Position: 0.4 m above base of Hagan

Rock Name: Quartzarenite

Grain Size:
- Maximum: 0.095 mm
- Minimum: 0.062 mm
- Mode: 0.075 mm

Sorting: Very well-sorted, θ=0.25

Roundness: Subangular

Sphericity: Low

Composition:
- Quartz (78%)
  - Monocrystalline (78%)
  - Polycrystalline (0%)
- Microcline (1.5%)
- Orthoclase (1%)
- Plagioclase (1%)
- Opaques (2%)
- Chert (1%)
- Chlorite (trace)
- Biotite (trace)
- Zircon (trace)
- Matrix (1%)
  - Fine-grained opaques, quartz and phyllosilicates.
- Cement (14%)
  - Calcite (12%)
  - Dolomite (1%)
  - Silica (1%)

Recalculated percent for Folk et al. (1970).
- Q = 96%
- F = 4%
- R = 0%

Other Features:
Very fine-grained, well-sorted, horizontally laminated, calcareous quartzarenite. Recrystallized quartz grains form a tight interlocking mosaic. Faint horizontal laminations composed of selectively precipitated calcite cement. Feldspar relatively unaltered.

Sample No: UH5-7B

Formation: Hagan Shale Member of the Clinch Sandstone

Stratigraphic Position: 7.5 m above base of Hagan

Rock Name: Siltstone

Grain Size:
- Maximum: 0.088 mm (rare)
- Minimum: 0.040 mm
- Mode: 0.050 mm

Sorting: Well-to very well-sorted, θ=0.27

Roundness: Subangular to angular

Sphericity: Low

Composition:
- Quartz (72%)
  - Monocrystalline (65%)
  - Polycrystalline (7%)
- Opaques (2%)
- Orthoclase (1%)
- Microcline (trace)
- Plagioclase (trace)
- Chert (trace)
- Muscovite (trace)
- Glauconite (trace)
- Zircon (trace)
- Matrix (0.5%)
  - Fine-grained opaques and phyllosilicates.
- Cement (24%)
  - Calcite (23%)
  - Silica (1%)
  - Dolomite (trace)

Recalculated percent for Folk et al. (1970).
- Q = 98%
- F = 2%
- R = 0%

Other Features:
Well-sorted, horizontally laminated siltstone. Recrystallized quartz grains form a tight interlocking mosaic. Laminations composed of concentrations of carbonate cement and phyllosilicates. Phyllosilicates show a preferred orientation with long axes parallel to bedding. Feldspars relatively unaltered. Some of the calcite cement occurs in large pools.

Sample No: UH5-7A

Formation: Hagan Shale Member of Clinch Sandstone

Stratigraphic Position: 7.4 m above base of Hagan

Rock Name: Quartzarenite

Grain Size:
- Maximum: 0.50 mm
- Minimum: 0.075 mm
- Mode: 0.075 mm and 0.40 mm

Sorting: Moderately sorted, θ=0.75

Roundness: Subangular (fine mode) and subrounded (coarse mode).

Sphericity: Low (fine mode), medium to high (coarse mode).

Composition:
- Quartz (79%)
  - Monocrystalline (78%)
  - Polycrystalline (1%)
- Trilobite Fragments (5%)
- Opaques (2%)
- Orthoclase (1.5%)
- Microcline (1%)
- Plagioclase (1%)
- Chert (0.5%)
- Zircon (trace)
- Chlorite (trace)
- Muscovite (trace)
- Matrix (1%)
  - Phyllosilicates and fine-grained opaques.
- Cement (8%)
  - Calcite (7%)
  - Silica (1%)
  - Hematite (trace)

Recalculated percent for Folk et al. (1970).
- Q = 96%
- F = 4%
- R = 0%

Other Features:
A bimodal (fine-and medium-grained), fossil-rich quartzarenite. Recrystallized quartz grains form an interlocking mosaic. Fabric more tightly packed within fine-grained layers. Preferred orientation of trilobite fragments and larger quartz grains with long axes parallel to bedding. Silica cement preferentially associated with the fine-grained size fraction, calcite cement with the larger grains. Also feldspars (with the exception of orthoclase) found mainly in the small size-fraction.

Sample No: P9-1

Formation: Poor Valley Ridge Member of the Clinch Sandstone

Stratigraphic Position: 9.8 m above base of PVR.

Rock Name: Quartzarenite

Grain Size:
- Maximum: 0.40 mm
- Minimum: 0.125 mm
- Mode: 0.250 mm

Sorting: Very well-sorted, θ=0.28

Roundness: Subrounded

Sphericity: Medium

Composition:
- Quartz (96%)
  - Monocrystalline (66%)
  - Polycrystalline (30%)
- Orthoclase (0.5%)
- Muscovite (0.5%)
- Chert (0.5%)
- Plagioclase (trace)
- Opaques (trace)
- Chlorite (trace)
- Zircon (trace)

- Matrix (1%)
  - Kaolinite and other phyllosilicates
- Cement (1%)
  - Silica, hematite and limonite.

Recalculated percent for Folk et al. (1970).
- Q = 99%
- F = 1%
- R = 0%

Other Features:
Very well sorted, fine-grained quartzarenite. Recrystallization of quartz grains forms a tight, interlocking fabric. Quartz overgrowths difficult to recognize. This sample was point-counted for 350 points.

Sample No: P3-1

Formation: Poor Valley Ridge Member of the Clinch Sandstone

Stratigraphic Position: 1.75 m above base of PVR.

Rock Name: Subarkose

Grain Size:
- Maximum: 0.130 mm
- Minimum: 0.065 mm
- Mode: 0.120 mm

Sorting: Very well-sorted, θ=0.30

Roundness: Subangular

Sphericity: Low

Composition:
- Quartz (85%)
  - Monocrystalline (65%)
  - Polycrystalline (20%)
- Albite (3%)
- Orthoclase (1%)
- Microcline (1%)
- Hornblende (trace)
- Chlorite (trace)
- Muscovite (trace)
- Chert (trace)
- Zircon (trace)
- Opaques (trace)
- Matrix (3.5%)
  - Phyllosilicates
- Cement (5.5%)
  - Calcite (4.5%)
  - Silica (0.1%)

Recalculated percent for Folk et al. (1970).
- Q = 94.5%
- F = 5.5%
- R = 0%

Other Features:
Very fine-grained, well-sorted, horizontally laminated subarkose. Recrystallization of quartz forms a tight, interlocking mosaic. Horizontal laminations consist of dense concentrations of phyllosilicates. Slight preferred orientation of quartz grains with long axes parallel to bedding. Feldspar shows only weak alteration to calcite (not as pronounced as P1-1 or P2-1). Some feldspars fresh. This sample was point-counted for 350 points.

Sample No: P5-A

Formation: Poor Valley Ridge Member of the Clinch Sandstone

Stratigraphic Position: 4.65 m above base of PVR

Rock Name: Quartzarenite

Grain Size:
- Maximum: 1.0 mm
- Minimum: 0.065 mm
- Mode: 0.075 mm and 0.8 mm

Sorting: Very poor, θ=1.75 to 2.0

Roundness: Subangular (fine mode) and well-rounded (coarse mode)

Sphericity: Medium (fine mode) and high (coarse mode)

Composition:
- Quartz (89%)
  - Monocrystalline (84%)
  - Polycrystalline (5%)
- Opaques (3%)
- Sedimentary Rock Fragments (1%)
- Microcline (0.5%)
- Orthoclase (trace)
- Plagioclase (trace)
- Chert (trace)
- Muscovite (trace)
- Chlorite (trace)
- Zircon (trace)
- Matrix (5%)
  - Phyllosilicates and fine-grained hematite.
- Cement (1%)
  - Hematite and Silica.

Recalculated percent for Folk et al. (1970).
- Q = 98%
- F = 1%
- R = 1%

Other Features:
Coarse-grained, poorly sorted, immature quartzarenite. Bimodal texture. The coarse size-fraction predominates, consisting of a wide array of quartz types, chert and sedimentary rock fragments. All others found in small size-fraction. Hematite cement predominates. Small size-fraction shows recrystallization of quartz forming a tight, interlocking mosaic. Intense bioturbation.

Sample No: P18-B

Formation: Poor Valley Ridge Member of the Clinch Sandstone

Stratigraphic Position: 27.4 m above base of PVR

Rock Name: Quartzarenite

Grain Size:
- Maximum: 0.710 mm (rare)
- Minimum: 0.080 mm
- Mode: 0.225 mm and 0.350 mm

Sorting: Well sorted within each mode, θ=0.35

Roundness: Subrounded

Sphericity: Medium

Composition:
- Quartz (98%)
  - Monocrystalline (95%)
  - Polycrystalline (3%)
- Muscovite (trace)
- Orthoclase (trace)
- Chert (trace)
- Tourmaline (trace)
- Opaques (trace)
- Matrix (0.5%)
  - Minor phyllosilicates
- Cement (1%)
  - Predominantly silica with rare, iron-stained phyllosilicate cement. Possible trace of hematite cement.

Recalculated percent for Folk et al. (1970).
- Q = 99.5%
- F = 0.5%
- R = 0%

Other Features:
Bimodal, well-sorted quartzarenite. Recrystallization of quartz grains forms a tight interlocking mosaic. Cross-laminations highlighted by slight differences in grain size. A slight preferred orientation of the coarse-grained mode with the long axis of quartz grains parallel to bedding. Some quartz grains have a very thin coating of hematite. This sample point-counted for 350 points.

Sample No: BH-1

Formation: Hagan Shale Member of the Clinch Sandstone.

Stratigraphic Position: 0.4 m above base of HS

Rock Name: Calcareous quartzarenite

Grain Size:
- Maximum: 0.10 mm
- Minimum: 0.050 mm
- Mode: 0.085 mm

Sorting: Well-sorted, θ=0.35

Roundness: Subangular

Sphericity: Low

Composition:
- Quartz (54%)
  - Monocrystalline (30%)
  - Polycrystalline (24%)
- Plagioclase (1%)
- Microcline (1.5%)
- Orthoclase (1.5%)
- Opaques (1%)
- Chlorite (trace)
- Muscovite (trace)
- Tourmaline (trace)
- Zircon (trace)
- Matrix (5%)
  - Quartz, feldspar, opaques and clay minerals.
- Cement (35%)
  - Calcite (33%)
  - Dolomite (2%)

Recalculated percent for Folk et al. (1970).
- Q = 93.1%
- F = 6.9%
- R = 0%

Other Features:
Where in contact, quartz grains are interlocking and show signs of recrystallization. Fabric is tightly packed due to heavy carbonate cementation filling in most of the pore space. No sedimentary structures observed.

Sample No: BH-2

Formation: Hagan Shale Member of the Clinch Sandstone.

Stratigraphic Position: 0.4 m above base of HS

Rock Name: Calcareous litharenite

Grain Size:
- Maximum: 3.5 mm
- Minimum: 0.125 mm
- Mode: 0.375 mm

Sorting: Poorly sorted, θ=2.0

Roundness: Subangular (fine grains), Subrounded (coarse grains)

Sphericity: Medium

Composition:
- Quartz (45%)
  - Monocrystalline (40%)
  - Polycrystalline (2%)
- SRF (12%)
- Albite (0.5%)
- Orthoclase (0.5%)
- Phosphate (0.5%)
- Glauconite (0.5%)
- Brachiopods (0.5%)
- Microcline (trace)
- Matrix (5%)
  - Quartz, feldspar, opaques and clay minerals.
- Cement (35%)
  - Calcite (30%)
  - Dolomite (5%)

Recalculated percent for Folk et al. (1970).
- Q = 77.6%
- F = 1.7%
- R = 20.7%

Other Features:
Framework of quartz shows loose packing with carbonate cement filling areas between grains. Various sedimentary rock fragments include: chert, mudstone, siltstone and sandstone clasts. All are highly rounded. No visible sedimentary structures.

APPENDIX III

MEASURED BED THICKNESS IN THE HAGAN SHALE

Bed Thickness (cm)	Meters Above Base of Hagan	Bed Thickness (cm)	Meters Above Base of Hagan
30.00	0.00	0.50	2.90
8.00	0.30	0.40	2.94
2.60	0.40	0.40	2.97
2.50	0.46	1.80	3.07
0.70	0.52	1.70	3.10
0.70	0.77	0.60	3.14
1.80	0.78	1.20	3.58
1.80	0.83	1.60	3.63
2.60	0.89	0.90	3.72
7.80	0.98	0.50	3.78
2.10	1.00	0.70	3.92
2.00	1.06	0.40	3.94
1.50	1.11	0.50	4.00
1.70	1.13	0.90	4.03
2.90	1.26	0.40	4.10
1.10	1.32	0.30	4.13
1.10	1.36	0.30	4.14
1.50	1.40	1.30	4.27
0.90	1.43	1.20	4.40
0.50	1.47	2.60	4.46
3.10	1.48	0.90	4.50
2.80	1.57	0.50	4.55
1.60	1.61	1.70	4.58
0.50	1.68	1.30	4.63
1.90	1.73	2.60	4.65
1.00	1.76	0.40	4.69
1.40	1.78	0.50	4.70
1.20	1.95	2.00	4.73
4.50	2.00	4.20	4.79
4.10	2.09	0.60	4.93
2.70	2.10	2.90	4.97
1.90	2.25	3.90	5.00
0.90	2.31	3.00	5.05
0.60	2.40	4.50	5.15
1.30	2.46	1.40	5.20
8.50	2.54	1.10	5.23
0.50	2.64	4.50	5.46
2.50	2.76	0.90	5.55
0.80	2.85	2.90	5.61

Bed Thickness (cm)	Meters Above Base of Hagan	Bed Thickness (cm)	Meters Above Base of Hagan
0.90	5.71	0.50	8.82
3.70	5.75	1.10	8.85
0.70	5.82	9.50	8.97
0.60	5.84	2.40	9.09
0.30	6.25	0.30	9.13
0.40	6.31	0.40	9.16
0.40	6.35	1.20	9.66
0.50	6.38	2.30	9.19
0.80	6.41	3.10	9.29
0.30	6.43	4.30	9.36
0.40	6.45	7.40	9.42
0.80	6.51	1.10	9.50
0.70	6.53	4.80	9.54
5.50	6.64	1.80	9.60
0.60	6.73	0.50	9.65
1.00	6.75	0.30	9.69
3.10	6.79	0.20	9.70
1.00	6.89	0.70	9.72
0.20	6.90	0.60	9.73
1.60	6.94	1.40	9.76
0.20	6.97	1.50	1.85
1.10	6.98	1.70	1.87
0.60	7.11	0.20	10.17
0.50	7.16	1.30	10.25
3.20	7.22	0.90	10.39
2.80	7.30	0.60	10.44
0.60	7.41	0.60	10.50
4.70	7.45	6.50	10.90
0.40	7.49	0.70	11.00
0.30	7.50	3.00	11.11
1.70	7.59	0.70	11.19
2.00	7.75	2.20	11.27
0.80	7.87	1.00	11.31
3.10	7.93	0.20	11.50
0.40	7.99	0.20	11.55
0.30	8.02	1.00	11.69
0.40	8.03	1.10	11.80
0.90	8.09	0.60	11.87
1.40	8.10	7.00	11.93
1.50	8.32	0.40	12.03
2.20	8.48	1.90	12.15
1.00	8.52	3.20	12.19
1.70	8.56	1.80	12.28
0.80	8.63	0.80	12.34
0.90	8.66	0.50	12.42

Bed Thickness (cm)	Meters Above Base of Hagan	Bed Thickness (cm)	Meters Above Base of Hagan
0.70	12.58	0.60	15.47
0.20	12.68	0.90	15.50
3.30	12.75	1.50	15.65
0.60	13.03	0.50	15.71
7.00	13.11	1.00	15.75
3.10	13.19	1.10	15.82
1.00	13.27	2.20	15.85
0.70	13.30	0.20	15.88
0.60	13.32	0.20	15.91
0.70	13.36	0.20	15.96
1.20	13.40	0.20	16.08
1.60	13.46	1.60	16.28
0.40	13.48	0.80	16.48
0.30	13.49	1.60	16.53
0.50	13.60	1.80	16.56
0.90	13.72	1.10	16.61
1.00	13.75	1.70	16.67
0.50	13.79	1.50	16.78
0.30	13.81	0.40	16.83
1.10	13.83	0.50	16.87
0.60	13.85	0.40	16.93
1.20	13.90	1.40	16.96
0.20	13.96	0.40	17.00
0.20	13.98	1.90	17.08
2.10	14.13	17.10	18.22
2.10	14.17	0.40	18.43
0.40	14.22	0.70	18.47
0.40	14.24	0.80	18.50
2.60	14.28	0.60	18.73
0.90	14.32	1.30	18.85
2.40	14.35	0.70	19.00
2.60	14.38	0.30	19.13
1.10	14.41	1.20	19.16
0.60	14.50	1.90	19.21
1.20	14.57	0.80	19.25
1.80	14.63	1.80	19.28
1.10	14.83	0.70	19.34
0.30	14.87	0.20	19.40
0.20	14.92	1.20	19.41
0.90	14.99	1.20	19.86
0.20	15.10	7.00	20.25
0.30	15.13	3.80	20.45
4.40	15.22	1.00	20.58
2.50	15.30	1.20	20.62
1.00	15.44	1.10	20.69

Bed Thickness (cm)	Meters Above Base of Hagan	Bed Thickness (cm)	Meters Above Base of Hagan
2.40	20.73		
1.80	20.78		
0.70	20.80		
0.70	20.83		
0.40	20.95		
0.30	21.00		
0.30	21.03		
0.20	21.08		
0.40	21.13		
0.30	21.20		
0.60	21.27		
0.50	21.30		
0.60	21.35		
1.30	21.50		
0.30	21.71		
0.20	21.86		
0.20	21.95		
0.20	22.20		
0.20	22.29		
0.10	22.45		
0.20	22.47		
0.20	22.49		
0.70	22.59		
0.60	22.78		
0.50	23.05		
0.30	23.12		
0.40	23.13		
0.50	23.15		
0.50	23.16		
0.40	23.18		
0.40	23.20		
0.30	23.21		
1.00	23.23		
0.50	23.24		
0.30	23.24		
0.50	23.25		
0.30	23.26		
1.80	23.28		

VITA

Gregory Thomas Marks was born in Cleveland, Ohio and raised on a small farm in nearby Olmsted Falls, Ohio. After attending elementary and secondary school, the author enrolled at Wilmington College, a private school in southwestern Ohio. Summers were spent working on an oil rig in central Ohio for Midwest Drilling, Inc. After spending two years studying agricultural science, he enrolled at The Ohio State University to start a curriculum in the geological sciences. He graduated from that institution in March, 1984 with a Bachelor of Science degree. Before attending graduate school at the University of Tennessee in the fall of 1984, the author was awarded a summer research internship at NASA-Johnson Space Center and The Lunar and Planetary Institute, Houston, Texas. Research was aimed at analyzing fluid inclusions trapped within Archean sediments with the neodymium laser microprobe. In the winter of 1985, Gregory accepted a teaching assistantship from the Department of Geological Sciences, University of Tennessee. During the summer and winter of 1985, the author was awarded an internship with Mobil Oil, Petrophysics and Computer Geology Division, Dallas, Texas. Gregory was awarded a Master of Science with a concentration in Geological Sciences in the summer of 1987.